

Accurate Sorption Measurements on Coal and Activated Carbon using Accurate Equations of State

Elisa Battistutta

Accurate Sorption Measurements on Coal and Activated Carbon using Accurate Equations of State

Proefschrift

ter verkrijging van de graad van doctor
aan de Technische Universiteit Delft,
op gezag van de Rector Magnificus prof. ir. K.C.A.M. Luyben
voorzitter van het College voor Promoties,
in het openbaar te verdedigen op
dinsdag 29 november 2011 om 12.30 uur

door

Elisa BATTISTUTTA

Dottore Magistrale in Ingegneria per l'Ambiente ed il Territorio
Universita' degli Studi di Trieste
geboren te Palmanova (Italy)

Dit proefschrift is goedgekeurd door de promotor:
Prof.dr. J. Bruining

Copromotor:
Dr. K-H.A.A. Wolf

Samenstelling promotiecommissie:

Rector Magnificus	voorzitter
Prof.dr. K.C.A.M. Luyben	Technische Universiteit Delft,
Prof.dr. J. Bruining	Technische Universiteit Delft, promotor
Dr. K-H.A.A. Wolf	Technische Universiteit Delft, copromotor
Prof.dr.ir. P.L.J. Zitha	Technische Universiteit Delft
Prof.dr. S. Durucan	Imperial College, London
Prof.dr. C.J. Spiers	Utrecht University
Dr. E.S.J. Rudolph	Technische Universiteit Delft
Dr. F. van Bergen	TNO Institute
Prof.dr. W.R. Rossen	Technische Universiteit Delft, reserve

E quanto intendo più, tanto più ignoro.
Tommaso Campanella

To all the people I love

The research described in this thesis is performed at the Department of Geoengineering, Faculty of Civil Engineering and Geosciences, Delft University of Technology, The Netherlands. The research has been financial supported by the european program GRASP (Green-House Gas Removal Apprenticeship) and by the Dutch CATO2 program for the capture, transport and storage of carbon dioxide.

Summary

Since industrial revolution, due to the increasing demand of energy, anthropogenic emissions in the atmosphere are constantly growing. The International Energy Agency (IEA) predicted a 57% increase of energy demand from 2004 to 2030 (IEA, 2004) of which, 85% consists of fossil fuels. Actions need to be taken in order to mitigate CO₂ emissions generated through human activities. In the last twenty years CO₂ emissions became a political and industrial priority in many governmental and commercial institutions; Carbon Capture and Storage (CCS) is one of the main options but it is a temporary solution. CCS is based on capturing CO₂ from large point sources. The gas is transported via pipelines and injected in deep underground formations, such as depleted gas and oil fields, deep saline aquifers and unminable coal seams. The last method is the option that will be treated in this thesis. Coal can be favorable if CO₂ replaces coal gas that mostly consists of methane (CH₄). This is called CO₂- Enhanced Coal Bed Methane (CO₂-ECBM) production.

The feasibility and economical viability of CO₂-ECBM depend on geological factors such as heterogeneities of coals and their pore systems. This is why the development and implementation of reservoir simulators for ECBM production and CO₂ storage require detailed and reliable information on the physical and chemical processes that are initiated by injection of gases in the coal layers. The most important processes to deal with are sorption behavior, of the coal competitive sorption of the different gases presents, multi-phase transport, permeability behavior and initial amount and compositions of the gas injected.

In this study the main objective is to get a better understanding of the coal-water-gases system. The activities involved experimental work and theory development to acquire data and theory for field scale modeling. Thinking in terms of real case scenarios we consider the use of an impure CO₂ stream, i.e., impurities in the CO₂, either flue gas components or water, and their ef-

fect on coal behavior. The activities in this research involve the experimental results of sorption on dry and wet coal and the sorption of flue gas type of gas mixtures measured with a manometric set up at 318 K and up to 160 bar. A new aspect of the thesis is to focus on the different ways to obtain sufficiently accurate Equations of State (EoS) to be used in a manometric set up.

The experimental results allowed us to interpret and test different models concerning sorption and thermodynamic behavior of gases. The results in general show that sorption and desorption of CH₄ and N₂ on coal are fully reversible, meanwhile this is not happening for CO₂. The equilibration time for the CO₂ sorption on coal is much larger than for N₂ and CH₄. An increase in temperature is negatively affecting the sorption capacity of the coal. The swelling induced by CO₂ injection on coal is a fully reversible phenomenon and it is positively related to the sorption.

The sorption of CO₂ on wet coal is inhibited by the presence of water. The density of the CO₂-H₂O gas phase in the temperature and pressure range of the study can be calculated using the Span and Wagner EoS for pure CO₂. The CO₂ dissolved in water, assuming that water in its sorbed phase behaves as in its free phase, can be described by a Peng-Robinson-Stryjek-Vera EoS that is optimized for the CO₂-water system.

The adequacy of an EoS to predict the density of a mixture can be tested by using a combination of the manometric set up with a density meter. A Helium mixture containing 1% O₂ and 1% NO₂ can be described with the Mc Carty EoS for pure Helium. In this case, the maximum relative difference from the experimentally determined density is of $6 \cdot 10^{-3}$. A CO₂ mixture containing 1% O₂, 1% He and 1% NO₂ cannot be described accurately with any of the existing EoS. Results concerning the excess sorption isotherm are influenced by the choice of a specific EoS. The maximum of the excess sorption can vary 25.88%, depending on which EoS is used for the calculations. A combination of different EoS for different pressure ranges gives an accurate result, with a maximum relative difference from the experimentally determined density of 0.05. In this case the maximum excess sorption gives a value of 7.81 mol/kg, which is in agreement with the literature concerning pure CO₂ sorption on activated carbon. In the desorption process from activated carbon with the two mixtures mentioned previously, the mass spectrometer measurements show that for the specified P,T range, no reactions occur between the gas and the activated carbon.

The results of this research give an alternative direction with respect to the use of impure CO₂ in ECBM.

Samenvatting

Sinds het begin van de industriële revolutie, is door de toenemende vraag, de antropogene emissie in de atmosfeer een constante groei ontstaan. Het internationale energie-agentschap voorspelt een toenemende vraag naar energie van 57% in de periode tussen 2004 tot 2030 (IEA, 2004), waarvan 85 % bestaat uit fossiele brandstoffen. Om de uitstoot van deze door menselijk handelen veroorzaakte CO₂ emissies te matigen, moet actie worden ondernomen.

In de afgelopen twintig jaar zijn de CO₂ emissies zowel een politieke als industriële prioriteit geworden voor vele zowel publieke als private instituties. De afvang en opslag van CO₂ (CCS) is een van de belangrijkste opties om dit probleem - tijdelijk - op te lossen.

CCS is gebaseerd op het afvangen van CO₂ bij grote uitstootlocaties. Het gas wordt getransporteerd via pijpleidingen en geïnjecteerd in diepe ondergrondse formaties, zoals uitgeputte gas- en of olievelden, diep gelegen zoutwater voerende lagen en of niet te delven kolenlagen. De laatste opslagmethode zullen wij in deze thesis nader beschouwen.

Kolen hebben hierbij de voorkeur voor de opslag van CO₂ als het kolengas, dat meestal bestaat uit methaan (CH₄). Deze methode staat ook wel bekend als CO₂ verbeterd-kolenlaag-methaan (CO₂-ECBM) productie.

De uitvoerbaarheid en economische levensvatbaarheid van CO₂ hangt af van geologische factoren zoals de heterogeniteit van de kolen en de petrofysische eigenschappen van het poreuze medium.

Dit is de reden waarom bij de ontwikkeling en implementatie van een ECBM en CO₂ opslag reservoir simulaties, gedetailleerde en betrouwbare informatie m.b.t. de fysische en chemische processen die optreden tijdens de injectie van gas in kolenlagen vereist is. De belangrijkste processen zijn sorptie van de kolen, competitieve sorptie van verschillende gassen, meer-fasen transport, permeabiliteits gedrag en de initieel aanwezige samenstelling van de hoeveel-

heid geïnjecteerd gas.

In deze studie is het hoofddoel om een beter begrip in water-kolen-gas systemen te krijgen. De activiteiten houden zowel experimenteel als theoretisch werk in, om data en het bijbehorende theoretische inzicht te verkrijgen om deze processen op makroschaal te modelleren.

Denkend in realistische scenario's, is het als gebruik van onzuiver CO₂ stoom te beschouwen, waarbij de onzuiverheden in de CO₂, of rookgas componenten of water en zijn effect op het gedrag van kolen is. De activiteiten in dit onderzoek hebben betrekking op het experimenteel bepalen van sorptie met droge en natte kolen en de sorptie van rookgasmengsels, die bepaald zijn met de manometrische opstelling op 318 K tot waarden van 160 bar. Een nieuw aspect is de afwijkende manier om voldoende nauwkeurige evenwichtsvergelijkingen (EoS) te bepalen voor deze manometrische opstelling.

De experimentele resultaten maakten het ons mogelijk verschillende modellen m.b.t. sorptie en thermodynamisch gedrag van gassen te interpreteren en te onderzoeken. De resultaten laten in het algemeen zien dat de sorptie en desorptie van CH₄ en N₂ op kolen volledig omkeerbaar is, terwijl dit niet het geval is voor CO₂.

De tijd om tot een evenwichtstoestand van CO₂ sorptie in kolen te komen is veel langer dan die voor N₂ en CH₄. Een toename in temperatuur beïnvloedt de sorptie-capaciteit van kolen negatief. Het opzwellen dat geïnduceerd wordt door CO₂ injectie in kolen is een volledig omkeerbaar fenomeen en is positief gecorreleerd met de sorptie.

De sorptie van CO₂ in natte kolen wordt geremd door de aanwezigheid van water. De dichtheid van de CO₂-H₂O gas fase in de temperatuur en het drukgebied dat we bestuderen, kan berekend worden m.b.v. de Span en Wagner EoS voor zuiver CO₂. De CO₂ die opgelost is in water, onder de aanname dat de geabsorbeerde fase zich gedraagt als in een vrije fase, kan beschreven worden door de Peng-Robinson-Stryjek-Vera EoS dat geoptimaliseerd is voor het CO₂-watersysteem.

De adequaatheid van de EoS om de dichtheid van een mengsel te bepalen, kan getest worden m.b.v. een combinatie van de manometrische opstelling met een dichtheidsmeter. Een Helium mengsel dat 1% O₂ en 1% NO₂ bevat, kan worden beschreven met de McCarty EoS voor zuiver Helium. Een CO₂ mengsel dat 1% O₂, 1% He en 1% NO₂ bevat kan niet accuraat door de huidige EoS beschreven worden. De resultaten die de overvloedige sorptie-isothermen beschrijven, zijn afhankelijk van de de specifiek gekozen EoS. De maximale exces-sorptie kan variëren tussen 25.88%, afhankelijk van de EoS die gebruikt zijn voor de berekening. Een combinatie van verschillende EoS

voor verschillende drukgebieden, geven een accuraat resultaat met een maximaal relatieve afwijking van de experimenteel bepaalde dichtheid van 0.05. In dit geval is de maximale excessorptie, 7.81 mol/kg, wat overeenkomt met de literatuur over CO₂ sorptie van actieve kool.

Tijdens het desorptie proces van actieve kool met de twee eerder genoemde mengsels, liet de massaspectrometer zien, dat voor het specifieke P,T bereik, geen reacties plaatsvinden tussen het gas en de actieve kool.

De resultaten van dit onderzoek geven een alternatieve richting m.b.t. het gebruik van onzuivere CO₂ voor ECBM.

Contents

1	Introduction	1
1.1	General introduction	1
1.2	Storage opportunities and CCS projects	2
1.3	CCS energy consumption and costs	4
1.4	Current state of knowledge of gas sorption in coal	6
1.5	research objectives, scope and outline of the thesis	10
2	Swelling and Sorption Experiments of Pure Gases on Coal	15
2.1	Introduction	16
2.2	Experimental method and materials	18
2.3	Results and discussions	23
2.4	summary of observations	36
2.5	Conclusions	38
2.6	Aknowledgement	39
3	Sorption of CO₂ on Moisture-Equilibrated Coal	41
3.1	Introduction	42
3.2	Experimental method and materials	44
3.3	Data analysis	47
3.4	Conclusions	55
3.5	Aknowledgement	56
4	Adequacy of Equation of State Models	57
4.1	Introduction	58
4.2	Theory	59
4.3	Experimental method and materials	62
4.4	Volume ratio measurements using a Helium mixture	65

CONTENTS

4.5	Volume ratio measurements using a CO ₂ mixture	72
4.6	Conclusions	78
4.7	Aknowledgement	79
5	Determiration of Adsorption of Gas Mixtures in a Manometric Set Up	81
5.1	Introduction	82
5.2	Experimental method and materials	84
5.3	Conclusions	97
5.4	Aknowledgement	98
6	Conclusions	99
A	Absolute sorption	103
B	Error determination	105
C	UNIFAC model	109
D	Peneloux volume correction	113
	References	115

List of Figures

2.1	Technical drawing of the manometric set up.	20
2.2	Examples of pressure decrease steps during sorption	24
2.3	N ₂ sorption on Selar Cornish coal.	27
2.4	CH ₄ excess sorption on Selar Cornish coal at 318 K and 338 K. .	28
2.5	CO ₂ excess sorption in Selar Cornish coal at 318 K and 338 K. .	29
2.6	Volumetric swelling induced by CO ₂ sorption.	33
2.7	Excess sorption isotherm of CO ₂ on Selar Cornish coal at 318K. .	34
2.8	Absolute sorption of CO ₂ on Selar Cornish coal at 318 K.	36
3.1	The set up for density measurements.	45
3.2	Density experimentally determined with a DMA 512 Paar density meter	48
3.3	CO ₂ excess sorption isotherms	50
3.4	CO ₂ Excess sorption isotherms with error bar	51
3.5	CO ₂ excess sorption isotherm in water (dissolution)	52
3.6	CO ₂ absolute sorption isotherm on water (dissolution)	53
3.7	Absolute sorption of CO ₂ on coal and absolute sorption of CO ₂ in water	54
4.1	Volume ratio of the sample cell and reference cell.	66
4.2	Probability plot obtained using the measured volume ratio data. .	67
4.3	The volume ratio computed with different EoS.	68
4.4	The volume ratio deduced from different EoS.	69
4.5	The volume ratio deduced from different EoS.	70
4.6	The relative difference of the calculated density.	72
4.7	The volume ratio computed with different EoS.	73
4.8	The relative difference of the calculated density.	73

LIST OF FIGURES

4.9	Density experimentally determined with a DMA 512 Paar density meter.	74
4.10	Density of the CO ₂ mixture at various pressures and at a constant temperature of 318 K.	75
4.11	The relative error of the densities.	76
5.1	Ion current measurements conducted with the mass spectrometer.	86
5.2	Ratio of the ion current measurements.	87
5.3	Excess sorption isotherm on activated carbon (Filtrisorb 400) of a He mixture.	89
5.4	Montecarlo simulation of the density of the CO ₂ mixture versus pressure.	90
5.5	Volume correction parameter.	92
5.6	The relative difference of the calculated density versus the experimentally determined density.	93
5.7	Excess sorption isotherm on activated carbon of a CO ₂ mixture.	95
5.8	Excess sorption isotherm on 4 different activated carbon samples.	96
B.1	Probability plot of an excess sorption value.	105
B.2	Standard deviation of pressure steps plotted versus pressure . .	106
B.3	Standard deviation of pressure steps plotted versus pressure . .	107

List of Tables

1.1	Overview of geological storage options	2
1.2	Exergy requirement in the CO ₂ capture process.	5
1.3	Overview of ongoing CCS projects.	12
1.4	Overview proposed CCS projects.	13
2.1	Properties of the U.K. Selar Cornish coal.	19
2.2	Critical properties and purity of the gases used	19
2.3	Experimental conditions and parameters of the sorption experiments.	22
2.4	Literature overview of sorption experiments.	26
2.5	Langmuir parameters of the different isotherm fitting.	38
3.1	Properties of the Tupton coal samples	44
3.2	Averaged values of pressure, temperature and CO ₂ molar composition	49
3.3	Moisture content of the samples used in this study	49
4.1	The Mathias Copeman coefficients.	63
4.2	Critical properties of the gases used.	63
4.3	The group binary interaction parameters a_{nm}	80
5.1	molecular weight of the molecules measured with the MS.	85
5.2	P,T of the lowest and highest data point of the void volume ratio measurements	89
5.3	Fitting parameters of the volume correction calculated as a function of pressure.	94
B.1	Accuracy of data measurements	105

Chapter 1

Introduction

1.1 General introduction

CO₂ emissions became a political and industrial priority in many governmental and commercial institutions in the past two decades. Since industrial revolution, due to the increasing demand of energy, anthropogenic emissions in the atmosphere are constantly growing. The International Energy Agency (IEA) predicted a 57% increase of energy demand from 2004 to 2030 (IEA, 2004) of which 85% consists of fossil fuels. In 2000, power plants were responsible for about the 40% of the total anthropogenic CO₂ emissions (Yang et al., 2008). Together with large industrial manufacturing plants they produced 14.2 Gt/y (IEA, 2007). The predictions for the year 2010 have been increased by a 63% to 18 Gt/year (IEA, 2004), an estimation that in 2007 was already overtaken (CDIAC)¹. Without preventive measures the prognoses for 2020, compared to 2004, increase with 76%, or 23.31 Gt/year.

There are different ways to mitigate CO₂ emissions, i.e., through the reduction of energy and material demand, by efficiency improvements and changes in consumption patterns (Damen, 2007). In addition, a shift towards less carbon-rich fuels and an increase of renewable energy will be essential. One of the options concerning the CO₂ emission reduction is provided by the Carbon Capture and Storage technology (CCS). The capture phase mainly concerns catching CO₂ from coal fired power plants, steel and cement industries as they are the best candidates regarding volumes produced. However, in the long term

¹Carbon Dioxide Information Analysis Center

CCS is considered to be an intermediate solution in the evolution towards a sustainable energy society (Bachu, 2008; Damen, 2007; Herzog, 2001; Metz et al., IPCC 2005; Riahi et al., 2004; Rubin et al., 2007). Transfer to low or no CO₂ emitting systems should be done before the end of the century.

1.2 Storage opportunities and CCS projects

Concerning the storage of CO₂, there are two main options, which have potential sufficient storage capacities, i.e., geological storage and ocean storage. The first includes the use of depleted gas and oil fields, deep saline aquifers and unminable coal seams. The second option involves large scale transport to the deep ocean, where P, T environments are able to trap CO₂ as a supercritical or liquid zone surrounded by water. This option is out of the scope of the thesis and will not be discussed any further.

Table 1.1: Overview of geological storage options (Metz et al., IPCC 2005)

Storage option	Global capacity (Gt of CO ₂)	Status of CO ₂ injection
Depleted oil and gas fields	675-900	Proven in commercial projects
Deep saline aquifers	At least 1000, but possibly up to 10 ⁴	Proven in commercial projects
Unminable coal seams	3-200	Demonstration phase

The global capacity for each different option can be found in Table 1.1. The estimation for the capacity of storage opportunities is made on the basis of a step procedure (Damen et al., 2003) that is considering:

- A Geographical Information System (GIS) that links high purity CO₂ point sources to oil and gas reservoirs (not more distant than 100 km).
- A multi-criteria analysis, based on source and reservoir characteristics and country specific features.
- A mass energy balance accounting for possible CO₂ stored and gas produced.

1.2 Storage opportunities and CCS projects

- Economic analysis for the determination of CO₂ mitigation costs.

The steps have been chosen based on economic arguments rather than geo-technical information. The estimate of seam storage capacity is between 3 - 200 Gt of CO₂, which is much less when compared to the one offered by the vast potential of aquifers (Metz et al., IPCC 2005). The estimates concerning coal seams are not very accurate due to the complexity of the geological reserve calculations (thickness, lateral continuity, tectonics). Interactions of coal with the gas-water system and behavior under in situ conditions have not been taken into account. If so, the upper estimates could be even lower.

The technique of gas injection in the deep underground has already been developed and used over more than 50 years, mostly in the US, for applications such as steam injection and Enhanced Oil Recovery (EOR) (Bachu, 2008; Moritis, 2006). CO₂-EOR is in use since the early seventies. In 1998 about 60 million m³/day of CO₂ have been injected at 67 commercial EOR projects (Herzog, 2001). Besides commercial projects, there are pilot operations, which are not developed for commercialization and are mainly run by government and research agencies. The final goal of these projects is to acquire technical information on geosequestration processes, technologies and monitoring and economics. Furthermore, they are essential to help informing the public, politics and industry decision-makers in order to provide assurance. Concerning the CO₂ injection in deep saline aquifers, there are projects running since the mid-nineties. In the Sleipner field (North Sea) and at the In Shala project (Algeria), CO₂ and other unwanted gases are separated and re-injected respectively in the upper located Utsira formation and the original reservoir formation (Riddiford et al., 2004; Torp and Gale, 2004). One pilot project run by the industry is ZeroGen in Queensland (Australia), where the goal is to demonstrate power generation from coal with associated CO₂ storage in a deep saline aquifer. This project can be compared with the FutureGen5 project in the USA that will start either in Illinois or in Texas in 2012. Other non-commercial projects of CO₂ storage in the deep saline aquifers are running at Frio in Texas (US), at Ketzin near Berlin (Germany) and at Otway (Australia). In these projects storage characterization and monitoring are the main issues. Comparable, is the K12B gas field (Dutch sector of the North Sea), a semi-commercial program of TNO and GdF. Here CO₂ was separated from the natural gas and re-injected for storage, to keep the reservoir pressure higher and to see whether productivity around the wells and in the reservoir was increased by using CO₂ as a cleaning agent (Cook, 2009; Forster et al., 2006; Horkova et al., 2006; van der Meer et al., 2005).

The only successful project concerning injection of CO₂ in coal bed layers with enhancing the methane extraction (CO₂-ECBM) was run between 1995 and 2001 at the Allison Unit in the San Juan Basin in New Mexico (USA) by Burlington Resources as a pilot for CBM production (Reeves, 2003). However, because of commercial reasons, limited monitoring data is available. Projects with some degree of success have been run in Canada (Fenn Big), Poland (RE-COPOL), China (Qinshui Basin) and Japan (Ishikari Coal Basin) (van Bergen et al., 2006; Gunter et al., 2005; Wong et al., 2007; Yamaguchi et al., 2006). A list of the CCS activities can be found in Table 1.3 and 1.4 at the end of this chapter.

1.3 CCS energy consumption and costs

CCS can be divided into three main activities: capture, transport and injection. The way these activities are developed depends on the CO₂-source (type of coal, pre/post combustion capture, etc.), transportation type and distance and type and characteristic of the reservoirs (Herzog, 2001). Each of these activities contribute to the total energy consumption of the CCS process. The realization of CCS projects is also related to exergy and costs analysis. Exergy analysis investigate the feasibility of the processes by calculating the recovery factor which is the net exergy gain divided by the extracted exergy of the energy resource (Eftekhari and Bruining, 2011). In a standard ECBM case it can be assumed that an injection point is located 100 km away from the CO₂ separation facilities. Furthermore the CO₂ is transported via steel pipelines with the aid of compressor stations and it is injected into a coal seam at the depth of around 1000 m. In this case the exergy consumption in terms of transportation and injection will be about 2000 kJ/kg CO₂ (Eftekhari and Bruining, 2011). Exergy transportation and injection are low compared to the energy consumption for capture and separation. For example, a power plant equipped with a CO₂ separation technology consumes about 10-40% more energy than without capture (Metz et al., IPCC 2005). The CO₂ concentration in the flue gas is typically low, ranging from 3% (in a gas plant) to 15% (in a coal plant). The rest of the flue gas is mainly N₂, H₂O and O₂, with traces of SO_x and NO_x. The high energy consumption concerning the capture are mainly due to the expensive separation technologies in order to strip the CO₂ from the flue gas. Table 1.2 reports the energy required to capture CO₂ per kg of CO₂ produced for different processes.

1.3 CCS energy consumption and costs

Table 1.2: Exergy requirement in the CO₂ capture process. (Eftekhari and Bruining, 2011)

Process	Exergy consumption [kJ/kg CO ₂]	Ref.
Aqueous MEA ¹	3000-7000	Oyenekan and Rochelle (2006)
Chemical absorption	4000-6000	Oyenekan and Rochelle (2006)
MEA ¹	3766	Mimura et al. (1997)
MEA ¹	4200	Chapel and Mariz (1999)
KS-2 ²	2930	Mimura et al. (1997)
Membrane system	500-6000	Brunetti et al. (2010)
Cryogenic	6000-10000	Brunetti et al. (2010)
Wet mineral carbonation	3600	Huijgen et al. (2006)

The cost analysis are complex since new and existing CCS technologies have to be prepared for large mass bulk processes in which globally 0.5 Gt of CO₂ have to be processed per year (IEA, 2007). Besides, the regular known or predictable costs, alternative costs and income have to be expected from governmental regulations and (negative) tax benefits. In 2005 the transportation costs were estimated around \$1 and \$3 per tonne of CO₂ per 100 km of pipeline and costs of injection were estimated at 5-25\$ per tonne (van Bergen et al., 2006). Again the cost associated with capture are high compared to transportation and injection costs, i.e. about 75% of the overall CCS costs. In addition, capture causes an increase of the electricity production costs by 50% (Feron and Hendriks, 2005). Recent results show even higher costs due to escalation in capital and operating costs (Rubin et al., 2007).

If the carbon sinks tolerate NO_x and SO_x, it is possible to eliminate separation steps and sequester an impure CO₂ stream (Herzog, 2001). This may result in a near zero-emission power plant and also will reduce CCS energy consumption for capture. The presence of the impurities is one of the aspects

¹Chemical absorption with a monoethanolamine (MEA) solvent

²Chemical absorption with solvents - sterically hindered amines

that have been taken into account in this thesis.

1.4 Current state of knowledge of gas sorption in coal

The feasibility and economical viability of ECBM depend on geotechnical factors such as texture heterogeneities and coal structure, the transport process in a cleat system, sorption behavior, permeability behavior and the initial amount and composition of the injected fluid, etc (White et al., 2005). With respect to the mentioned processes, the development and implementation of reservoir simulators for ECBM production and CO₂ storage requires detailed and reliable information. Data acquired are often from sample sizes which are representative for a certain volume of coal. Hence, an improved understanding at different scales is important for the accurate prediction of gas and water production rates as well as optimal CO₂ injection rates (Busch et al., 2004).

Coal structure

Coals contain both organic and inorganic phases. The latter consists of minerals such as quartz, clays and pyrite that may have a sedimentological or an authigenic origin. The organic part, defined as macerals, can be divided in three major groups: vitrinite, liptinite and inertinite. The vitrinite group is as 50 to 90 volume percent and has been derived primarily from cell walls and woody tissues. The liptinite group makes up about 5 to 15 volume percent and originates mostly from waxy or resinous plant parts, such as cuticles and spores. Inertinites are derived from strongly oxidized plant material. In essence, the mineralogical structure of coal is considered to be amorphous.

CO₂ can be stored in the coal layers as a free phase, trapped by the impermeable layers of the reservoirs and as an adsorbed phase, on the internal surface of the pore structure. The coal structure can be divided in two distinct porosity systems (Shi and Durucan, 2005): (1) a network of fractures (fracture system) defined as butt cleats and face cleats where the fractures become smaller until they envelope the matrix system and (2) the coal matrix system consisting of a highly heterogeneous pore structure (pore system), which varies from a few angstrom to a micrometer size.

1.4 Current state of knowledge of gas sorption in coal

Transport processes

The transport process of gas is complicated by the heterogeneity of the previously described porous medium and can be divided in two processes at the two different scales that characterize the porous system. The first process, the flow at the cleat scale, is pressure driven and can be described by Darcy's law. The second transport process is controlled by diffusion in the pore system. At this scale also gas storage by physical adsorption occurs (Harpalani and Chen, 1997).

Two decades ago researchers got aware about coal-CO₂ interaction and developed, based on experimental work, complex models on transport processes. One of the models mostly applied is the Ruckenstein's bidisperse (Ruckenstein et al., 1971), which describes the adsorption rate in spherical microporous particles of uniform size embedded in a macroporous particle system. As major contributors in the development of this theory in this field can be mentioned: Ciembroniewicz and Marecka (1993), Marecka and Mianowski (1998), Bustin and Clarkson (1998), Shi and Durucan (2003), Siemons et al. (2003), Cui et al. (2004), Busch et al. (2004), Siemons et al. (2007), Yi et al. (2008), Yi et al. (2009), Fathi and Akkutlu (2009). These studies analyze experimental data on sorption and desorption rates of gases on coal assuming a diffusion process where the gas transport is considered fickian and the geometry of the porous medium is a bimodal pore structure. Other models are summarized in the papers of Bhatia (1987) and King and Ertekin (1995), and recently Wang et al. (2009b). These models are not used in this study and will not be discussed further.

Diffusive transport processes within the coal matrix particles or in the cleat system could be the rate-limiting step for adsorption during gas injection and production operations.

In this thesis we determined the characteristic times for equilibration of gases in the matrix particles.

Swelling effect

Besides diffusion, the volumetric and mechanical effects on the coal structure have to be considered. Sorption of CO₂ and other gases on coal induces gas dependent sorption and swelling. Experimental work showed that this increase in matrix volume has a negative correlation with cleat permeability behavior (Mazumder and Wolf, 2007). Swelling can be measured at a laboratory scale using photometric techniques (Robertson, 2005) or conventional strain

measurement techniques (Levine, 1996; Syed, 2011). Swelling follows the form of the adsorption isotherm and the experimental results can be described using a Langmuir type of curve, showing that adsorption and swelling are positively related. The most commonly used models are from Connell et al. (2010); Levine (1996); Palmer and Mansoori (1998); Pekot and Reeves (2003); Robertson (2005); Shi and Durucan (2003); Wang et al. (2009a). They derive the equations to predict the permeability behavior of a fractured sorptive-elastic media under variable stress conditions. The permeability measurements are obtained in core flooding experiments conducted in the laboratory. These models are derived for cubic or matchstick geometry under uniaxial, biaxial or hydrostatic confining pressures. The models are also designed to handle changes in permeability caused by adsorption and desorption of gases from the matrix blocks.

There is no comprehensive theory in terms of the matrix of coal, i.e. heterogeneity at different scales. Such a theory should include also the ash and maceral composition of coal as mentioned above. Ritger (1987) proposed the use of the theory developed by Thomas and Windle (1982). In this theory the coal is considered to be a glassy polymer, which is transformed to a rubber like polymer after sorption and induces an increase of the diffusion coefficient (Mazumder and Bruining, 2007; Mikelic and Bruining, 2008; Romanov, 2007).

Water effect

Due to its competitiveness in occupying sorption sites, water reduces the gas sorption capacity of the coal. This phenomenon has been already mentioned in many experiments (Busch et al., 2007; Clarkson and Bustin, 2000; Day et al., 2008b; DeGance et al., 1993; Fitzgerald et al., 2005; Goodman et al., 2007; Krooss et al., 2002; Mastalerz et al., 2004; Mohammad et al., 2009b; Prinz and Littke, 2005; Siemons and Busch, 2007). In addition, the CO₂ in such a system will be adsorbed by the coal surface but also by the water. At the same time water will be present in the system as free water and as adsorbed on the matrix. There is a lot of literature concerning the water-CO₂ system. The dissolution of CO₂ in water can be described either using the Henry's law or other models such as the model of Duan and Sun (2003), which is based on a specific particle interaction theory for the liquid phase and a highly accurate equation of state for the vapor phase. Also in this case the effect of water can be predicted based on experimental data but the theory behind this coal-CO₂-water interaction is still not clear. There are still open questions, e.g., how the water competes with the CO₂; the value of the density of water in the adsorbed state; whether if water occupies the same sites as

1.4 Current state of knowledge of gas sorption in coal

CO₂; etc.

Equation of state

The use of an accurate Equation of State (EoS) is important for two aspects:

- to quantify the amount of CO₂ stored in the free phase in the coal layers;
- to measure the excess sorption isotherm with a manometric set up, in order to convert pressures, volumes and temperatures to density values.

The EoS can be divided into two categories (Li and Yan, 2009a), (1) the more general such as the cubic EoS or the virial EoS and (2) the specific ones such as the Span and Wagner for the CO₂ (Span and Wagner, 1996). In the first category the accuracy is lower meanwhile in the second one the accuracy is much higher. However, the latter can only be used for a specific gas by the use of many fitting parameters. The majority of sorption experiments on coal are dealing with pure gases, for which the use of the specific EoS is suggested. If dealing with gas mixtures, as in the case of the experimental work in this thesis, the EoS has to be adapted with the use of mixing rules, which is only possible with the EoS expressed in the general form. In this case the accuracy is again lower than in the case of a specific targeted EoS. The density values cannot be anymore described accurately as in the case of a single gas component. Therefore, the final excess sorption curves can depend on which EoS has been used.

Excess and absolute sorption isotherm

The experimental results on the gas sorption on coal are important for its physical characterization. Therefore, it is essential for the scientific community to have common references in order to allow results to be compared (Gens-terblum et al., 2010, 2009). The excess sorption isotherm measured in the laboratory is used to estimate the amount of CO₂ that can be stored on coal. This curve assumes that the coal volume does not change and that the CO₂ is not occupying any volume when it is adsorbed. These assumptions allow the use of the experimental data without introducing any unknown in the system. However, the excess sorption isotherm cannot offer sufficient information about the total mass of CO₂ adsorbed per unit mass of coal, which is the required information for any further field scale application. The absolute sorption gives such information and can be derived from the excess sorption isotherm.

The only problem to the absolute sorption description is that the void volume accessible to the gas is not any more constant and is changing due to the swelling of the matrix and the volume occupied by the adsorbed phase (Battistutta et al., 2010; Hol et al., 2011; Mohammad et al., 2009a; Romanov et al., 2006; Sakurovs et al., 2009). Hence, we have to assume the density of the CO₂ in the adsorbed phase, because there are no direct measurements.

1.5 research objectives, scope and outline of the thesis

Regarding the physical mechanism of gas sorption in coal, literature shows that results in this field of coal research are little and still many aspects have to be investigated. Experimental sorption data provide insight and give further details to develop more suitable theories. Questions and topics mentioned in the previous section are the base for the research as described in this thesis. Using different experimental set ups and physical models, the influence of the gas sorption on coal by gas types, temperature and time dependency, swelling effects, impurities and water is studied.

All sorption experiments have been conducted using manometric set ups. The manometric method is a common tool for sorption determination in Earth Science and Chemical Engineering; it is based on the principle of mass conservation and the equipment measures pressures, temperatures and volumes of the system. All the experiments have been conducted at pressures ranging up to 160 bar. To improve the quality of the measurements, a mass spectrometer and a density meter have been used.

- In Chapter 2 the sorption isotherms on Selar Cornish coal have been measured for CO₂, CH₄ and N₂, at 318 K and 338 K. All these gases are relevant for the ECBM field, i.e., N₂ and CO₂ are two of the main constituent of the flue gas and CH₄ is the product gas. The measurements have been done at two different temperatures, to test their influence on the equilibration time and the sorption. CO₂ induced swelling and shrinking have been measured on Selar Cornish, at 318 K; the influence of the latter has also been tested on the absolute sorption isotherm.
- In Chapter 3 the sorption isotherms have been measured for CO₂ on dry and wet Tupton coal, at 318 K, checking the relevance of the water in the sorption. The density of the gas phase has been measured using a

1.5 research objectives, scope and outline of the thesis

density meter to test the effect of the water in the gas phase. To estimate the sorption of CO₂ in water, a sorption isotherm has been measured on non adsorptive wet unconsolidated sand. The result was used to check the relevance of the water contribution in the case of wet coal sorption.

- In Chapters 4 two different gas mixtures with NO_x have been used to test the validity of different EoS using experimental data coming from two different experiments. The first is based on void volume measurements between the empty sample cell and the reference cell of the manometric set ups. The second consists of density measurements using a density meter.
- In Chapter 5 the sorption isotherms have been measured on activated carbon at 318 K for the same two gas mixtures mentioned in Chapter 4. The gases concentrations have been measured during the desorption experiments using a mass spectrometer.

Table 1.3: Overview of ongoing CCS projects (Scottish Centre for Carbon Storage, School of Geosciences, University of Edinburgh).

Project	Location	Start up	Injection rate [t of CO ₂ /day]	Storage
Sleipner	Norway	1996	3000	Aquifer
San Juan Basin	USA	1989	277000 total	ECBM
RECOPOL	Poland	2001	15-2	ECBM
Weyburn	USA	2000	3-5000	CO ₂ -EOR
In-Salah	Algeria	2004	5-6000	Gas field
K12B	NL	2004	2-3000	Gas field
Salt Creek	USA	2004	5-6000	CO ₂ -EOR
Snøvit	Norway	2006	2000	Aquifer
La Barge	USA		11000	Gas field
Fenn Big	Canada	test phase		ECBM
Ishikari Coal Basin	Japan	2002	1.8-2.8	ECBM
Qinshui Basin	China	2002	17	ECBM
Ketzin	Germany	2008	82	Aquifer
Frio	USA	2002	-	Aquifer
Nagaoka	Japan	2000	-	Aquifer
Mountaineer	USA	2009	270	Aquifer
Otway	Australia	2005	60	Gas field

1.5 research objectives, scope and outline of the thesis

Table 1.4: Overview of proposed CCS projects (Scottish Centre for Carbon Storage, School of Geosciences, University of Edinburgh).

Project	Location	Start up	Injection rate [t of CO ₂ /day]	Storage
Northeastern	USA	2011	4000	CO ₂ -EOR
Antelope Valley	USA	2012	2-3000	CO ₂ -EOR
WA Parrish	USA	2012	2-3000	CO ₂ -EOR
Hydrogen Energy	USA	2014	5000	CO ₂ -EOR
Tenaska	USA	2015		CO ₂ -EOR
AMPGS	USA	2015	-	-
Kaarsto	Norway	-	3000	CO ₂ -EOR
Mongstad	Norway	2010	270	CO ₂ -EOR
Sargas Husnes	Norway	2011	7000	CO ₂ -EOR
Gorgon	Australia	2011	7000	CO ₂ -EOR
Teesside	UK	2012	13000	-
Aalborg	Denmark	2013	5000	CO ₂ -EOR
Abu Dhabi	UAE	2013	5000	CO ₂ -EOR
Rotterdam	Netherlands	2014	-	-
Huerth	Germany	2014	7000	-
Kedzierzyn	Poland	2014	7000	-
RWE	Germany	2015	-	-
Zerogen	Australia	2015	-	Aquifer
Jansschwalde	Germany	2015	3000	CO ₂ -EOR
Boundary Dam	Canada	2015	3000	CO ₂ -EOR
Nuon Magnum	Netherlands	2015	-	-
Union Fenosa	Spain	2016	3000	-
ENEL CCS1	Italy	2016	3000	-
Green Gen	China	2018	-	-
Energy FutureGen	USA	2012	2700-5500	-

Chapter 2

Swelling and Sorption Experiments on Methane, Nitrogen and Carbon Dioxide on Dry Selar Cornish Coal

Abstract

Sorption isotherms of CO₂, CH₄ and N₂ are determined at 318 K and 338 K for pressures up to 160 bar in dry Selar Cornish coal using the manometric method. Both equilibrium sorption and desorption were measured. The desorption isotherms show that there is no hysteresis in N₂, CH₄ sorption and desorption on coal. The time to achieve equilibrium depends on the gases and is increasing in the following order: He, N₂, CH₄, CO₂. The results show that the sorption ratio between the maximum in the excess sorption N₂:CH₄:CO₂ = 1:1.5:2.6 at 318 K and 1:1.5:2.0 at 338 K. Obtained ratios are within the range quoted in the literature.

Swelling and shrinkage induced by CO₂ injection and extraction from Selar Cornish coal have been measured. The experiments have been conducted on unconfined cubic samples using strain gauges measurements at 321 K for pressures up to 41 bar. It has been found that the mechanical deformation is fully reversible.

The density of CO₂ in its adsorbed phase, has been extrapolated from the

excess sorption isotherm calculated including the swelling. The resulting value is unrealistically high. This can indicate that either the line extrapolation is not a valid method or the model of adsorbate storage is oversimplified. Absolute sorption for CO₂ has been estimated considering also the change in the coal volume due to swelling. The resulting isotherm calculated with or without the swelling is almost the same.

2.1 Introduction

Concerns about global warming generated interest in reducing the emissions of the main greenhouse gas - carbon dioxide (CO₂). Large quantities of CO₂ are produced during the combustion of fossil fuels. Methods intended to reduce CO₂ emission include its storage in geological formations, e.g., saline aquifers and (depleted) gas reservoirs. One of the options is CO₂ injection into underground coal in combination with the production of CH₄ originally present in coal seams. Another idea is to inject flue gas, i.e. a mixture of N₂ and CO₂ (Mazumder et al., 2006a; Reeves, 2001). In these cases N₂ acts as a stripping agent. This technology is known as flue gas-Enhanced Coalbed Methane (flue gas-ECBM) recovery.

The effectiveness of enhancing methane production by CO₂ and/or N₂ depends on the sorption behavior of the main constituents. Therefore, knowledge about sorption behavior of CO₂, CH₄ and N₂ is required. Many experimental dry coal-sorption studies have been published in the last years (e.g., Busch et al. (2007); Chaback et al. (1996); Clarkson and Bustin (1999b); Day et al. (2008a); Gruskiewicz et al. (2009); Majewska et al. (2009); Ottiger et al. (2006); Prusty (2008); Saghafi et al. (2007); Siemons and Busch (2007)). The measurements quantify the sorption capacity of CO₂, CH₄ and N₂ in different kinds of dry coal.

The time required for attaining thermodynamical equilibrium for the gas adsorbed by the coal is an important factor in any *in situ* application. Recent literature stresses the importance of the latter as an essential factor in establishing proper excess sorption isotherms for gases (Day et al., 2008a; Gruskiewicz et al., 2009; Majewska et al., 2009; Prusty, 2008). The equilibration time depends on gas, temperature of the system and the grain sizes of coal used in the experiments. A few authors studied the kinetics of the gas sorption on coal (Busch et al., 2004; Clarkson and Bustin, 1999b; Goodman et al., 2006; Gruskiewicz et al., 2009; Siemons et al., 2003; Solano-Acosta et al., 2004). CH₄ and CO₂ adsorption occurs much faster in fine grained fractions. Siemons

2.1 Introduction

(2003) reported that equilibration time is proportional to the grain size up to 1500 μm ; above it is more or less constant. The grain size used in sorption experiments usually ranges between 63 μm and 2000 μm (Busch et al., 2006) with the exception of the work of Majewska (2009), who used coal blocks. Equilibration times reported by these authors vary between 1 hour to 440 hours. Mazumder (2006) in his coal measured that the cleat spacing in coal is between 500 μm and 5000 μm . In order to maintain the structural integrity of the coal, in this study the chosen particle size is between 1.5 - 2 mm, that leads to long equilibration time.

Sorption/desorption of gases on coal induces a relevant effect on its mechanical structure: the swelling/shrinkage of the matrix. Coal swelling induced by gas adsorption is a phenomenon extensively studied either using optical systems (Robertson, 2005) or strain gauges (Levine, 1996). Literature data concerning experimental results is remarkable and results are relatively consistent amongst different laboratories (van Bergen et al., 2009; Cui et al., 2007; Day et al., 2007; Durucan et al., 2009; Levine, 1996; Mazumder and Wolf, 2007; Pini et al., 2009; Reucroft and Patel, 1986; Robertson, 2005; Shi and Durucan, 2005). CO_2 sorption on coal induces a bigger swelling effect on the coal matrix than CH_4 and N_2 . It has been shown that at high pressure the coal is almost saturated and no sorption and swelling are observed anymore. At pressures above 200 bar, as the rate of change in adsorbed gas content becomes small, matrix compression dominates and can decrease the volumetric strain (Pan and Connell, 2007).

In this study, the isotherm curves of N_2 , CH_4 , CO_2 were determined at 318 K and 338 K for pressures up to 160 bar in dry Selar Cornish coal using the manometric method (Hemert et al., 2009). In here the interest is not yet addressed to the mixed gas sorption but focus on pure gas (de)sorption. The chosen range is representative for *in situ* conditions. In Europe usually seams suitable for CO_2 storage are at depths over 500 meters, with correspondingly high reservoir pressures and temperatures (308-338 K, 60-150 bar).

Swelling/shrinkage measurements have been conducted on Selar Cornish coal with CO_2 using strain gauges on unconfined cubic samples at $T=321$ K up to 41 bar.

Excess sorption isotherms provide insufficient information for ECBM applications because they are considering the void volume that can be occupied by the gas as a constant disregarding that it is reduced by the volume of the gas in its adsorbed phase and by the swelling induced by the gas absorption. Therefore it is preferable to use the absolute sorption isotherm which is the total amount of gas that can be adsorbed per unit mass of coal. The absolute

sorption is considering also the volume occupied by the CO₂ in its adsorbed phase. In this study the absolute sorption has been recalculated considering also the changes in volume of the coal induced by the swelling.

In this study all the experimental results are fitted with the Langmuir model (Sakurovs et al., 2007), which adequately represents gas sorption in coal and provides values of parameters that can be used in many reservoir simulations.

2.2 Experimental method and materials

2.2.1 Sample preparation

Sorption measurements

All experiments are performed with a semi-anthracite, from the Selar Cornish, South Wales Coalfield (vitrinite reflectance is $R_{max}=2.41$). Maceral and ash content are reported in Table 2.1.

For the sorption experiments the stored coal blocks are broken, crushed and then sieved. The fraction between 1.5 and 2.0 mm is used in the study. Sieving was brief in order to avoid dust production. Batches of 50 to 70 cm³ are sealed and stored at about 276 K until used in the experiments. Before placing the sample in the cell, it has been dried in oven for 24 hours at 378 K under vacuum conditions in order to remove all the moisture content. After placing the sample in the cell, at the beginning of each experiment, the cell is evacuated at 322 K for at least 24 hours under vacuum conditions. The sample weights after evacuation are reported in Table 2.3. All gases are supplied by Linde Gas b.v. with the purities and critical constants as specified in Table 2.2.

Swelling measurements

For the swelling experiments coal blocks have been cut to obtain cubic samples with an average dimension of 10x10x10 cm. The selected samples are not presenting any consistent fracture, and are considered to be homogeneous. Gases have been provided by BOC Gases (UK) Ltd; purity of gases is reported in Table 2.2.

2.2 Experimental method and materials

Table 2.1: *Properties of the used U.K. Selar Cornish coal.*

Proximate analysis				
Moisture mass-%	Vol. matter mass-% (w.f.)	Fix. Carbon mass-% (w.f.)	Ash mass-% (d.a.f.)	
0.64±0.04	9.61±0.02	85.37±0.01	4.38±0.06	
Ultimate analysis				
Carbon mass-%	Hydrogen mass-%	Nitrogen mass-%	Sulfur mass-%	Oxygen mass-%
85.2±1.3	3.28±0.03	0.77±0.05	0.92±0.01	5.60±0.01
Microscope analysis				
R _{max} %	Vitrinite vol-%	Liptinite vol-%	Inertinite vol-%	Minerals vol-%
2.41	73.6	24.6	0.0	1.8

Table 2.2: *Critical properties and purity of the gases used.*

Gas	T _c [K]	P _c [bar]	ρ _c [mole/m ³]	Purity [%]
He	5.1953	2.2274	17399	99.996
N ₂	126.192	33.958	11183.9	99.9995
CH ₄	190.564	45.992	10139	99.9995
CO ₂	304.1282	73.773	10624.9	99.9995

2.2.2 Experimental setups

Sorption measurements

For the sorption experiments two setups were used. One of the setups, that has a higher accuracy, is extensively described in Hemert et al. (2009) and is used for the experiments with CO₂. Thus, CO₂ sorption behavior is accurately described in the critical pressure and temperature range. Here we describe the other setup, used for N₂ and CH₄ experiments. The manometric apparatus (Fig. 2.1) consists of 5 stainless-steel cells: two sample cells, two reference cells and one common reservoir. Two sorption experiments can be performed simultaneously in part A and part B of the setup. Pressures are measured using the pressure transducers PTX611 manufactured by Drück. Their accuracy is 0.08% FS. The entire setup is immersed in a water-filled thermostatic bath. The

Swelling and Sorption Experiments of Pure Gases on Coal

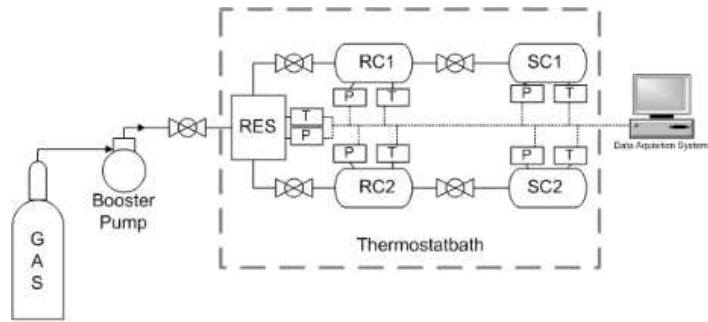


Figure 2.1: *Technical drawing of the manometric set up. RES is the reservoir, RC 1 is the reference cell 1 and RC 2 is the reference cell 2, duplicate of 1, SC 1 is the sample cell 1 and SC 2 is the sample cell 2, duplicate of 1, P indicates the pressure transducers and T are the thermocouples.*

temperature is constant within 0.05 K. Experimental temperatures are determined with a PT100 sensor, manufactured by Automated System Laboratories, with an accuracy of 0.02 K. Thermocouples monitor temperature during the experiments to ensure that the temperature is constant. The PTX611 and the K-type thermocouple were connected to a Keithley KPCI-3108 data acquisition and control card connected to a PC with a 16 channel, 16 bits single ended analog input. The valves are controlled with a PC via the data acquisition and control card. Control of the valves is on a time interval basis. The acquisition software is written in Testpoint V3.4. The acquisition software scans the measurements every second and records them every 10 seconds.

Swelling measurements

For the swelling experiments strain gauges were glued to the coal blocks in order to reveal the microstrain induced by gas injection. The set up used has been provided by the Department of Earth Science and Engineering at Imperial College London. A full description of the equipment can be found in Durucan et al. (2009). Measurements have been performed up to a pressure of 41 bar due to the technical limitations of the used set up.

2.2 Experimental method and materials

2.2.3 Experimental procedure

Sorption measurements

An experiment for sorption measurements consists of four or five consecutive procedures: (1) He leak rate determination, (2) determination of the volume accessible to gas by a He sorption experiment, (3) actual sorption and desorption experiment with CO₂, N₂, or CH₄, (4) control measurement of the He sorption and, if necessary, (5) a second leak rate determination.

The leak rate of helium is determined at approximately 200 bar and at the experimental temperatures of 318 K or 338 K for more than 24 hours. Leakage tests are performed until the influence of leakage is determined to be less than 10⁻⁴ mm³/s. At this stage, leakage is not explicitly considered anymore (Hemert et al., 2009). The setup is evacuated at the experimental temperature for 24 hours before the start of the sorption experiment. A sorption experiment consists of two parts: (1) determination of the sorption isotherm and (2) determination of the desorption isotherm. For the sorption isotherm, gas is added step-wise to the evacuated sample cell until a pressure of 140 to 160 bar is reached. For the desorption isotherm, gas is extracted sequentially from the sample cell until a pressure of 20 to 50 bar is reached. Table 2.3 reports the time lag between each step needed to achieve pressure stability.

Swelling measurements

For the experimental procedure concerning the swelling experiments a full description of it can be found in the article by Durucan et al. (2009). Swelling has been measured using strain gauges placed on a clean and plane surface of the cubic sample. Measurements have been taken from pure gas (Helium and CO₂) injections. For each Helium injection an interval of one hour is respected in order to attain equilibrium. For CO₂ a longer time has been respected, between three to six days. Gas is added step-wise to the sample cell until a pressure of 41 bar is reached. The experiment has been performed inside an oven with a constant temperature of 319.4±0.2 K.

Table 2.3: *Experimental conditions and parameters of the sorption experiments.*

Exp.	T [K]	τ_w [h] ¹	M [g]	χ [-]	ρ_{coal} [g/mm ³]
N ₂	318.20	~10	38.44	6.458±0.005	1.65±0.01
			38.59	7.027±0.004	1.85±0.01
	338.06	~27	31.51	7.034±0.008	1.68±0.01
			35.05	7.015±0.008	1.67±0.01
CH ₄	318.11	~252	35.05	6.995±0.004	1.66±0.01
			31.51	6.979±0.003	1.64±0.01
	338.06	~30	35.05	6.995±0.004	1.66±0.01
			31.51	6.979±0.003	1.64±0.01
CO ₂	318.05	~72	38.17	3.969±0.028	1.38±0.02
			37.78	4.102±0.012	1.33±0.01
	337.55	~72	37.20	4.084±0.002	1.30±0.01

¹ Values reported represent the waiting time respected between each pressure step

2.2.4 Data analysis

Sorption measurements

Accurate values of the excess sorption strongly rely on the use of an accurate Equation of State (EoS). In this study, the equation of state for He published by McCarty (1990) is used. For N₂ and CH₄ the equation of state developed by Wagner and Span (1993) is used. For CO₂ the equation of state developed by Span and Wagner (1996) is used. Equations of state give densities ρ [mol/m³] of the gases as a function of pressure P [bar] and temperature T [K]. The excess sorption m^N [mol/kg] for measurement N is obtained from

$$m_{\text{exc}} = \frac{V_{\text{ref}}}{M} \left[\sum_{i=1}^N (\rho_{\text{fill}}^i - \rho_{\text{eq}}^i) - \chi \rho_{\text{eq}}^N \right], \quad (2.1)$$

where χ is the volume ratio, M is the mass of the sample and respectively ρ_{fill} is the density of the filling phase and ρ_{eq} is the density of the equilibrium phase. The volume accessible to gas in the sample cell, V_{sc} [m³] and the reference cell volumes V_{ref} [m³], are determined using helium expansion. There is no discernible helium sorption effect and it is assumed to be negligible for the determination of χ .

2.3 Results and discussions

$$\chi = \frac{V_{sc}}{V_{ref}} = \frac{\rho_{eq}^i - \rho_{fill}^i}{\rho_{eq}^{i-1} - \rho_{eq}^i}. \quad (2.2)$$

Equation 2.2 is adopted for all the measurements; no leakage was detected during the experiments. Table 2.3 reports all the averaged values of volume ratio obtained in each single experiment including the standard deviation.

Swelling measurements

For the swelling experiments, microstrain are measured using the strain gauges. The coal sample, under hydrostatic gas pressure loading experiences a mechanical deformation in addition to the sorption-induced swelling. The strain associated to the compression can be estimated using Helium experiments, where no sorption is occurring. The strain can be related to pressure by:

$$\epsilon_p = -c_p P \quad (2.3)$$

where c_p [bar^{-1}] is the mechanical compliance coefficient of the sample. The matrix swelling induced by CO_2 injection can then be measured as the net strain between the experimental value and the mechanical compression.

$$\epsilon_m = \epsilon_{exp} - \epsilon_p \quad (2.4)$$

where ϵ_m is the matrix swelling strain and ϵ_{exp} is the measured strain.

2.3 Results and discussions

2.3.1 Equilibration time for the sorption experiments

In total eight sorption experiments were performed. All experiments, except the one with CO_2 were carried out in duplicate. Two sorption experiments have been conducted with N_2 at 318 K and two, always with N_2 at 338 K. In the methane experiments, the temperature for the first two pressure steps was maintained at 318 K. For the following steps the temperature was 338 K. An extra point at 318 K was measured at the last pressure step, before desorption. This procedure was motivated by the long equilibration time needed for CH_4 at 318 K (about ten days). Three experiments were conducted with CO_2 , in the set up with higher accuracy (Hemert et al., 2009); two at 318 K and one at 338

Swelling and Sorption Experiments of Pure Gases on Coal

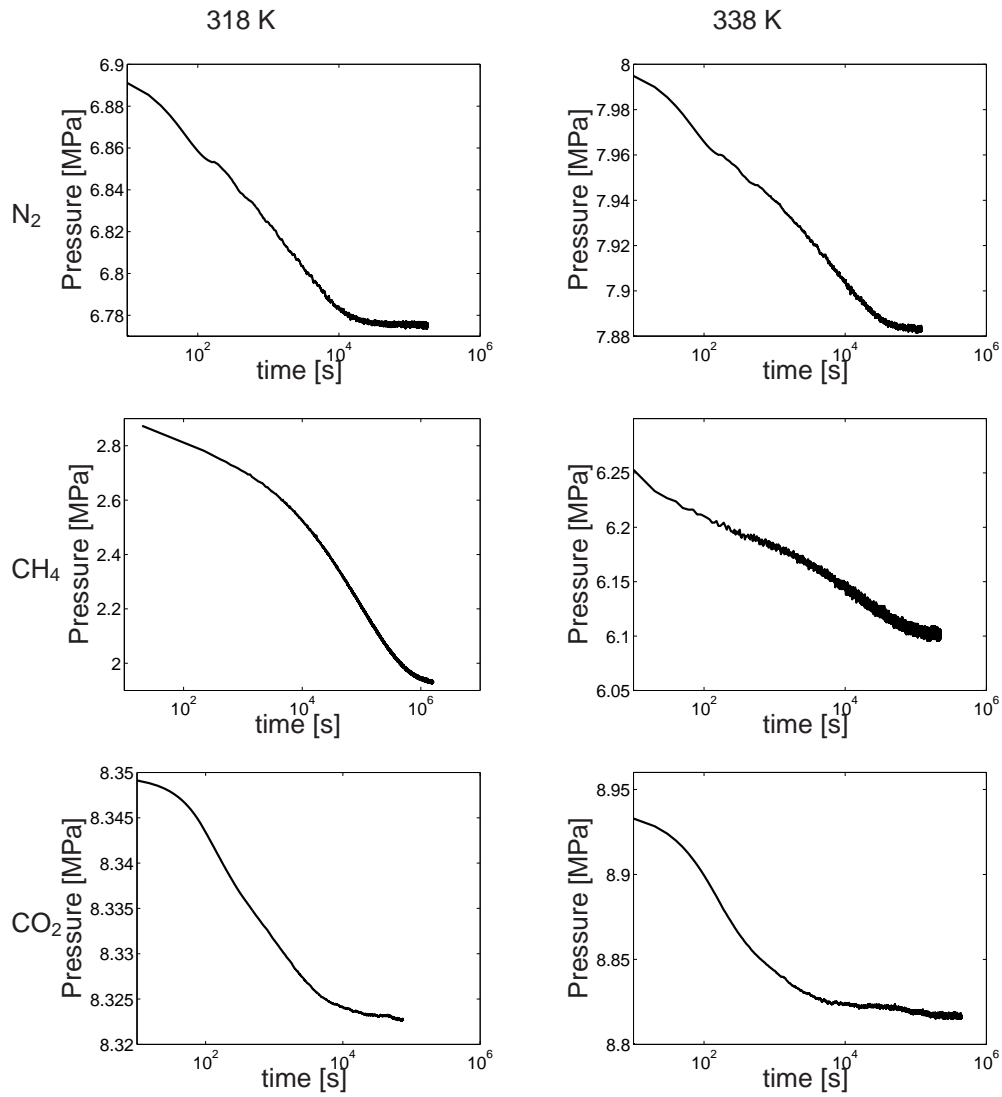


Figure 2.2: Some examples of pressure decrease steps during sorption of N_2 , CH_4 and CO_2 at 318 and 338 K in Selar Cornish coal particles. It is clear that the sorption behavior is different for the different gases and varies with the temperature.

2.3 Results and discussions

K. According to the experimental measurements, the equilibration in the CO₂ experiments was not fully attained.

Equilibration time for each pressure step is obtained from the pressure versus logarithmic time plot. Therefore, the entire pressure plots (Fig. 2.2) are discussed (Clarkson and Bustin, 1999b; Gruszkiewicz et al., 2009). Immediately after adding gas to the sample cell, the pressure transducer shows an increase in pressure caused mainly by an "adiabatic" temperature effect. A combination of adiabatic compression in the sample cell and expansion in the reference cell takes place. Temperature equilibration is fast; then the pressure steadily decreases until equilibrium is reached. This has also been observed by other authors. In order to improve legibility of the plots, the first erratic one hundred seconds of the pressure step are eliminated when necessary, therefore the "adiabatic" effect is not included in the plots.

Figs. 2.2 show the pressure decline history after an adsorption step for N₂, CH₄ and CO₂ at 318 K and 338 K. The logarithmic time scale allows a better assessment of the equilibration time, i.e., the time required to attain a constant pressure value. Proper assessment of the equilibration time after every gas injection step is essential because incomplete sorption results in a non-equilibrated excess sorption curve. In figs. 2.2 CH₄ experiment at 318 K shows the largest pressure decrease. This is so because the Langmuir surface is becoming saturated but also, to a lesser extent, because the difference between the gas in its free phase and the gas in the adsorbed phase is decreasing. For N₂ and CH₄ equilibration times do not change significantly with pressure, but it does change with gas type and temperature (Table 2.3). Helium has, at both temperatures, a short equilibration time (one hour) and is not plotted. CH₄ at a temperature of 318 K has an equilibration time of about 10 days as opposed to the much shorter equilibration time at 338 K, i.e., approximately 27 hours. The equilibration time of N₂ shows much less variation, i.e., 10 hours at 318 K and 27 hours at 338 K. Discussion of possible causes for these differences is outside the scope of this thesis.

CO₂ experiments have been conducted with a fixed interval between each pressure step of 72 hours. Results show that equilibration, after this interval is not fully attained. Equilibration has been checked for a longer time interval for just two pressure steps, during desorption (avoiding the superposition of any possible leak effect on the measurements). Results obtained from these two measurements show that after 2 weeks, CO₂ is still desorbing from coal, at a very low rate.

For the definition of equilibrium, it is very important to consider the set up accuracy and the time scale we are considering. The same results obtained for

Swelling and Sorption Experiments of Pure Gases on Coal

the CO₂ sorption, if plotted on a linear scale, or measured on a less accurate set up, appear to be equilibrated already after a few hours.

Table 2.4: *Literature overview of sorption experiments on different dry coals from other laboratories.*

Author	Grain size [μm]	Temperature [K]	waiting time [hours]
Chaback et al. (1996)	93-300	300-320	6-18
Clarkson and Bustin (1999a)	1840	273	7
Busch et al. (2006)	63-2000	318	1
Goodman et al. (2004)	250	295-328	0.5-12
Siemons and Busch (2007)	200	318	20
Day et al. (2008a)	500-1000	326	4
Gruskiewicz et al. (2009)	1000-2000	308-313	50
Majewska et al. (2009)	20000x20000x40000	298	440
Goodman et al. (2006)	250	328	96
this study	1000-2000	318-338	336

Coal particles with sizes above 0.5 mm are interdispersed with microcleats (Mazumder et al., 2006c) in which diffusion is relatively fast. Therefore, particles above 0.5 mm do not show a large size dependence on equilibration time (Siemons et al., 2003). If coal size particles are below 0.5 mm, the particles between the cleat system are crushed and a much shorter equilibration time is observed as mentioned in other reports (Busch et al., 2004; Siemons et al., 2003; Solano-Acosta et al., 2004).

Our equilibration times are much longer than the one reported in Table 2.4, apart for Majewska et al. (2009) who was working with coal blocks and Goodman et al. (2006) who plotted pressure decrease versus the squared root of time.

The decision of taking big or small grain size needs to be the result of a good compromise between many factors and this will have an important consequence for estimations on a field scale or for obtaining an excess sorption isotherm.

2.3 Results and discussions

2.3.2 Excess Sorption Isotherm

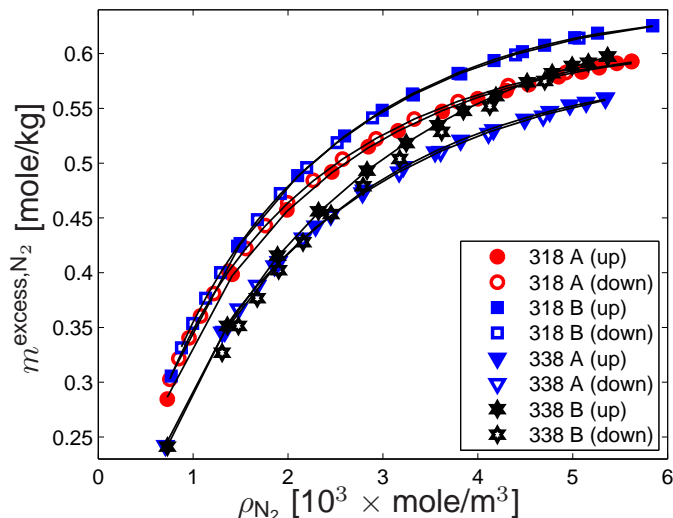


Figure 2.3: N_2 excess sorption on Selar Cornish coal at 318 K and 338 K. All the curves are fitted using the Langmuir model with two free parameters (m_a , the saturation capacity of coal and b_v , the Langmuir equilibrium constant, see Table 2.5).

This section discusses the excess sorption isotherms determined from the mass balance.

Figs. 2.3, 2.4 and 2.5 show the excess sorption isotherm of N_2 , CH_4 and CO_2 .

The N_2 curve does not show a maximum and the isotherm is monotonically increasing. The maximum error for the duplicate measurements is 0.04 mole/kg at 318 K and 0.07 mole/kg at 338 K. The sorption at $\approx 5.5 \times 10^3$ mole/ m^3 decreases from 0.60 ± 0.02 mole/kg at 318 K to 0.53 ± 0.05 mole/kg at 338 K. For a single sample the sorption and desorption curves almost coincide.

CH_4 excess sorption isotherm reaches a maximum of 0.92 at 338 K at high pressures, at 6.2×10^3 mole/ m^3 . The maximum error of the duplicate measurements is 0.01 mole/kg at 318 K and 0.02 mole/kg at 338 K. The sorption at approximately 6.2×10^3 mole/ m^3 decreases from 0.94 mole/kg at 318 K to

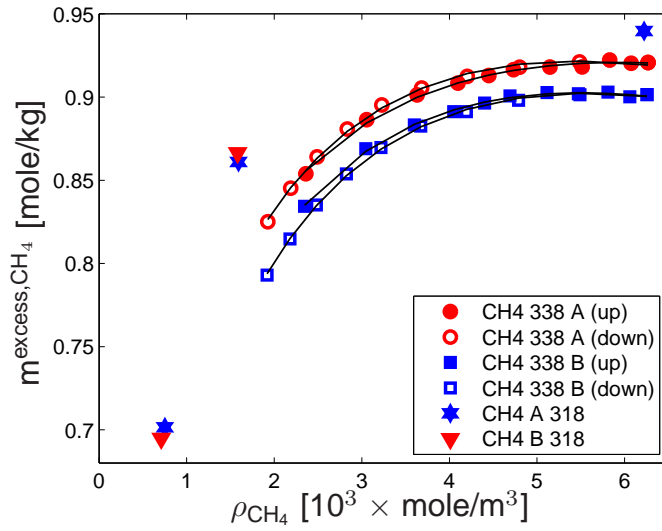


Figure 2.4: CH_4 excess sorption on Selar Cornish coal at 318 K and 338 K. All curves are fitted using the Langmuir model with two free parameters (m_a , the saturation capacity of coal and b_v , the Langmuir equilibrium constant, see Table 2.5). For the 318 K sorption isotherm only three points have been measured.

2.3 Results and discussions

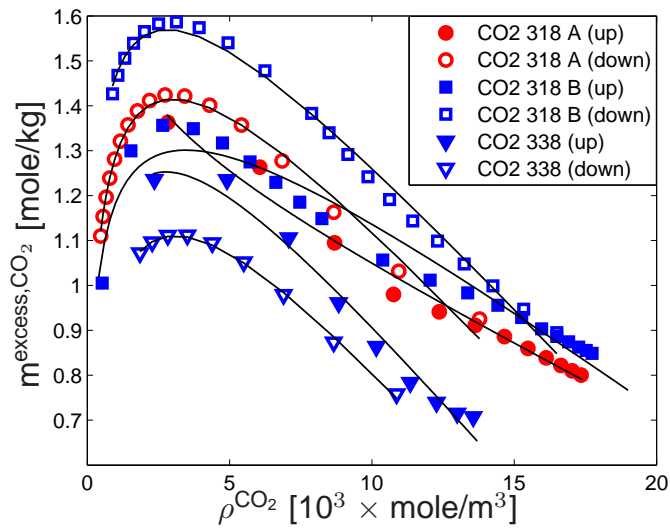


Figure 2.5: CO₂ excess sorption in Selar Cornish coal at 318 K and 338 K. All the curves are fitted using the Langmuir model with three free parameters (m_a , the saturation capacity of coal, b_v , the Langmuir equilibrium constant and ρ_a , the density of CO₂ in its adsorbed phase, see Table 2.5).

0.92±0.01 mole/kg at 338 K. For a single sample the sorption and desorption curves almost coincide.

Fig. 2.5 shows the excess (de)sorption of CO₂ plotted against density of the CO₂ in its free phase. Plotted versus pressure the isotherms cross over; however, plotted versus density they become linear at high density values. The isotherms show a higher excess sorption value than the one calculated for N₂ and CH₄. The desorption isotherm (338 K) in fig. 2.5 is lower than the sorption isotherm. The desorption isotherms (338 K) are higher than the sorption isotherms. The error at 318 K is 0.07 mole/kg for sorption data and 0.2 mole/kg or less for desorption data. The error at 338 K could not be determined as only one curve has been measured. When increasing the temperature from 318 K to 338 K, the estimated sorption maximum at 3.5×10^3 mole/m³ decreases from 1.36±0.03 mole/kg to 1.24 mole/kg. For the desorption isotherm the variation is much bigger. Note that the "318 A up" intersects with other isotherms, which is considered to be caused by an insufficient number of data points at low pressures.

Isotherms increase up to a maximum around $3.4\text{-}5.6 \times 10^3$ [mol/m³], as reported also by Day et al. (2008) and then decrease linearly. The linearity is the result of the free phase density increase which approaches the density of the adsorbed phase. If it were possible to reach higher pressures in the experiment, the density of the free phase would be equal to the density of the adsorbed phase. Thus, an excess sorption would be zero. In the N₂ and CH₄ excess sorption this apparent decrease in the sorption is not visible because the gas density in the free phase is much lower than the gas density of the adsorbed phase.

CO₂ measurements cannot represent an equilibrated excess sorption isotherm. None of the data points in fig.2.5 represent a situation where equilibrium has been attained. Reason to this limitation have been explained in the previous section (see Section 2.3). Measurements on CO₂ are in agreement with the recent literature data (Ottiger et al., 2008; Sakurovs et al., 2007). The grain size distribution is not influencing the excess sorption isotherm but just the equilibration time (Siemons et al., 2003).

The ratios between the maximum in the excess sorption are N₂:CH₄:CO₂ = 1:1.5:2.6 at 318 K and 1:1.5:2.0 at 338 K. This is within the range mentioned in the literature (Busch et al., 2003). The temperature dependence of the N₂ equilibrium sorption is lower than for CO₂ and CH₄.

The hypothesis that sorption on coal is reversible, given appropriate waiting time at each pressure step, is confirmed in the experiment with N₂ and CH₄. There are several reasons that may cause the apparent hysteresis in the CO₂

2.3 Results and discussions

sorption.

- The sample have been dried following a specific procedure (see Section 2.2) but the remaining moisture content in the coal sample actually is not known. The water in the sample is dispersed creating chemical bonds with coal surface. Even a small amount of water then can affect CO₂ sorption kinetics and sorption processes.
- Another reason that can explain the apparent hysteresis might be the insufficient waiting time. In view of the extremely long equilibration times, the reversibility of CO₂ sorption in coal is still an open question.
- The absorption process creates chemical interactions between coal and CO₂ molecules that can be not fully reversible (van Bergen, 2009).

The reversibility of the sorption process is a new observation but results are in agreement with existing literature on activated carbon (Dreisbach et al., 1999; Salem et al., 1998; Sebastian and Jasra, 2005) and with the reversibility of the swelling and shrinkage process caused by the CO₂ sorption and desorption on coal (see section 2.3.3).

In this study the Langmuir (L) isotherm model has been chosen in order to fit our data. The Langmuir equation is based on the concept of an equilibrium between the gas molecules in the adsorbed state at a sorption site and gas molecules in the free gas phase. In order to maintain the linearity in the CO₂ excess sorption isotherm and to lead to a closer connection to the fugacity term, the Langmuir equation was adapted (Sakurovs et al., 2007):

$$m_{\text{exc}} = \frac{m_a \rho_g}{b_v + \rho_g} \left(1 - \frac{\rho_g}{\rho_a} \right), \quad (2.5)$$

where m_{exc} is the excess sorption, m_a is the saturation capacity per unit mass of coal, b_v is the Langmuir equilibrium constant, ρ_a is the adsorbed phase density of the gas and ρ_g is the density of the gas in the free phase. The bracketed term converts to excess sorption (Mavor et al., 2004).

Figs. 2.3, 2.4 and 2.5 show the fitted Langmuir isotherms as drawn lines.

For CH₄ and N₂, Eq.2.5 have been used with two free parameters: m_a and b_v . The densities of the adsorbed phase are assumed equal to the densities of the liquid phase: $25.02 \times 10^3 \text{ mol/m}^3$ and $22.04 \times 10^3 \text{ mol/m}^3$, respectively for N₂ and CH₄ (Sudibandriyo et al., 2003). The resulting averaged parameters are presented in Table 2.5. The Langmuir isotherm show excellent agreement

with the experimental data . The sum of the squared difference of the sorption data with respect to the fitted curve is always equal or less than 0.01.

For the carbon dioxide data, the two parameters fit is not adequate to represent the excess sorption isotherm. This is so because the gas phase density of carbon dioxide in our experiment starts to approach the density of the adsorbed phase. Therefore, the density of the adsorbed phase has been kept as a fitting parameter. Results of the fitted parameters are displayed in Table 2.5 In the literature there is a large variety of densities used (Siemons and Busch, 2007). In the experiments described in this study, the fitted density of the adsorbed phase varies between $21.86 \times 10^3 \text{ mol/m}^3$ and $44.01 \times 10^3 \text{ mol/m}^3$. The density of the gas in its adsorbed phase obtained with the model fitting have been compared with the one extrapolated from the excess sorption isotherm, following the methodology described by Sudibandriyo (Sudibandriyo et al., 2003). Values obtained are in good agreement with the models results. The density of CO_2 in its adsorbed phase measured on activated carbon gives much smaller values, e.g. $22.72 \times 10^3 \text{ mol/m}^3$ (Hemert et al., 2009). The increase in the density of the CO_2 in its adsorbed phase during sorption on coal can be attributed to specific dissolution processes on the coal matrix when CO_2 is in its supercritical phase (Huang et al., 2005).

2.3.3 Swelling measurements

Free swelling has been measured on two different cubic samples of Selar Cornish coal. The strain gauges on one sample are placed over a plane surface and on the other sample are placed on two normal plane surfaces. In total three different linear strains have been measured. Fig.2.6 shows the volumetric swelling (in percentage) of the two different samples of Selar Cornish coal induced by CO_2 injection, at a constant temperature of $321 \pm 0.2 \text{ K}$. The swelling in the two plane is almost the same, which means that the swelling is isotropic for this coal. The volumetric strain is three times the linear strain. The data show that swelling is a fully reversible process, as already noticed by other laboratories (Chikatamarla et al., 2004; Day et al., 2007). Free swelling is proportional to the volume of gas adsorbed and the amount of gas on coal is related to the density by a Langmuir equation. Thus also the swelling effect can be described by a Lanmguir type curve (Levine, 1996), see Fig.2.6. Experimental results have been fitted with a Langmuir type curve .

$$\epsilon_v = \frac{\epsilon_{\max} \rho_g}{b_V + \rho_g}, \quad (2.6)$$

2.3 Results and discussions

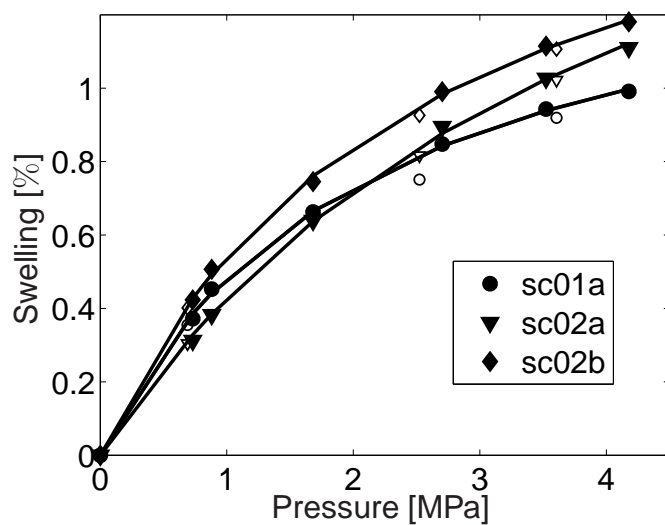


Figure 2.6: Volumetric swelling induced by CO_2 sorption on two different samples of Selar Cornish coal (sc01 and sc02) at 321 ± 0.2 K. Letters a and b in the legend indicate that the calculated swelling is obtained from measurements on two different planes of the same cubic sample. The unfilled symbols represent shrinkage induced by desorption. Experimental results have been fitted with a Langmuir isotherm. Parameters values are reported in Table 2.5.

where ϵ_v is the volumetric swelling, ϵ_{\max} is the maximum volumetric swelling and b_v is the Langmuir constant.

2.3.4 Absolute sorption isotherm

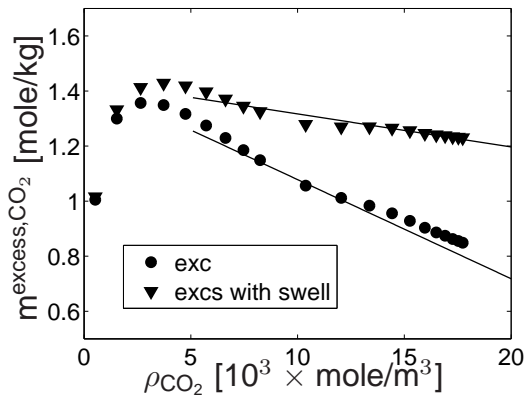


Figure 2.7: Excess sorption isotherm of CO_2 on Selar Cornish coal at 318K. The circles represent the excess sorption considering a constant sample cell volume. The triangles are estimated considering also the change in volume due to the swelling of coal during CO_2 sorption.

For ECBM application the absolute sorption isotherm as well as the excess sorption are of interest. The absolute sorption is the total amount of gas residing in the coal per unit mass, it is taking in account also the gas in its adsorbed phase; this leads to a decrease of the volume accessible to the gas because sorption sites are occupied by the gas after every injection. At low pressure the gas has a substantially lower specific density than the one in the adsorbed phase and the volume of the latter can be neglected. At higher pressure values, the density of the gas in its supercritical phase is of the same order of magnitude of the density of the adsorbed phase. The measurements are affected by the non-ideality of the gas phase and the volumetric effects of the condensed phases (coal swelling, increase of the adsorbed phase volume, etc.) are no longer negligible.

The transformation methods from excess sorption to absolute sorption either

2.3 Results and discussions

use constants ρ_a (density of the gas in the adsorbed phase) or constant V_a (volume of the gas in the adsorbed phase)(Murata et al., 2001). Some authors prefer to develop the isotherm curve from assuming a constant V_a (Ottiger et al., 2006) and some, as in this study, assume ρ_a constant. This leads to the following equation (Mavor et al., 2004):

$$m_{exc} = m_{abs} \left(1 - \frac{\rho_g}{\rho_a} \right) \quad (2.7)$$

The above equation for the absolute sorption isotherm takes into account the gas in its adsorbed phase but it ignores any swelling effect. The absolute sorption isotherm has been rewritten incorporating coal volume changes due to the CO₂ absorption

$$m_{abs} = n_T - \rho_g[V_{sc} - (\rho_a m_a) - (V_0(\epsilon_v + 1))], \quad (2.8)$$

where n_T is the total amount of CO₂ in moles and V_0 is the initial volume of the unswollen coal. Parameters derivation is included in the Appendix A.

In Fig.2.7 plots of the excess sorption are compared. One has been calculated assuming a constant volume accessible to the gas in the free phase and the other one assuming a volume reduction due to swelling. The adsorbed density values have been calculated as described in section 2.3.2. For the case of a constant volume accessible to the gas, the extrapolated value is $\rho_a=42.06 \times 10^3 \text{ mol/m}^3$. For the case of a volume reduction due to swelling, the extrapolated value is $\rho_a=114.03 \times 10^3 \text{ mol/m}^3$. The extrapolated value obtained for the case of a volume reduction due to swelling is unrealistic if it is interpreted as the adsorbed density of the CO₂. Possible reasons for this high values are:

- CO₂ is also affecting the coal structure (absorption)
- It has been assumed that the swollen coal has the same porosity as the unswollen coal, $\phi=0.03$ (Mazumder, 2007)

Fig. 2.8 presents the two absolute sorption isotherms, one considering just the effect of the volume occupied by the gas in its adsorbed phase and the other one including also the effect induced by the swelling of the coal. Using excess sorption data and Eq.3.2 and using excess sorption data with Eq.2.8 leads to the same sorption isotherm. This similarity is the result of the mathematical procedure.

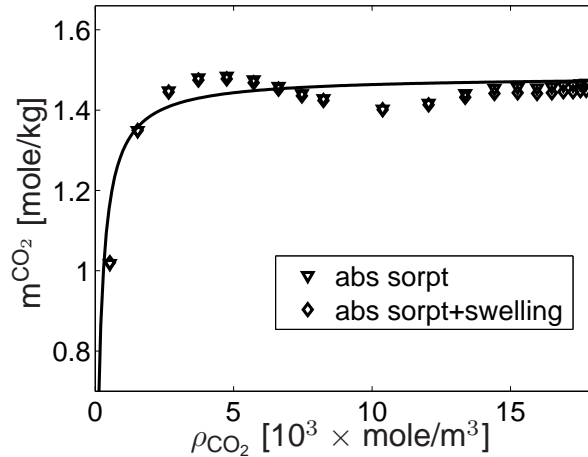


Figure 2.8: Absolute sorption of CO_2 on Selar Cornish coal at 318 K. The triangles represent the absolute sorption curve and the diamonds represent the absolute sorption curve including also the swelling effect. The Langmuir equation is fitted to the absolute sorption isotherm (continuous line), the parameters are displayed in Table 2.5 .

2.4 summary of observations

For the experiments with Selar Cornish coal the following observations are made:

- Experimental results indicate that the time required for attaining sorption equilibrium for N_2 is 10 h at 318 K and 27 h at 338 K; for CH_4 it is 10 days at 318 K and 30 hours at 338 K; for CO_2 it exceeds 72 h at 318 K and 338 K. It has been proved by the experiments that the time required for equilibration varies with the type of gas, temperature. Thus, results are in line with the expectation that during flue gas injection methane is produced first and subsequently nitrogen will reach the production well while carbon dioxide lags behind. In the field case, methane desorbs first as a consequence of its in situ presence and pressure drop near the production well.
- The excess sorption isotherm of nitrogen monotonically increases to a

2.4 summary of observations

maximum of 0.60 ± 0.02 mole/kg at 318 K and 0.53 ± 0.05 mole/kg at 338 K. The excess isotherm of N_2 shows no hysteresis.

- The excess sorption of methane monotonically increases to a plateau of 0.92 ± 0.01 mole/kg at 318 K and 0.94 ± 0.01 mole/kg at 338 K. The excess isotherm of CH_4 shows no hysteresis.
- The excess sorption of carbon dioxide increases with increasing gas density up to a density of approximately 4×10^3 mole/ m^3 with a maximum of 1.36 ± 0.03 mole/kg at 318 K and a maximum of 1.24 mole/kg at 338 K. After the maximum is reached, the excess sorption decreases strongly with increasing density. This behavior is in agreement with recent gravimetric measurements in the literature for CO_2 sorption in coal. The excess isotherm of CO_2 shows hysteresis. Whether this is due to insufficient waiting time after each pressure step or other phenomenon is still an open question.
- Swelling measurements on unconfined cubic samples reveal that CO_2 sorption induces a swelling effect on coal. The phenomenon is fully reversible. Data are fitted with a Langmuir isotherm. Langmuir parameters are: a maximum swelling of $\epsilon_{max} = 1.42 \pm 0.17$ % and a Langmuir constant of $b_v = 1.38 \pm 0.33$ MPa.
- The absolute sorption for CO_2 has been calculated in two different ways. First no correction for swelling was made and the density of the sorbed phase extrapolated from the excess sorption was used in order to obtain the absolute sorption isotherm. In the second case, swelling correction was used and again the extrapolated density of the adsorbed phase was used in a correction factor to convert the excess sorption isotherm to the absolute sorption isotherm. The two absolute sorption isotherms are almost the same. However, the extrapolated density for the swelling corrected case is unrealistically high. The absolute sorption isotherm curve has been fitted with a Langmuir type of curve. The saturation capacity per unit mass of coal is $m_a = 1.8$ mole/Kg and the Langmuir equilibrium constant is $b_v = 3.9 \times 10^3$ mol/ m^3 .

Table 2.5: Langmuir parameters of the different isotherm fitting. ρ_a is the density of the gas in its adsorbed phase, b_v is the Langmuir equilibrium constant and m_a is the saturation capacity per unit mass of coal. The parameters calculated for the absolute sorption are not presented with an error analysis because they were calculated over a single experiment.

	N ₂ ¹	CH ₄ ¹	CO _{2,exc}	CO _{2,abs}	swelling ²
ρ_a [$\times 10^3$ mol/m ³]	25.02	22.04	21.86-44.01	42.06	-
b_v [$\times 10^3$ mol/m ³]	1.33 \pm 0.32	0.34 \pm 0.05	0.37 \pm 0.11	1.8	1.38 \pm 0.17
m_a [mol/Kg]	0.73 \pm 0.04	0.97 \pm 0.01	1.63 \pm 0.18	3.9	1.38 \pm 0.33

¹ the density of the gas in the adsorbed phase has been taken from literature (Sudibandriyo et al., 2003)

² the second parameter of the swelling is not the total mass adsorbed (m_a), but the maximum swelling ($\epsilon_{m.a.x.}$ [%])

2.5 Conclusions

Equilibration time in each of the pressure step in a sorption experiment using a manometric set up can be established when after injection of the gas in the sample cell, there is not any more noticeable change in pressure. To assess it correctly, it is necessary to plot the pressure in a logarithmic time scale. This can be accomplished for N₂ and CH₄. The equilibrium cannot be accomplished for CO₂ due to extremely long experimentation time. For N₂ and CH₄ the excess sorption isotherm does not show any hysteresis. CO₂ excess sorption isotherm shows hysteresis. One of the causes can be ascribed to the insufficient waiting time. Other cause can be the residual water content in the coal sample. Even a small amount of water can affect CO₂ sorption kinetics and sorption processes. Other reason can be ascribed to the fact that during absorption the gas seems to react with the coal molecules creating bonds that could be not fully reversible.

All the excess sorption and desorption isotherms and the swelling/shrinkage measurements can be fitted using a Langmuir curve. The physical meaning of the extrapolated absolute density of CO₂ obtained from the excess sorption isotherm is not clear. This can indicate that either the line extrapolation is not a valid method or the model of adsorbate storage is oversimplified. Other factors, besides coal swelling and the volume of the adsorbed phase, could affect the excess sorption isotherm. Excess sorption data may not provide enough in-

2.6 Acknowledgement

formation to accurately determine all unknowns and explain molecular-scale phenomena.

The free swelling results show that coal swelling accounts for most of the decline in the CO₂ excess sorption at high pressures.

2.6 Acknowledgement

The experiments have been performed under the GRASP (Green-House Gas Removal Apprenticeship) programme. We are really thankful to the Mining and Environmental Engineering Research Group at Imperial College of London and particularly to Sevket Durucan for allowing the internship and Shafiuddin Amer Syed for all the laboratory work concerning the swelling experiments. Experiments of gas sorption on coal have been performed at Dietz Laboratories of TUDelft, we are really thankful to Henk Van Hasten for his technical help.

Chapter 3

Manometric Sorption Measurements of CO₂ on Moisture-Equilibrated Bituminous Coal

Abstract

Gas sorption isotherms have been measured on dry and wet Tupton coal at 318.15 K up to a pressure of 160 bar with the manometric method. The aim of this chapter is to determine the relevance of the presence of water for CO₂ sorption on coal. The manometric method requires an accurate equation of state (EoS). Experimental measurements conducted with a density meter show that the density of the CO₂-H₂O mixture in the gas phase can be calculated using the Span and Wagner EoS for pure CO₂ gas. The density of the CO₂-H₂O mixture in the aqueous phase can be described by a Peng-Robinson-Stryjek-Vera EoS optimized for CO₂-water system. For the interpretation of the coal experiments we also measured the adsorption of CO₂ in a wet unconsolidated sand sample. We show that adsorption experiments follow the computations with the PRSV-EoS. These experiments also allows to determine the partial molar volume of CO₂ in water which agree well with literature data. Given the small amount of water in the coal, adsorption of CO₂ in water only gives a small contribution. For the coal experiments a Monte Carlo simulation has been used

to establish the error on the excess sorption measurements. Errors are ranging from a minimum of 0.6% to a maximum of 4.2%. Comparison of the dry and wet coal samples shows that the presence of 4.6% of water in the coal reduces the maximum sorption capacity by 16%.

3.1 Introduction

In this chapter the sorption of CO₂ on coal under wet conditions has been investigated. Water is always present in coal layers in the deep underground. The water content in coals varies from less than a few percent to more than 70% in brown coals and lignite (Day et al., 2008b). Even if water is withdrawn prior to the ECBM (Enhanced Coal Bed Methane) procedure, it will never be possible to fully dry the coal in situ (Ozdemir and Schroeder, 2009).

The presence of water can affect the sorption capacity of CO₂ because of competitive adsorption of water on the coal surface, though coverage of micropores by water is only a fraction of that found for CO₂ (Busch and Gens-terblum, 2011; Walker et al., 1988). Furthermore, the water molecules form clusters which can obstruct pore access to the CO₂ molecules, though this effect may not be important after proper equilibration (van Bergen et al., 2009). The first accurate experiments measuring CO₂ sorption on coal were mainly dealing with dry coal, but there is an increasing number of papers that deal with wet coal (Busch et al., 2007; Clarkson and Bustin, 2000; Day et al., 2008b; DeGance et al., 1993; Fitzgerald et al., 2005; Goodman et al., 2007; Joubert et al., 1974; Krooss et al., 2002; Mastalerz et al., 2004; Mohammad et al., 2009b; Prinz and Littke, 2005; Siemons and Busch, 2007). The existing literature confirms that the presence of water reduces the sorption capacity of coal.

In dry conditions CO₂ diffuses into the gas field cleat system and is subsequently adsorbed in the matrix. It means that part of the CO₂ will be present as a free phase in the cleat system and part of it as adsorbed in the coal matrix. However in the case of wet coal the system is a 2-phase (liquid and gas) and a 2-component (CO₂ and H₂O) mixture. Therefore, in this case the CO₂ will be present in the system as gas in a free phase or adsorbed on coal and also as dissolved in water. There is a large database concerning the CO₂, H₂O phase diagram (Chapoy et al., 2004; Diamond and Akinfiev, 2003; King and Coan, 1971; Mather and Franck, 1992; Muller et al., 1988; Todheide and Franck, 1963; Wiebe and Gaddy, 1939, 1940, 1941). This experimentally well

3.1 Introduction

defined system leads to numerous theoretical thermodynamic models that are referring to these data bases.

A manometric set up can be used to measure the CO₂ sorption on coal. In presence of water, the gas in the system is a mixture of CO₂ and H₂O. The critical point of the CO₂ can be affected by the presence of water and hence may change the phase behavior in this region due to the impurities (IEA, 2004). Despite the small amount of H₂O present in the gas phase, it is important to check the pressure, temperature and volume behavior. In many papers the resulting excess sorption has been calculated using the Span and Wagner EoS (Span and Wagner, 1996) for pure CO₂. This is because the water in the gas phase is considered negligible (Diamond and Akinfiyev, 2003; King et al., 1992; Spycher et al., 2003).

The majority of experiments do not distinguish between CO₂ adsorption on coal and dissolution in the water. On the other side, the most recent literature (Busch et al., 2007; Fitzgerald et al., 2005; Goodman et al., 2007; Mohammad et al., 2009b) explicitly considers in the calculation also this contribution and splits the CO₂ adsorption into an adsorption part on the water and an adsorption on coal. For the dissolution of CO₂ in water the most commonly used model is the one from Duan and Sun (2003). This model is based on a specific particle interaction theory for the liquid phase. So far none of these articles have obtained direct measurements on the CO₂ dissolution in water.

The aim of this chapter is (1) to add more measurements to the data base, (2) to separate and quantify the contribution of adsorption on coal and dissolution in water and (3) to validate the applicability of the current EoS models to CO₂-H₂O mixtures, both in liquid and gas phase. Indeed the accuracy required in the density measurements using a manometric set up (Hemert et al., 2009) requires to test the adequacy of the Span and Wagner EoS for this gas mixture. Therefore we validated different EoS (Equation of State) for the CO₂-H₂O mixture, measuring the density of the gas using a density meter (DMA 512 Paar) at phase equilibrium at different temperatures and pressures. The excess sorption isotherm of CO₂ has been also measured on the same pressure range and temperature on a moisture equilibrated non-adsorptive medium, e.g. unconsolidated sand. This experiment has been conducted in order to compare the results with different models calculating the CO₂ dissolution in water and also to determine what is the relevance of the CO₂ dissolved in water during the process of CO₂ sorption on wet coal. We measured and compared 5 different excess sorption isotherms on Tupton coal under wet and dry conditions at a constant temperature of 318 K, on a pressure range from 0 to 160 bar.

3.2 Experimental method and materials

3.2.1 Sample preparation

In this study two different adsorbents have been used: coal and unconsolidated sand. Both materials have been granularized and sieved in a range between 1 and 1.5 mm. The unconsolidated sand have been previously dried in the oven for 24 hours at 1273.15 K in order to remove all the organic matter and which may lead to CO₂ sorption. The coal samples used in this study are from a bituminous coal from Tupton, Derbyshire Coalfield, England. Table 1 shows all the characteristic values measured in the laboratory.

Table 3.1: *Properties of the Tupton coal samples used in this study (Siemons and Busch, 2007)*

Grain size [mm]	VRr	Rank	Vitrinite [%]	Inertinite [%]	Liptinite [%]	Ash [%]	Moisture (a.r.) [wt. %]
1.5-2	0.53	hvb C	67.2	22.8	9.2	3.0	13.5

Concerning the experiments on the dry samples, the samples have been previously dried under vacuum in the oven for 24 hours at a temperature of 388.15 K. For the experiments conducted on the moisture samples, both the coal and the unconsolidated sand, have been moisture equilibrated following the standard ASTM D 1412 procedure. Samples were periodically measured until the weight was constant. Equilibration for unconsolidated sand was very fast (less than 1 day), while for coal equilibration took at least one week.

3.2.2 Set up description

In this study two different sets of measurements have been performed.

One set is the sorption measurements. They have been conducted using a manometric set up that has already been described in other articles (Battistutta et al., 2010; Hemert et al., 2009). The manometric apparatus consists of a reference cell and a sample cell, from where gas can be injected or extracted step-wise. All the data processing are based on the principle of mass conservation. Measuring the pressure increase or decrease in the sample cell,

3.2 Experimental method and materials

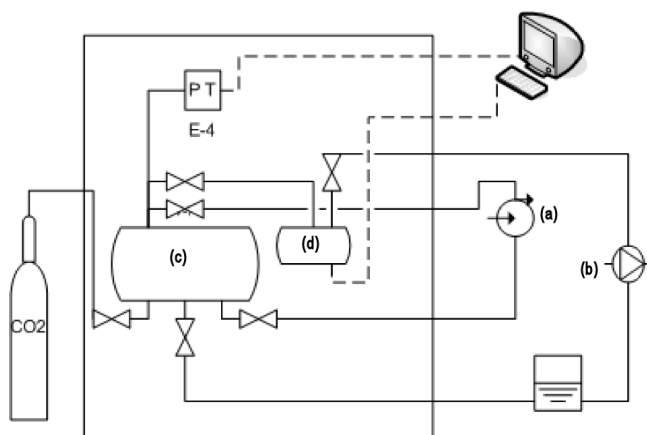


Figure 3.1: The set up for density measurements. The main elements are: (a) the circulating pump; (b) the vacuum pump; (c) the vessel filled with water and CO₂ and (d) the density meter. PT indicates the pressure and temperature sensors. The system is placed in a oven represented by the large rectangle.

makes it possible to determine the amount of gas that has been adsorbed, or desorbed in the porous medium.

The other set concerns the density of the CO₂, H₂O gas mixture measurements. The density has been measured using the set up schematically described in Fig.3.1. The entire set up has been placed in a oven in order to keep the temperature constant. A circulating pump allows to move the fluid in a circular pipe line from and to the vessel. The vessel is connected to the density meter with a valve on top of it. The density is measured with the DMA 512 Paar density meter. The accuracy of the density meter is 10^{-4} kg/dm³. The pressure is measured using a PTX611 manufactured by Drüeck, its accuracy is estimated to be less than 0.1 bar. The temperature is measured with a k-type thermocouple, with an accuracy of 0.02 K. The pressure transducer, the thermocouple and the density meter are connected to a data acquisition and control card connected to a PC. Samples are taken every 10 seconds.

3.2.3 Experimental procedure

Density measurements

The density measurements have been performed on a mixture of CO₂ and H₂O. The final aim is to measure the density of the gas phase. The density of the H₂O-CO₂ in the liquid phase is less relevant for the purposes of this thesis purposes and will be left for future work.

At a first stage the cell has been filled with water. The water has been previously degassed using a vacuum pump and pumped into the vessel. CO₂ has been subsequently injected into the same vessel until reaching the desired range of pressure. The amount of water placed in the system should be enough in order to assure that the gas phase can be fully saturated but at the same time not too abundant in order to reduce equilibration time for the liquid phase. The circulating pump made the mixing of the components more efficient reducing the equilibration time. After 30 hours, when no pressure changes were detected anymore, the system was considered to in equilibrium. At this stage, the valve, placed on the top part of the cell, connected to the density meter was opened. The gas present in the top part of the cell at this stage could flow to the density meter. In order to reduce as much as possible the pressure drop due to the opening of the valve, the pipe line to the density meter has been shortened as much as possible. The length of it is 5 cm. The procedure has been repeated to obtain measurements at different pressures.

Excess sorption measurements

The excess sorption measurements for the dry coal have been taken using the manometric set up with the procedure extensively described in Hemert et al. (2009). The procedure for the wet coal measurements has been modified in order to avoid any moisture loss. The moisture loss has been tested running several times the volume ratio measurements. In a volume ratio experiment, helium is released from the reference cell to the sample cell (or viceversa) to find the volume ratio, which is the ratio between the void volume of the sample cell and the reference cell. In the cases of gas removal, e.g., at the end of the volume ratio measurement, the system has to be evacuated before the injection of CO₂. The water bath is cooled down to 278 K, the temperature decrease reduces the vapor pressure, then the presence of water in the gas phase. The gas is extracted step-wise and passed through a still in order to monitor if any water loss through condensation happens. In this case it is not possible to

3.3 Data analysis

create vacuum conditions, then the system has been evacuated down to the atmospheric pressure and flushed several times with the gas used in the next experiment. Before every experiment temperature has been risen again to 318.15 K. Volume ratio measurements have been conducted repeatedly at the beginning and the end of each set of experiments. All of them showed a constant volume ratio meaning that there is no water loss in the system.

One of the two desorption experiments has been conducted on a wet coal sample. At every pressure step, the evacuation of the reference cell has been done without decreasing the temperature and evacuating the cell under vacuum conditions. In this case there is a partial loss of water from the system.

3.3 Data analysis

3.3.1 Density measurements of the gas mixture

Four different sets of about 30 density measurements have been taken concerning the CO_2 , H_2O gas mixture in four different pressure ranges. Fig. 3.2 shows the experimental values of the density, obtained using the Paar 512 density meter, versus the density calculated using two different EoS; the Span and Wagner EoS for pure CO_2 (S&W) and an optimized Peng and Robinson EoS (PRSV) for CO_2 -water system. The first one (Span and Wagner, 1996) considers the gas as pure CO_2 . The second one takes in account the presence of water in the gas mixture. The CO_2 molar fraction (y_{CO_2}) in the gas phase was always above 99% for the temperature and pressure conditions used in this research. Table 3.2 reports the averaged values of P, T, y_{CO_2} for each of the four single set of measurements. The PRSV equation has been selected because of its successful application in vapor-liquid equilibria (VLE) and liquid-liquid equilibria (LLE) of the same gas mixture (Wahanik et al., 2010). Resulting gas densities have been calculated using the Peng-Robinson-Stryjek-Vera equation of state (Stryjek and Vera, 1986) with the Modified Huron-Vidal second order (MHV2) mixing rule (Dahl and Michelsen, 1990) which is a modification of the Huron and Vidal mixing rule (Huron and Vidal, 1979a). For the calculation of the activity coefficient and Gibbs free energy the Non-Random Two-Liquid (NRTL) activity coefficient model has been used. To correct for the predicted liquid density of the model, the Peneloux volume correction parameters have been applied (Peneloux and Freze, 1982). The accurate description of the model and the parameter values are reported elsewhere (Wahanik et al., 2010). In Fig. 3.2 we apply a linear fitting to the data points. The S&W fitting

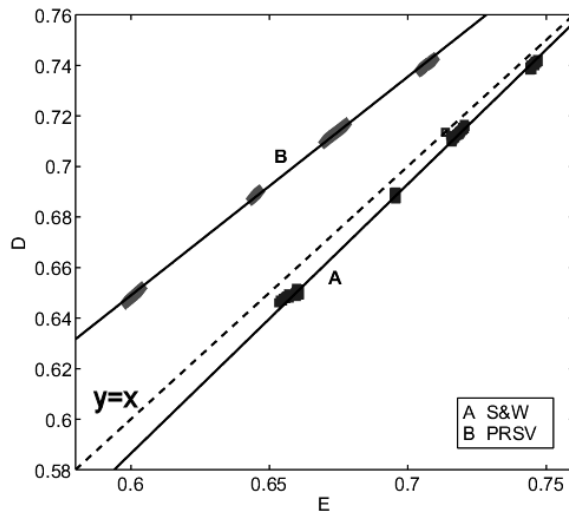


Figure 3.2: Density experimentally determined with a DMA 512 Paar density meter versus the densities calculated with an accurate EoS for CO₂ (A, Span and Wagner, 1996 (Span and Wagner, 1996), B, a modification of Peng Robinson by Stryjek et al., 1986 (Stryjek and Vera, 1986))

is described by the equation $y=1.0332x-0.0297$ and the PRSV is described by $y=0.8383x+0.1479$, where x is the density predicted by the EoS and y is the real experimental value at the same temperature, pressure and composition. As can be observed the S&W EoS performs better than the PRSV EoS. Therefore the Span and Wagner EoS is preferred.

3.3.2 Excess sorption measurements

Five different excess sorption isotherms have been measured on three different samples of Tupton coal (3 adsorption curves and 2 desorption curves). Table 3.3 reports the moisture content in each coal sample.

The water can be present in the sample cell as three different phases: in the aqueous phase, in the gas phase and in the adsorbed phase (Mohammad et al., 2009a). In this study the coal is assumed to be fully saturated with water,

3.3 Data analysis

Table 3.2: Averaged values of pressure, temperature and CO₂ molar composition of the CO₂, H₂O gas mixture. *P* and *T* are determined with the sensors of the set up. The molar concentration of CO₂ in its gas phase (*y*_{CO₂}) has been modeled with the PRSV EoS. Each *P*, *T*, *y*_{CO₂} value averages the four different sets of measurements.

T [K]	P [bar]	<i>y</i> _{CO₂}
319.36±0.02	121.9±0.1	0.9952
319.46±0.02	133.2±0.1	0.9949
319.67±0.02	141.8±0.1	0.9947
319.76±0.02	155.3±0.1	0.9945

Table 3.3: Moisture content of the samples used in this study

sample nr.	moisture content [%]
1	0
2	4.6
3	4.8

due to the procedure used for the coal preparation (ASTM D 1412). No water in the free aqueous phase is assumed to exist.

The void volume can be calculated, using Helium expansion (see Battistutta et al. (2011)), as the ratio between a known volume (the reference cell) and an unknown one, i.e., the void volume of the sample cell and can be expressed as

$$V_{void} = V_{sample} - (V_{adsorbent} + V_{adsH_2O}). \quad (3.1)$$

The results show a constant volume ratio between the sample cell and the reference cell with pressure. This means that (1) helium solubility in water is negligible (2) evaporation of water into helium is negligible (3) water can be considered incompressible in the range of pressure of interest (4) the volume of water in the system does not change with pressure. The presence of water does not influence the calculations of the void volume measurements.

Fig. 3.3 shows the five different isotherms on three different samples of Tupton coal at 318.15 K. In order to convert P,T,V data to densities, the S&W EoS has been used.

As can be observed the dry coal can adsorb more than the wet coal. The presence of 4.6% of water is reducing the maximum capacity adsorption by

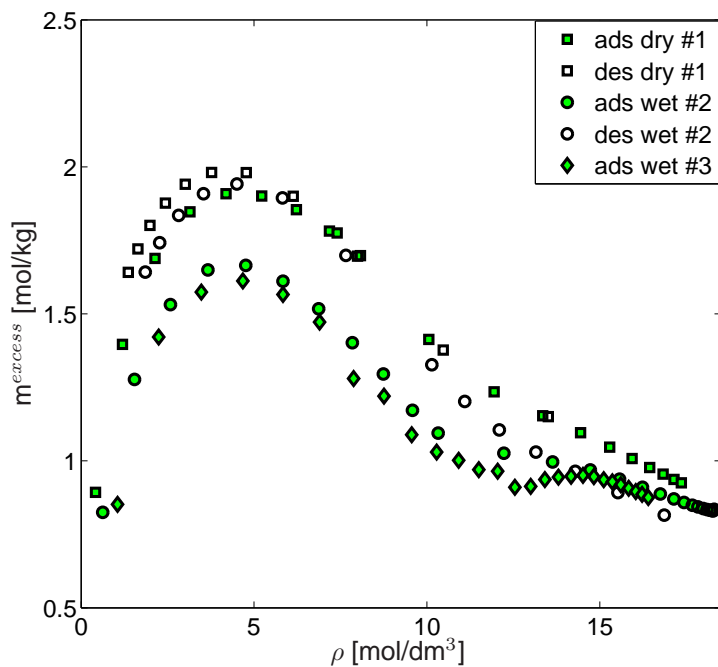


Figure 3.3: CO₂ excess sorption isotherms as a function of gas phase density on Tupton coal at 318.15 K, up to a pressure of 195 bar.

16%. The desorption curve concerning the wet coal (see Fig. 3.3, des wet #2) shows higher values than the adsorption curve. It is asserted that the reason for this is the experimental procedure that we followed. After every equilibrium step, the reference cell was placed under vacuum, like in the standard procedure. The water has been subsequently stepwise removed, restoring sorption sites for the CO₂ molecules. As can be observed, also for the dry coal, the adsorption curve shows lower values for the mass adsorbed than for the desorption curve. There are two reasons for the observed behavior. A reason is that accumulative errors cause this effect. However, the error analysis (as will be further described) shows that this can only be part of the reason. Another reason is that there is irreversible adsorption leaving some residual adsorption

3.3 Data analysis

on the coal.

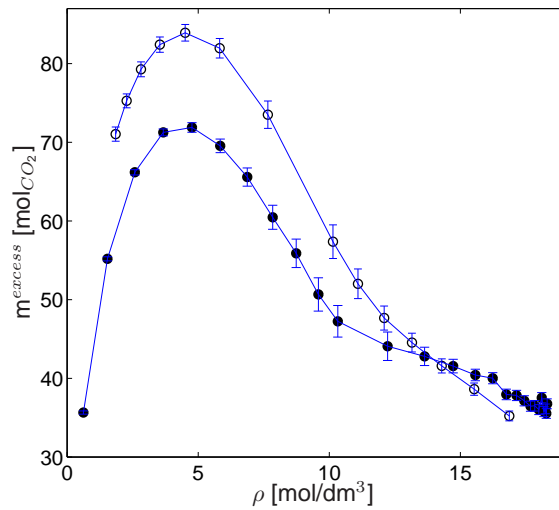


Figure 3.4: CO₂ Excess sorption isotherms on Tupton sample nr.2 with error bar. The full dots are sorption steps. The empty dots are desorption steps.

A Monte Carlo simulation has been derived in order to establish the error on the excess sorption measurements (see Fig.3.4 and the Appendix B for further details). It results that errors are ranging from a minimum of 0.6% to a maximum of 4.2%.

Influence of the moisture content on the measurements

The excess sorption isotherm gives the moles of CO₂ adsorbed per unit mass of coal as a function of density. In the case of wet coal, the excess sorption is defined as the moles of CO₂ adsorbed per the total mass of the sample (coal plus water), see Fig. 3.3.

In order to establish the contribution of water in the CO₂ storage process, a separate sorption experiment using a water saturated unconsolidated sand sample was run. The unconsolidated sand is a non adsorptive medium (see the section concerning the sample preparation), therefore, in this experiment

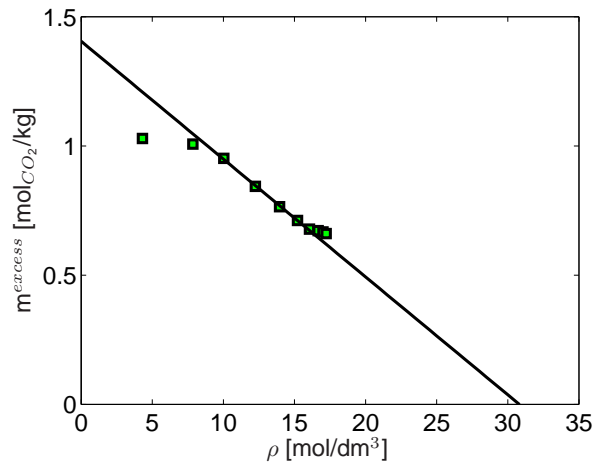


Figure 3.5: CO₂ excess sorption isotherm in water (dissolution) at 318.15 K using an unconsolidated sand sample. The linear part of the curve can be extrapolated in order to obtain the density of the CO₂ in its sorbed state.

all the CO₂ that is not in the free phase is assumed to be dissolved in water. Fujii et al. (2009) have studied the sorption of CO₂ on a sandstone sample. Their results give a maximum sorption of 0.38 mol/kg in a pressure range up to 200 bar at 323 K. Their sandstone has been prepared drying the sample under vacuum at a temperature of 378.15 K. There is no mineralogical analysis of the sample content. However, we still consider the sorption in the sand negligible. All the organic matter present, which is assumed to be responsible for the CO₂ sorption, has been removed heating the sample at a temperature of 1273.15 K. The experiment of this study has been run up to a pressure of 158 bar at a constant temperature of 318.15 K. Fig. 3.5 shows the sorption of CO₂ expressed as excess sorption versus CO₂ free phase density. The extrapolation of the linear part of the curve gives the inverse partial molar volume which can be interpreted as the density of CO₂ in its sorbed phase. By the way the excess sorption is defined it is zero, when the density of the gas in the free phase is equal to the density of the gas in the adsorbed phase. From the extrapolation, the density of the CO₂ in the adsorbed phase is $\rho_a=31 \text{ mol/dm}^3$, which is very close to literature data, which indicate that this density is around 30 mol/dm^3

3.3 Data analysis

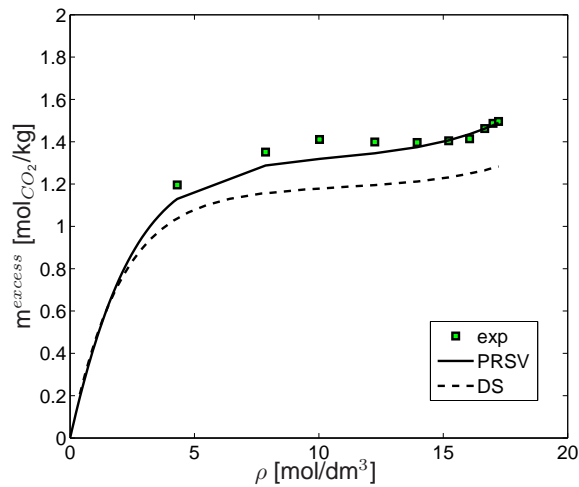


Figure 3.6: CO₂ absolute sorption isotherm on water (dissolution) at 318.15 K using an unconsolidated sand sample. The experimental data (squared dots) have been fitted with the PRSV model (drawn line) and the Duan and Sun model (dashed line).

(Gmelin, 1978).

The absolute density value has been used in order to convert the curve to the absolute sorption isotherm using the following equation (Mavor et al., 2004):

$$m_{exc} = m_{abs} \left(1 - \frac{\rho_g}{\rho_a} \right). \quad (3.2)$$

Fig. 3.6 shows the results. For the calculation of CO₂ dissolution in water, the curve has been fitted with two different models: the PRSV (see the section concerning the density measurements), and the Duan and Sun (Duan and Sun, 2003). Data are in good agreement with the PRSV model.

As the PRSV model is satisfactory for an estimation of the moles of CO₂ dissolved in water, it was assumed that it can be also used for CO₂ dissolved in water in coal. The quantity of CO₂ dissolved in water cannot be measured directly in a coal-CO₂-water system. It was assumed that the amount of CO₂ that dissolves in liquid water is the same as the amount that dissolves in adsorbed water. This assumption (1) disregards any possible change in the water

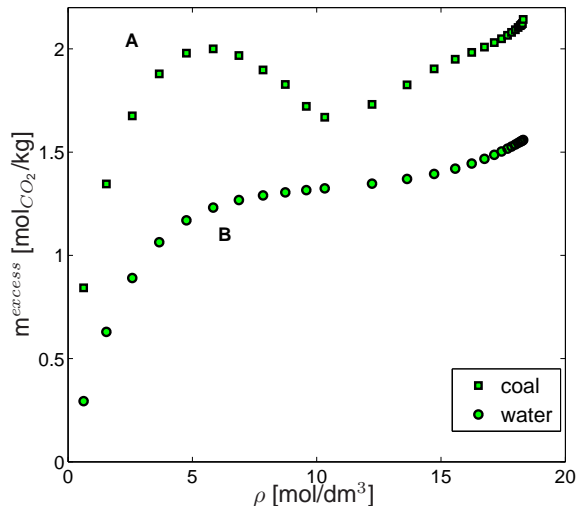


Figure 3.7: Absolute sorption of CO₂ on coal experimentally determined with the manometric set up and absolute sorption of CO₂ in water, obtained from the PRSV model.

properties in its sorbed state and (2) assumes that all the water is accessible to CO₂. Fig. 3.7 shows the absolute sorption of CO₂ on coal on sample 2 (see Table 3.3), using the previously calculated density of CO₂ in the sorbed phase ($\rho_a=31$ mol/dm³). Curve A represents the total moles of CO₂ sorbed per mass of wet coal (coal plus water) calculated using the S&W EoS. This kind of behavior is also reported by other laboratories (Krooss et al., 2002; Pini et al., 2009). One of the possible reasons for this behavior is due to the conversion from excess to absolute sorption. For the conversion, the density of CO₂ in its sorbed phase, which is unknown, is required. The value, in the present study, has been extrapolated from the CO₂ dissolution in water. This value can describe the CO₂ behavior in a condition where no further reaction is occurring between the gas molecules and the sorptive medium, i.e., activated carbon. This is not the case of coal. In Chapter 2, the sorbed density has been determined by fitting the parameters with a Langmuir type of curve. Then the shape was much closer to a Langmuir curve; however it was necessary to use an extremely high density value in order to satisfy the model. It suggests that in the

3.4 Conclusions

coal another mechanism applies. However, we do not know this mechanism yet and therefore we need to leave this for future work. Curve B describes the moles of CO₂ dissolved in water using the PRSV model expressed as moles of CO₂ per mass of water. It can be observed that the two different storage processes, i.e., sorption on coal and dissolution in water, have comparable values. However, the coal sample contains only 4.6% of water. Then for the 43.21 grams of wet coal sample, it is obtained that 71.94×10^{-3} moles of CO₂ are adsorbed on the coal part and 2.86×10^{-3} moles are dissolved in water. In this case the amount dissolved in water is almost negligible. However, the water presence in coal can vary from few percent up to around 70% for a lignite or brown coal. In this case the presence of water would not longer be negligible.

3.4 Conclusions

- It has been experimentally shown that the density of the CO₂-H₂O mixture in the gas phase can be calculated using the Span & Wagner EoS, when the mole fraction of CO₂ is above 99%, i.e., less than 1% of water. The mixture can be treated as a pure CO₂ gas.
- Measured values of the partial molar volume of CO₂ in water agree well with literature data.
- The dissolution of the CO₂ in water can be described using the PRSV (Stryjek and Vera, 1986) with Modified Huron-Vidal second order (MHV2) mixing rule (Dahl and Michelsen, 1990) which is a modification of Huron and Vidal mixing rule (Huron and Vidal, 1979a). For the calculation of the activity coefficient and Gibbs free energy the Non-Random Two-Liquid (NRTL) activity coefficient model has been used.
- A Monte Carlo simulation has been run in order to establish the error on the excess sorption measurements. Errors are ranging from a minimum of 0.6% to a maximum of 4.2%.
- Sorption of CO₂ on wet coal is reduced by the competitiveness of water molecules in occupying sorption sites. The presence of 4.6% of water in the coal reduces the maximum sorption capacity by 16%.

3.5 Acknowledgement

The experiments have been performed under the CATO-2 Program (Dutch national R&D program for CO₂ capture, transport and storage). Experiments of gas sorption on coal have been performed at GeoLab of the Department of Applied Earth Sciences, TU Delft. Many thanks go to Henk Van Asten for his technical support and expertise.

Chapter 4

Adequacy of Equation of State models for Determination of Adsorption of Gas Mixtures in a Manometric Set Up

Abstract

In Enhanced Coal Bed Methane (ECBM) usually CO₂ mixtures containing impurities such as NO_x, etc., are injected in the coal layer. This chapter investigates the adequacy of different Equations of State (EoS) for the determination of adsorption of gas mixtures in a manometric set up.

The viability of these EoS has been investigated by performing experiments in a reference cell and an empty sample cell at a constant temperature of 318.15 K. From these measurements we derive the volume ratio of these cells. A variety of EoS and mixing rules have been used to validate whether they can be applied, i.e., lead to the correct volume ratio. It is shown that for a He rich mixture (98% He, 1% O₂ and 1% NO₂) it is possible to use the McCarty EoS for pure Helium for this purpose but that none of the other EoS, including mixing rules, give acceptable results. With the use of the McCarty EoS, the maximum relative difference from the experimentally determined density is of $6 \cdot 10^{-3}$.

For a CO₂ rich mixture (97% CO₂, 1% He, 1% O₂ and 1% NO₂) none of the investigated EoS and mixing rules can be applied. Therefore, an experimental stepwise procedure based on the volume ratio measurements has been presented, to obtain correct density values with an error between 0.033% for high densities to 0.85% for low densities.

4.1 Introduction

A manometric set up can be used to determine sorption of gases on coal. To obtain a sorption isotherm with a manometric set up an accurate EoS to convert pressure and temperature data to densities is required.

In our previous experiments in the Dietz Laboratory, it has been investigated the sorption of pure gases such as CO₂, CH₄, He, N₂ on coal, for which an accurate Equation of State is usually available (Hemert et al., 2009). However impurities are always present in CO₂ streams coming from flue gas even after separation processes (Metz et al., IPCC 2005). Description of the possible post treatments of flue gas can be found in many articles (Cosam and Eiber, 2007; Li and Yan, 2009b; Li et al., 2009; Liu and Shao, 2010; Sass et al., 2005). In practice usually some NO_x remains (in a ppm range) and therefore CO₂ with minor impurities is injected in the coal layer.

The sorption behavior of gas mixtures on an adsorbate using a manometric set up has been already investigated. citeStevenson1991 and Zhou et al. (1994) focused on the development of an accurate EoS in combination with a mixing rule using experimental data. Other authors use conventional EoS in combination with mixing rules for the manometric set up to obtain adsorption data for binary and ternary mixtures of CO₂, N₂ and CH₄ (Fitzgerald et al., 2005, Mazumder et al., 2006b, Hall et al., 1994, Busch et al., 2007, Chaback et al., 1996, Arri et al., 1992, DeGance et al., 1993). However the adequacy of these EoS needs to be validated.

Mazumder (2006) studied the preferential sorption of a flue gas on coal by using a manometric set up. Here the preferential sorption of the components was quantified. However, the results based on the gas chromatographic analysis were not verified by theory using an accurate EoS.

In the storage phase, streams containing impurities have different physical properties and geochemical reactivity when compared to a pure CO₂ gas phase (Report IEA, 2005). CO₂-ECBM is an expensive technology due to the high costs of CO₂ purification. An option to reduce separation costs would be to inject the flue gas directly as an untreated mixture in deep coal seams (Wong

4.2 Theory

et al., 2000). Therefore, it is important to quantify the adsorption isotherm of a gas mixture on coal at a specific temperature. The purpose of this study is to investigate the effect of NO₂ in the gas mixture on the density calculations.

The manometric set up poses an high demand on the accuracy of the EoS. There are specific EoS such as the Span and Wagner EoS for pure CO₂ (Span and Wagner, 1996) and both for pure N₂ and pure CH₄ the Wagner and Span EoS (Wagner and Span, 1993) and for He the McCarty EoS (McCarty and Arp, 1990). These equations are very accurate and precise due to the fact that they use a large experimental data set, which make it possible to determine a large number of parameters. These equations cannot be used for mixtures. One approach to mixtures is to use a cubic EoS such as Soave Redlich Kwong (SRK) (Soave, 1972) or Peng and Robinson (PR) (Peng and Robinson, 1976) with appropriate mixing rules. There are many mixing rules for the cubic EoS (Valderrama and Silva, 2003) all of them based on the classical Van der Waals mixing rule (Kwak and Mansoori, 1986). They require extra information about the gases used in the mixtures such as the thermodynamic properties of the critical point, the Mathias Copeman coefficients (Mathias and Copeman, 1983) and the binary interaction parameters. Equations such as SRK and PR EoS are useful for industrial purposes and for hydrocarbon recovery but may not be suitable for other purposes (Agarwal et al., 2001a,b).

One of the purposes of this paper is to investigate whether the density obtained using such a specific EoS in combination with any of the mixing rule is accurate enough for manometric adsorption measurements.

This procedure has been illustrated by using two different mixtures: the first one is composed of 98% He, 1% O₂ and 1% NO₂; the second mixture is composed of 97% CO₂, 1% He, 1% O₂ and 1% NO₂.

4.2 Theory

In the following the applied EoS and mixing rules to compute density of the gas mixtures at a given temperature and pressure are given. The cubic EoS can be represented in a general manner by (Panagiotopoulos and Reid, 1986)

$$P = \frac{RT}{v - b_m} - \frac{a_m}{v^2 + uvb_m + wb_m^2}, \quad (4.1)$$

where, for the Soave-Redlich Kwong (SRK) EoS, $u=1$, $w=0$ and, for the Peng and Robinson (PR) EoS, $u=2$, $w=-1$. We used T [K] to denote the absolute

temperature, R is the gas constant [8.314 J/mol K], P is the pressure [Pa] and v is the specific molar volume [m³/mol].

The cubic EoS can also be applied to mixtures by introducing mixing rules. These so-called mixing rules have been modified with respect to the Van der Waals mixing rule and can be expressed as follows (Kwak and Mansoori, 1986)

$$a_m = \sum_{i=1}^{N_c} \sum_{j=1}^{N_c} x_i x_j a_{ij}, \quad (4.2)$$

$$b_m = \sum_{i=1}^{N_c} \sum_{j=1}^{N_c} x_i x_j b_{ij}, \quad (4.3)$$

where a_m accounts for the molecule-molecule interactions and b_m for the hard-core volume in the mixture. The force parameter, a_{ij} , and the volume parameter, b_{ij} , are expressed by

$$a_{ij} = a_i a_j (1 - k_{ij}), \quad (4.4)$$

$$b_{ij} = \frac{b_i + b_j}{2}. \quad (4.5)$$

The binary interaction parameters k_{ij} can be obtained by fitting to phase equilibrium data of the specific mixture. For the PR EoS (Peng and Robinson, 1976) the parameter b_i is independent of temperature and can be calculated knowing the critical point of each gas component, i.e.,

$$b_i = 0.07780 \frac{RT_c}{P_c}. \quad (4.6)$$

For the SRK EoS (Soave, 1972) b_i can be expressed as

$$b_i = 0.008644 \frac{RT_c}{P_c}. \quad (4.7)$$

For the determination of the parameter a_i the temperature dependence is incorporated according to Mathias and Copeman (Mathias and Copeman, 1983), i.e.,

$$a_i = a_{ci} \beta_i(T), \quad (4.8)$$

where for the PR EoS

$$a_{ci} = 0.45724 \frac{R^2 T_{ci}^2}{P_{ci}}, \quad (4.9)$$

4.2 Theory

and for the SRK

$$a_{ci} = 0.42188 \frac{R^2 T_{ci}^2}{P_{ci}}. \quad (4.10)$$

The effect of the temperature is described by

$$\beta_i(T) = [1 + c_{1i}(1 - T_{ri}^{0.5}) + c_{2i}(1 - T_{ri}^{0.5})^2 + c_{3i}(1 - T_{ri}^{0.5})^3]^2, \quad (4.11)$$

where c_{1i} , c_{2i} and c_{3i} are reported in Table 4.1. In the case of helium and NO_2 no coefficients are available, the Mathias Copeman coefficients have been replaced by the acentric factor. In this case $c_{2i}=c_{3i}=0$ and

$$c_{1i} = 0.48 + (1.574\omega) - (0.176\omega^2), \quad (4.12)$$

for the SRK EoS and

$$c_{1i} = 0.37464 + (1.54226\omega) - (0.26992\omega^2), \quad (4.13)$$

for the PR EoS; ω is the acentric factor. The experimental temperature divided by the critical temperature T_{ci} (see Table 4.2) of each component i is called the reduced temperature and is denoted as T_{ri} .

To improve the description of the interactions Panagiotopoulos et al.(1986) and Kwak et al.(1986) proposed to make the interaction parameter k_{ij} composition dependent, i.e.,

$$k_{ij} = \delta_{ij}x_i - \delta_{ji}x_j. \quad (4.14)$$

For a number of mixtures, values of the parameter δ_{ij} can be found. If no literature data exist, the value can be estimated by the modified Chueh-Prausnitz equation (Chueh and Prausnitz, 1967)

$$\delta_{ij} = 0.018 \left(1 - \frac{2V_{ci}^{\frac{1}{6}}V_{cj}^{\frac{1}{6}}}{V_{ci}^{\frac{1}{3}} + V_{cj}^{\frac{1}{3}}} \right)^6, \quad (4.15)$$

where V_{ci} is the critical volume of component i (see Table 4.2).

Peneloux and Freze (1982) introduced the so-called volume shift approach to improve the performance of both the SRK and the PR EoS. In this approach the so-called pseudo molar volume is calculated as follows

$$v = \bar{v} + \sum_{i=1}^{Nc} x_i c_i, \quad (4.16)$$

and

$$b_m = \bar{b}_m + \sum_{i=1}^{Nc} x_i c_i, \quad (4.17)$$

where $c = \sum_{i=1}^{Nc} x_i c_i$ is the volume correction dependent on the mole fraction x_i of each gas component. The values of c_i are found by optimizing Eq. 4.22 (see below).

Not all systems can be properly described using the classical mixing rules. Therefore, mixing rules have been developed that make use of the so-called g^E (excess Gibbs free energy) models for the determination of the parameter a_m of a mixture.

In this way a more accurate description of experimental phase equilibrium data could be achieved. Just as for the equations of state, a high number of g^E models exist. Only the UNIFAC g^E model (Fredenslund et al., 1977) is predictive. The combination of the Soave-Redlich Kwong EoS with the new kind of mixing rule and the UNIFAC g^E model gives the so-called Predictive Soave Reidlich Kwong EoS (PSRK) EoS (Holderbaum and Gmehling, 1991; Huron and Vidal, 1979b).

The UNIFAC g^E model is a so called group contribution model, thereby, it is assumed that the components are comprised of so-called functional groups. Further, it is assumed that the interaction between the functional groups are always the same, no matter in which component the functional group occurs.

The PSRK EoS is calculated using the following expression

$$\frac{a_m}{b_m RT} = \sum_{i=1}^{Nc} x_i \frac{a_i}{b_i RT} + \frac{1}{A} \frac{g_0^E}{RT} + \left(\sum_{i=1}^{Nc} x_i \ln \frac{b_m}{b_i} \right). \quad (4.18)$$

More details can be found in the Appendix C. The limitation of this model is that it is targeted for hydrocarbons (Chen et al., 2002).

4.3 Experimental method and materials

4.3.1 Gas mixtures

Two mixtures have been chosen for the experiments: the first one is a so-called He mixture composed of $97.94 \pm 0.04\%$ He, $0.996 \pm 0.04\%$ O₂ and $1.03 \pm 0.04\%$

4.3 Experimental method and materials

Table 4.1: *The Mathias Copeman coefficients (c_1, c_2, c_3), the acentric factor (ω) and the parameters R_k and Q_k for each gas component.*

Gas	c_1 (SRK)	c_2 (SRK)	c_3 (SRK)	ω	R_k	Q_k
CO ₂	0.867	-0.674	2.471	0.2236	1.3	0.982
He	-	-	-	-0.39	0.885	0.985
O ₂	0.545	-0.235	0.292	0.0222	0.733	0.849
NO ₂	-	-	-	0.849	1	1.1

NO₂; the second is a so-called CO₂ mixture composed of 96.99±0.04% CO₂, 1±0.04% He, 1.003% O₂ and 1.007±0.04% NO₂.

The first mixture has been introduced to test the procedure with a rather simple example. The second mixture is representative for the flue gas after removing N₂ which is commonly done to reduce the volume of the exhaust stream. The concentration of NO₂ in the gas mixture is much higher than in practice because the purpose of this study is to investigate the effect of NO₂ in the gas mixture on the density calculations. The gas mixture contains NO₂ and not NO, which is also one of the primary combustion products in the flue gas. This is due to the fact that NO is very reactive and in the presence of oxygen it reacts to NO₂ according to the reaction



This also motivated the choice of including O₂ in the mixture.

All the gases, including the mixtures, have been provided by Linde gas. Critical properties of the components have been summarized in Table 4.2.

Table 4.2: *Critical properties of the components used in this study.*

Gas	T_c [K]	P_c [bar]	V_c [cm ³ /mol]
CO ₂	304.1282	7.3773	94
He	5.1953	0.2274	57.3
O ₂	154.58	50.45985	73.4
NO ₂	431.35	101.33	82.49

4.3.2 Experimental procedure

Volume ratio measurements

The manometric apparatus consists of a reference cell and a sample cell, from where gas can be injected or extracted step-wise. All the data processing are based on the principle of mass conservation. In this work the manometric set up has been used for the determination of the density of a gas mixture from pressure and temperature data using the separately measured volume ratio, i.e., the ratio between the sample cell and the reference cell. The system used in this study is built as a duplicate set up, meaning that there are two set ups running in parallel using the same thermostatic bath. The manometric apparatus used in these experiments has been already described in Chapter 2. The accuracy of the pressure measurements is below 0.1 bar and for the temperature is 0.02 K. In this section the experimental procedure is described. Volume ratio measurements consist of two consecutive procedures: (1) He leak rate determination, (2) determination of the volume accessible to the gas.

The first procedure is done in order to ensure that the set up is leak free. Therefore, the system is filled with He up to approximately 200 bar at the temperature of the experiment (318 K). Then the pressure drop in the system is monitored for the next 24 hours. Leakage test are performed by observing the pressure decline. The leakage rate has been measured as

$$k = \frac{V_{cell}}{t} \ln \frac{P_i}{P_0}, \quad (4.20)$$

where t is the duration of the leakage test, P_0 is the initial pressure value and P_i is the final one. An acceptable leakage rate is when it is less than 10^{-4} mm³/s (Hemert et al., 2009).

After the leak rate test the set up is evacuated at the experimental temperature for 24 hours before the start of the actual volume ratio experiment. The sample cell is empty and no sorption occurs in the system. Gas can either be added step-wise to the evacuated sample cell until a pressure between 140 and 160 bar is reached. Viceversa, gas can be extracted step-wise starting around 150 bar until a pressure of 20-30 bar is attained. Every new step has been initiated after equilibrium has been attained. The criteria for equilibrium can be found in Chapter 2. In this set of experiments the equilibration time is very fast because no sorption occurs inside the empty sample cell.

4.4 Volume ratio measurements using a Helium mixture

4.3.3 Data analysis

Volume ratio measurements using Helium

The volumes of the reference cell and the sample cell are constant, e.g., we assume they are independent of temperature and/or pressure. Thus, the volume ratio, χ , is also constant. However, due to the compressibility of gases, the amount of gas in the reference cell and sample cell varies with temperature and pressure. This can be expressed in terms of densities using a mass balance, i.e.,

$$\chi = \frac{V_{sc}}{V_{ref}} = \frac{\rho_{eq}^i - \rho_0^i}{\rho_{eq}^{i-1} - \rho_{eq}^i}. \quad (4.21)$$

where V_{sc} is the volume of the sample cell, V_{ref} is the volume of the reference cell and ρ_0^i is the density of the gas during the filling of the reference cell (or depletion, depending of whether we are increasing or decreasing the pressure in the system). The density of the gas after the equilibration steps is denoted by ρ_{eq}^i . The volume ratio (Eq. 4.21) can be accurately measured using He because the density of He can be described by a highly accurate EoS (Mcarty, 1990). The results show a constant value for the volume ratio (see fig. 4.1). A probability plot of the data set (fig. 4.2) shows that system A has a volume ratio of $\chi_A=9.741\pm 0.022$ and system B has a volume ratio of $\chi_B=9.573\pm 0.020$. The volume ratio obtained with this set of measurements will be used as a reference for the other experiments.

4.4 Volume ratio measurements using a Helium mixture

After testing the accuracy of the measurements of the volume ratio between the empty sample cell and the reference cell using pure helium, the experiment can be repeated using other gases (or gas mixtures, as in this case). The values for the volume ratio obtained using other gases can be compared with the one obtained with the pure helium measurements. This method allows testing the accuracy of each specific EoS. The void volume measurements have been repeated using a mixture of 98% He, 1% O₂ and 1% NO₂. Different EoS and mixing rules have been tested in order to establish whether they can be used to determine the correct volume ratio. Based on these calculations

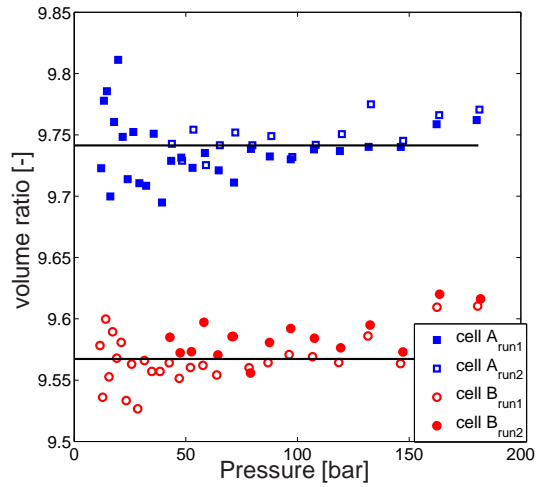


Figure 4.1: Volume ratio of the sample cell and reference cell A and of the duplicate reference cell and sample cell B deduced from Eq 4.21 using the McCarty EoS for pure Helium. The experiments have been repeated twice (with open symbols and full symbols indicating the two separate experiments) using pure Helium.

4.4 Volume ratio measurements using a Helium mixture

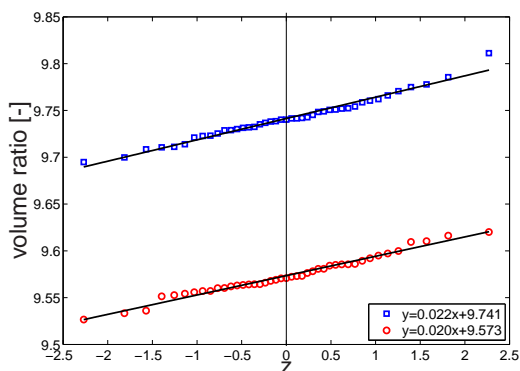


Figure 4.2: Probability plot obtained using the measured volume ratio data from system A (9.741 ± 0.022 , open squares) and from system B (9.573 ± 0.020 , open circles). The obtained values are plotted versus the variable Z in its standard normal form. The average is obtained for $z=0$ and the slope is equal to the standard deviation.

and experimental data from runs with pure helium, see Section 4.3.3, it can be identified which EoS can be used for manometric sorption studies.

The McCarty (McCarty and Arp, 1990), the PR (Peng and Robinson, 1976) and the SRK (Soave, 1972) EoS were used to obtain the molar density of the gas mixture from pressure and temperature data. As a first estimate the presence of O_2 and NO_2 was omitted, i.e., assuming that the gas consists of pure He. The resulting volume ratios as function of pressure are given in Fig. 4.3. The McCarty EoS for pure He predicts the volume ratios for pressures higher than around 50 bar correctly. However at lower pressures the predicted volume ratio is too low. The PR EoS generally performs poorly. At low pressure (< 50 bar) the computed volume ratios are lower than the experimentally determined. For higher pressures (> 50 bar) the calculated volume ratios are significantly higher than the experimentally determined ones. The volume ratios computed with the SRK EoS show in general the same behavior but with smaller deviations than the PR EoS in the high pressure range.

Because the volume ratios computed with the PR and SRK EoS differ strongly from the experimental data, an alternative method was formulated, which allows the adjustment of the EoS to the experimental data. Thereby, the computation of the molar density values of the gas mixture has been proposed

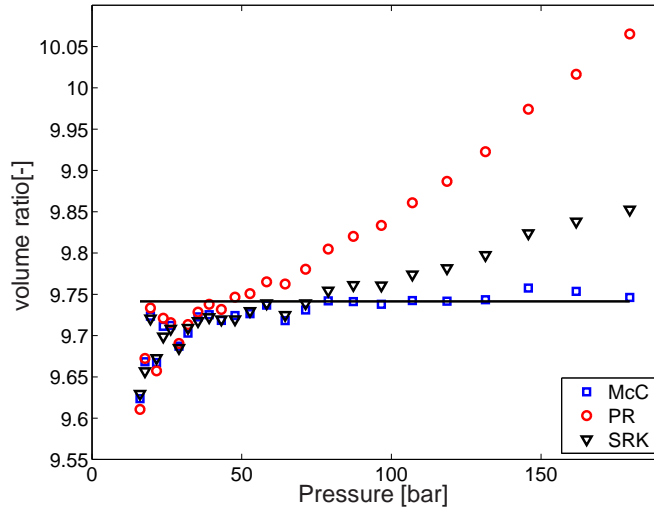


Figure 4.3: The volume ratio computed with Eq. 4.21 using the McCarty, the PR and the SRK EoS for pure Helium to describe the Helium mixture. The constant volume ratio has been obtained from pure helium measurements (see Fig. 4.1, 4.2).

4.4 Volume ratio measurements using a Helium mixture

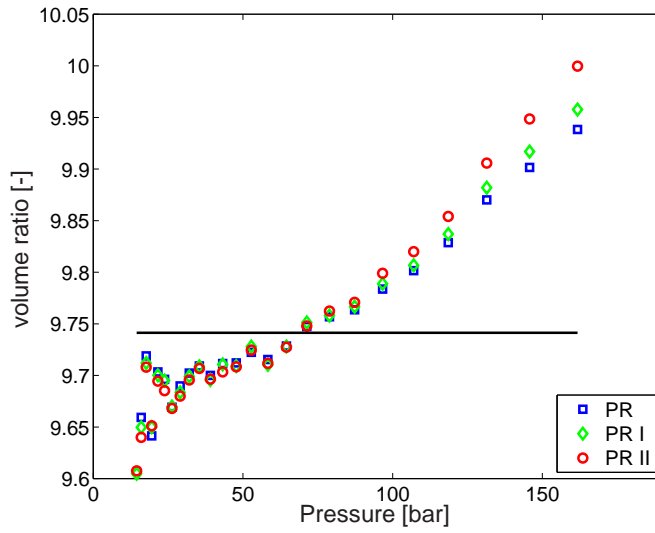


Figure 4.4: The volume ratio deduced from Eq.4.21 using the PR EoS considering the gas mixture as pure He (PR) and combining PR with two different mixing rules (PR I and PR II). All the calculated density values have been optimized using the Peneloux volume shift operation, optimizing the objective function Eq. 4.22. The constant volume ratio has been obtained from pure helium measurements (see Fig. 4.1, 4.2).

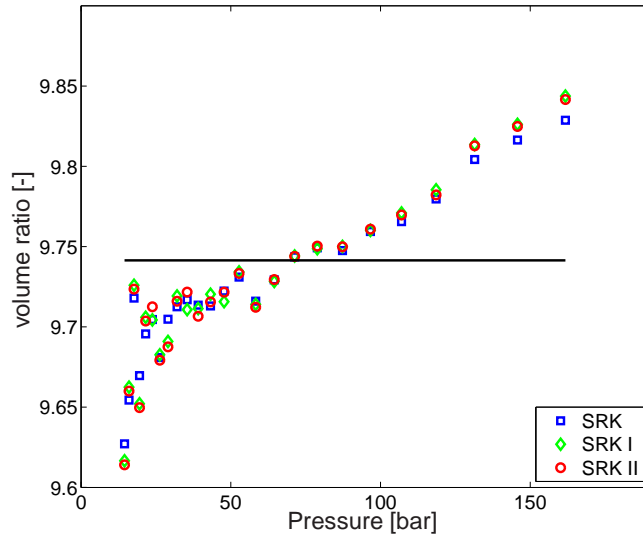


Figure 4.5: The volume ratio deduced from Eq.4.21 using the SRK EoS considering the gas mixture as pure He (SRK) and combining SRK with two different mixing rules (SRK I and SRK II). All the calculated density values have been optimized using the Peneloux volume shift operation, optimizing the objective function Eq. 4.22 over the entire pressure range. The constant volume ratio has been obtained from pure helium measurements (see Fig. 4.1, 4.2).

4.4 Volume ratio measurements using a Helium mixture

starting from an experimental point of view. In Eq. 4.21, ρ_i can be calculated from ρ_{i-1} . In this way all the densities can be calculated based on one reliable value of ρ_{i-1} . For this work the density at 318 K and 107.03 bar was used as reference value. In the range between 118 and 70 bar the computed volume ratios calculated with the McCarty EoS (see Fig. 4.3) represent the experimental values quite accurately. At 318 K and 107.03 bar the density of the helium mixture computed with the McCarty EoS is equal to 3.867 mol/L, which gives a volume ratio of $\chi = 9.7416$. This value has been used in Eq. 4.21 to find all the other density values for $i=1, \dots, N$. We can use these values to optimize the EoS minimizing the following objective function:

$$\sum_{i=1}^N (\rho_{exp,i} - \rho_{EoS,i})^2 = min, \quad (4.22)$$

where $\rho_{exp,i}$ for $i=1, \dots, N$ are the densities obtained from the known initial density value $\rho=3.867$ mol/L and $\rho_{EoS,i}$ is the density calculated using an EoS with or without mixing rule.

In Figs. 4.4 and 4.5 the volume ratios computed with the SRK and PR EoS with the adjusted parameters are shown. Two different mixing rules were applied depending on how we consider the binary interaction parameter k_{ij} . In method I we use Eq. 4.14 and Eq. 4.15 in Eq. 4.4 to obtain the force parameter a_{ij} . In Figs. 4.4 and 4.5 it is given by PRI and SRKI. In model I, the δ_{ij} parameter can be estimated instead of using Eq. 4.15, by minimizing Eq. 4.22. This method is equivalent to an estimation of the δ_{ij} parameter using Eq.4.15. The influence of the parameter δ_{ij} on the molar density is very small.

In model II we can freely choose the values of the binary interaction parameters k_{ij} and optimize the results using as an initial condition the values obtained for k_{ij} from model I. The objective function to be minimized is again given by Eq. 4.22.

Finally the volume correction (Eq. 4.16, 4.17) suggested by Peneloux has been applied to all the different models described above. With this procedure new densities have been calculated minimizing Eq.4.22 to find the volume shift parameters (c_i). Figs. 4.4 and 4.5 include this correction in their plots.

After introducing the volume shift correction the computed volume ratios using the three different models almost coincide. Thus, incorporating a mixing rule does not improve the results. Surprisingly the McCarty EoS for pure He gives better results than the PR and SRK EoS with or without mixing rules.

Figs. 4.4 and 4.5 show that even with adjusting the parameters to improve the prediction of the density, the resulting volume ratios differ a lot from the

experimentally determined ones. For low pressures the volume ratios are under predicted, for higher pressures they are over predicted. At low pressures the scatter between the data can be attributed to the fact that the volume ratio is affected by the small value of the denominator of Eq. 4.21. However there is a systematic error leading to a low volume ratio. Even though the error is small, it is relevant in the determination of the volume ratio for a volumetric set up.

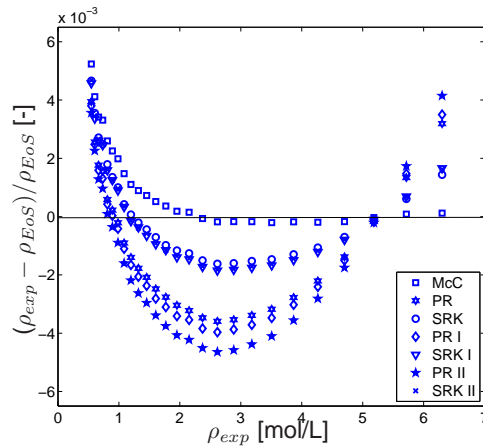


Figure 4.6: The relative difference of the calculated density versus the experimentally determined density.

Fig. 4.6 shows the relative difference between the calculated density and the experimentally derived density. It is relevant to notice that even a small difference in the density calculation (0.1%) leads to wrong estimates of the volume ratio (see Figs. 4.4 and 4.5).

4.5 Volume ratio measurements using a CO₂ mixture

The volume ratio of the two duplicated sample cells have been determined using the Span and Wagner EoS for CO₂ as a pure gas (Span and Wagner, 1996) and the SRK and PR EoS applied to the mixture using the mixing rules

4.5 Volume ratio measurements using a CO₂ mixture

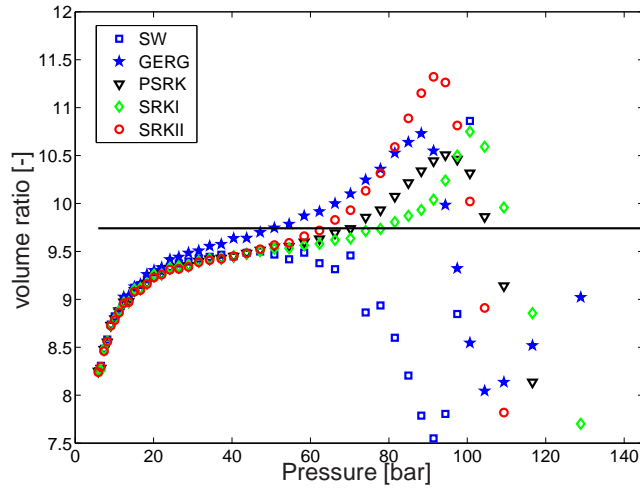


Figure 4.7: The volume ratio computed with Eq. 4.21 using the CO₂ mixture. The plot shows the volume ratio obtained with the density derived from five different EoS; the PR I and PR II have not been displayed because of their high inaccuracy.

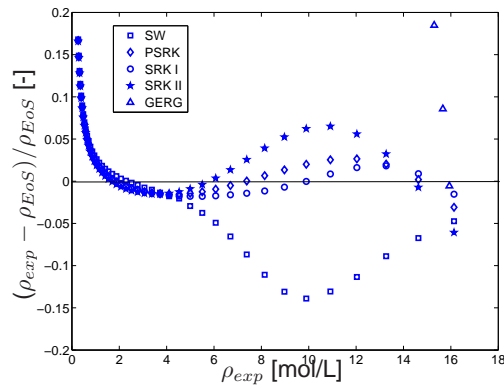


Figure 4.8: The relative difference of the calculated density versus the experimentally determined density.

1

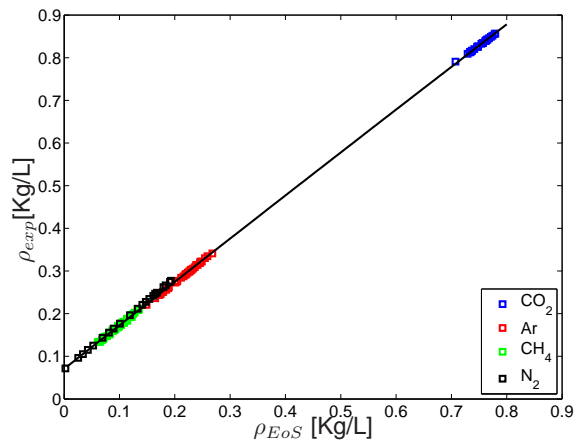


Figure 4.9: Density experimentally determined with a DMA 512 Paar density meter versus the densities calculated with accurate EoS for CO_2 (Span and Wagner, 1996), Ar, CH_4 and N_2 (Wagner and Span, 1993).

4.5 Volume ratio measurements using a CO₂ mixture

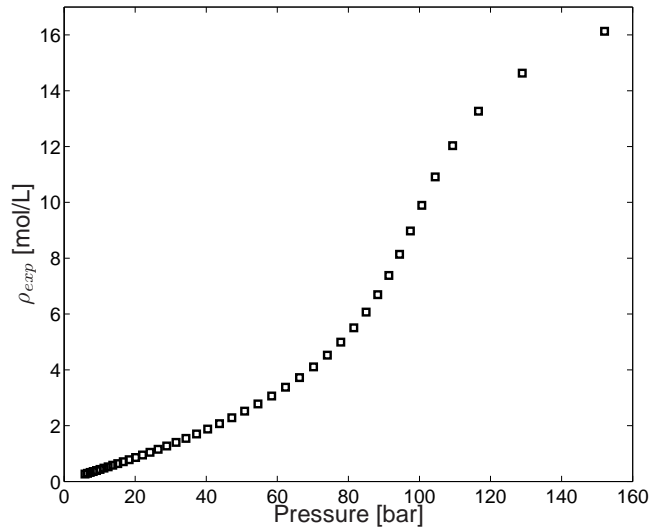


Figure 4.10: Density of the CO₂ mixture at various pressures and at a constant temperature of 318 K. The density at $P=152.08$ bar has been measured using the DMA 512 Paar density meter, all the other values have been computed using Eq. 4.21.

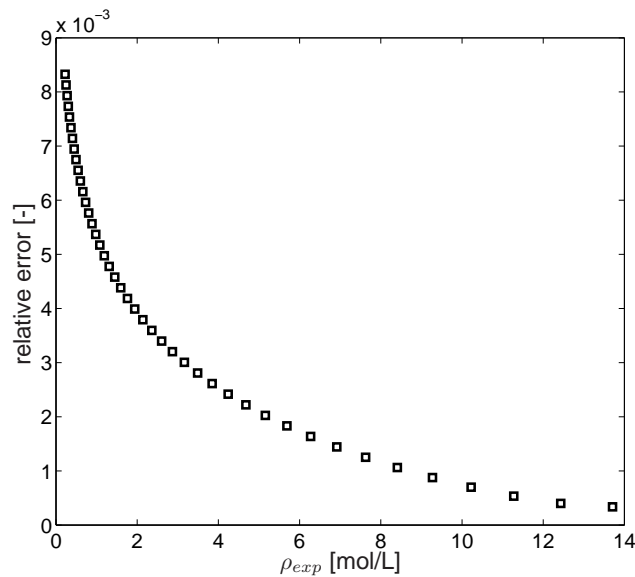


Figure 4.11: The relative error of the densities calculated from Eq. 4.21, see Fig. 4.10. The relative error is measured using a Montecarlo simulation. The relative error is the ratio between the standard deviation and the averaged value of each single density measurement.

described in the previous section, see Fig.4.7. Here the volume ratio in the low pressure range (up to 40 bar) and close to the critical point of CO_2 (between 80 and 120 bar) are not described very accurately in all cases. There is a large discrepancy between the volume ratio measured with pure He (see Section 4.3.3) and the volume ratio obtained using the SRK and PR EoS, see Fig. 4.7. As an attempt to get better agreement between measured and predicted densities, two more different EoS have been tested. The GERG-2004 Wide Range EoS for Natural Gases and other Mixtures (Kunz et al., 2007) has been used in order to convert the P,T data to densities. The software has been used thanks to the collaboration with Aachen University. Because the software does not provide data concerning NO_2 , the mixture of CO_2 has been considered disregarding the presence of NO_2 and assuming a molar concentration of 98% of CO_2 . The so-called PSRK EoS was tested. Thereby, the force parameter

4.5 Volume ratio measurements using a CO₂ mixture

a_m (see Eq. 4.1) was computed using the non-classical Huron-Vidal mixing rule in combination with the UNIFAC model (see Appendix C). Additionally, the volume correction as suggested by Peneloux (Eq. 4.16 and 4.17) was incorporated. The volume shift parameters c_i were adjusted to minimize the objective function (Eq. 4.22). Fig. 4.7 shows the volume ratio obtained with the density derived from five different EoS; the PRI and PRII have not been displayed because of their high inaccuracy.

None of the applied EoS reaches the accuracy necessary to allow the determination of sorption of gas mixtures containing CO₂.

The inadequacy of the EoS to predict the volume ratios correctly shows that it is necessary to obtain experimental data of the density. For the CO₂ mixture it is not possible to start with a single value of the density obtained with any of the discussed EoS to calculate backward the other density values as has been done in Section 4.4. Indeed, the fact that one accurate volume ratio for the CO₂ mixture was computed, does not mean that the density value is correct, but just that the difference between the two consecutive densities is correct. Indeed, as can be observed in Fig. 4.8, the GERG-2004 EoS gives a volume ratio that is in the same range as those determined with the other EoS (see Fig. 4.7). However, it is affected by a bigger relative error in the density than the other models. In Fig. 4.8 just two points are plotted, the rest are off the scale. The density of the CO₂ mixture, therefore, has been experimentally determined using a density meter (DMA 512 Paar) connected to a thermocouple sensor and a pressure transducer. The temperature has been kept constant by placing the density meter cell in a thermostatic bath at a constant experimental temperature of 318.15 K \pm 0.02. The accuracy of the density meter is 10⁻⁴ kg/dm³. The DMA 512 Paar density meter has been calibrated using different gases with known densities, see Fig. 4.9. We can use the density values obtained with the DMA 512 Paar density meter for the CO₂ mixture to get a single density value at a specific temperature and pressure in order to calculate backward all other densities using the volume ratio (see Eq. 4.21) as described in the previous section. Densities have been experimentally measured with the DMA 512 Paar density meter for the CO₂ mixture in a range between 138 and 155 bar in order to interpolate the density value of the first data point for the volume ratio measurement which is $\rho=13.7073$ mol/dm³ at P=152.08 bar. Fig. 4.10 shows the resulting density of the CO₂ mixture at various pressures and at a temperature of 318 K. The density has not been measured over the whole pressure range using the DMA 512 Paar density meter because the accuracy of the density meter measurements in the lower pressure range is low.

The error in the density values obtained from the volume ratio in Eq. 4.21 can be estimated by carrying out a Montecarlo simulation. For this we start with the initial value of the density $\rho_N=13.7073 \text{ mol/dm}^3$ with a standard deviation of $\Delta\rho=0.0045 \text{ mol/dm}^3$, which is inferred from the accuracy of the density meter. We proceed by generating a vector row of $M = 183$ initial density values to which we add a normally distributed random number with an average of zero and a standard deviation of $\Delta\rho$. For each vector component we generate a column that consists of a sequence of N density values by modifying Eq. 4.21 to

$$\rho_i = \frac{\rho_0}{\chi + 1} + \left(\frac{\chi}{\chi + 1} \right) \rho_{i-1}. \quad (4.23)$$

In this way we generate a matrix with indexes k, l , where $1 \leq k \leq M$ is the column index and $1 \leq l \leq N$ is the row index. The matrix has $M = 183$ columns and $N = 43$ rows. In our case $\rho_0 \simeq 0$ and thus the first term in Eq. 4.23 can be neglected. Each column starts with a random number with an average of ρ_N and a standard deviation of $\Delta\rho$. For each column we choose a single value of χ to which we added a normally distributed random number with an average of zero and a standard deviation of $\Delta\chi = 0.022$. Density values are generated down to a value of about $\rho_1 \simeq 0.23 \text{ mol/dm}^3$. For each l^{th} row we determine the average value and the standard deviation. The results are shown in Fig. 4.11, where we plot the coefficient of variation (standard deviation / average), which denotes the relative error as a function of the density. We observe that the relative error changes from 0.85% for low densities to 0.033% for high densities. The accuracy of the obtained density values is in the same range as the accuracy of the density meter DMA 512 Paar. Therefore our measurements show that in the absence of a density meter, it is possible to use the manometric set-up to obtain sufficiently accurate density values provided that one has a single reliable and accurate density value from another source. Such a density value can be obtained outside the critical region.

4.6 Conclusions

In order to test the adequacy of the EoS in a manometric set up we measured at different pressures the volume ratio between the empty sample cell and the reference cell. The volume ratio between the reference cell and the sample cell of the manometric set up is determined by expanding helium from the reference

4.7 Acknowledgement

cell to the sample cell and using the Mc Carty EoS in order to convert pressure and temperature data in to density for the computation of the volume ratio. The volume ratio can also be computed using a Helium mixture (98% He, 1% O₂ and 1% NO₂) . This is so because the density can be sufficiently accurately described by the McCarty EoS for pure Helium. Therefore this EoS can be used for this specific mixture to perform sorption experiments. A deviation occurs between the correct volume ratio and the volume ratio measured in a low pressure range (20-40 bar) for the He mixture. It is not likely that this error can be attributed to an error in the EoS but to an adsorption on the vessel walls. The PR and SRK EoS with or without mixing rule are not adequate to obtain a correct density from pressure and temperature data.

None of the considered EoS and mixing rule can be used for the experimental sorption determination in a volumetric set up with sufficiently high accuracy for the CO₂ mixture (97% CO₂, 1% He, 1% O₂ and 1% NO₂). Measurements concerning CO₂ mixtures are more sensitive to an accurate EoS because the experimental conditions are close to the CO₂ critical point and also it is well known that the other gases in the mixture change the location of the critical point and thus have a large influence on the densities, reducing the adequacy of the EoS. The manometric set up can be used to measure the density values of a gas mixture provided that at least a single density value has been measured at the same conditions with another available technique, e.g., with a density meter. This experimental values can be used in order to determine an accurate EoS to process sorption experiments on coal.

4.7 Acknowledgement

The experiments have been performed under the GRASP (Green-House Gas Removal Apprenticeship) Marie Curie programme. Experiments of gas sorption on coal have been performed at GeoLab of the Department of Applied Earth Sciences, TU Delft. We thank Henk Van Asten for his technical support and expertise. We also thank the LEK RWTH-Aachen group, in particular Yves Gensterblum for providing us the data concerning the GERG-2004 EoS.

Table 4.3: *The group binary interaction parameters a_{nm} .*

Gas	CO ₂	He	O ₂	NO ₂
CO ₂	0	565.20	208.14	0
He	55.66	0	758.30	0
O ₂	32.043	247	0	0
NO ₂	0	0	0	0

Chapter 5

Determination of Adsorption of Gas Mixtures in a Manometric Set Up

Abstract

Research concerning ECBM until now mainly focused on pure gas adsorption. Application of the manometric set up to mixtures to be used in ECBM requires an accurate description of the thermodynamic behavior of these mixtures. To illustrate the applied methodology the behavior of two different mixtures have been studied: a helium rich mixture (98% He, 1% O₂ and 1% NO₂) and a CO₂ rich mixture (97% CO₂, 1% He, 1% O₂ and 1% NO₂) on activated carbon.

Sorption experiments have been conducted using a manometric set up at a constant temperature of 318.15 K and up to a pressure of 160 bar. The composition of the gas mixture has been measured after every desorption step. For this we used a mass spectrometer. It turns out that when equilibrium is reached, the concentration of the different components of the mixture is constant throughout the desorption experiment. Consequently, no reaction, in this range of pressures and temperatures, occurs between the gas and activated carbon.

So far no existing Equation of State (EoS) is able to describe the CO₂ rich mixture sufficiently accurately for application in a manometric set up. The use of different EoS is affecting the excess sorption isotherm results. In order to

choose between different EoS some density measurements have to be performed. Combining different EoS for different pressure range it is possible to obtain a sufficiently accurate EoS in order to find the excess sorption of mixtures.

5.1 Introduction

There are many options to reduce the anthropogenic CO₂ emissions in the atmosphere, e.g., the improvement of energy efficiency in industrial processes, the implementation of renewable energies (Li and Yan, 2009b). An alternative option is also represented by the Carbon Capture and Storage (CCS). One of the possible solutions in this framework is Enhanced Coal Bed Methane (ECBM). A vast amount of literature concerning this topic has recently been produced (Mazzotti et al., 2009; Reeves, 2006). The CO₂ to be stored is a component of flue gas, which varies considerably depending on the used fuels for the energy conversion and the applied combustion process. The main components of the flue gas are O₂, CO₂, N₂, H₂O and traces of SO_x and NO_x. Most of the research however generally uses pure CO₂, disregarding the presence of impurities as being the most important component of the flue gas stream. However, the three main carbon capture technologies, i.e. pre-combustion, post-combustion and oxyfuel combustion do not lead to a pure CO₂ stream (Liu and Shao, 2010). A simple chemical process configuration and high CO₂ purity cannot be achieved at the same time (Li et al., 2009). As in the case of current gas recovery projects such as in Sleipner and In-Salah, the CO₂ stream is not pure (Jacquemet et al., 2009), i.e., at Sleipner this stream contains up to 150 ppm H₂S and up to 5% of non-condensable gases.

CO₂-ECBM is an expensive technology also due to the high costs of CO₂ purification. An option to reduce separation costs would be to inject the flue gas directly as a partly treated mixture in the deep coal seams (Wong et al., 2000). However, a limited removal of the main gas impurities, e.g., N₂, would reduce the compression costs and maintain the volume efficiency in the storage phase, e.g., 5 mol % N₂ at a storage depth of 1 km and 2 km, leads to a reduction of the storage capacity of 22 % and 9 % respectively (Li and Yan, 2009b). In all the practical cases, in the storage phase, the stream to be sequestered would still contain traces of N₂, NO_x and SO_x.

Streams containing impurities have different physical properties and geochemical reactivities compared to a pure CO₂ gas phase (IEA, 2004). Therefore, it is important to quantify the thermodynamic behavior of, among others,

5.1 Introduction

the CO₂-NO₂ mixtures and the adsorption isotherm of these gas mixtures on coal. Data concerning CO₂-NO₂ mixtures in the literature are very scarce. In the CCS field there are no studies concerning this gas mixture (Jacquemet et al., 2009). Recent papers are dealing with CO₂ mixtures containing also SO₂ (Li and Yan, 2009a,b). This combination is not a part of this study.

The NO_x present in the flue gas is generally removed using specific De-NO_x techniques. The most widely used is the SCR (Selective Catalytic Reduction), where the NO₂ is reduced to N₂ using ammonia as reactant and then adsorbed by a catalyst. This process can reach an efficiency of 90%. Literature concerning this topic is abundant. In the nineties the adsorption of NO₂ on activated carbon for the optimization of De-NO_x processes has been investigated (Gray and Do, 1993; Neathery et al., 1997; Rubel and Stencel, 1996, 1997; Stanmore et al., 2008; Zhu et al., 2005). All experiments concerning the adsorption of NO₂ on activated carbon are carried out using a microbalance or a thermo gravimetric analyzer coupled to a mass spectrometer. Rubel and Stencel (1996) reports that the maximum amount of NO₂ adsorbed on activated carbon can be as high as 200 mg per g of carbon. The pressure range of the studies is going up to 28 bar and to temperatures up to 623 K. At temperatures higher than 373 K NO_x reacts with the C molecules of the activated carbon producing oxygen and carbon dioxide (Gray and Do, 1993; Stanmore et al., 2008). This reaction is not significant for temperatures below 373 K, as in our case study. The absence of experimental results above 28 bar leads to a lack of data in this range of interest.

In this study the results of a manometric set up used to measure the excess sorption isotherm are discussed. We derive an accurate EoS to interpret the pressure and temperature data. The EoS can be divided into two categories (Li et al., 2009), 1) the more general such as the cubic EoS (SRK, PR) and 2) the specific ones as the Span and Wagner (Span and Wagner, 1996). In the first category the accuracy is lower while in the second one the accuracy is much higher but can only be used for a specific gas and the use of many fitting parameters. As has been shown previously (Chapter 4) the majority of the existing EoS and mixing rules used in reservoir models are not sufficiently accurate for manometric measurements. For this reason different excess sorption isotherms using different EoS are compared.

To illustrate these ideas, this study analyzes the sorption behavior of two different gas mixtures, one mainly composed of helium, as a reference gas, and one mainly composed of CO₂. The helium mixture has been chosen in order to test the procedure. The CO₂ mixture has been used to validate whether the presence of NO₂ in the flue gas has an effect on the density calculations.

The gas composition has been analyzed during the desorption experiments to establish the concentration of the components. The excess sorption isotherm on activated carbon at 318.15 K and up to 160 bar has been calculated for both gases on 6 different activated carbon samples.

5.2 Experimental method and materials

Two mixtures have been chosen for the experiments: the first one is a so-called He mixture composed of $97.94 \pm 0.04\%$ He, $0.996 \pm 0.04\%$ O₂ and $1.03 \pm 0.04\%$ NO₂; the second one is a so-called CO₂ mixture composed of $96.99 \pm 0.04\%$ CO₂, $1 \pm 0.04\%$ He, 1.003% O₂ and $1.007 \pm 0.04\%$ NO₂.

The first mixture has been introduced to test the procedure with a gas of which the EoS can be easily obtained. The second mixture is representative for the flue gas after removing N₂. The concentration of NO₂ in the gas mixture is much higher than in practice because the purpose of this study is to investigate the effect of NO₂ in the gas mixture on the density calculations in the supercritical region. The gas mixture contains NO₂ and not NO, which is also one of the primary combustion products in the flue gas. This is due to the fact that NO is very reactive and in the presence of oxygen reacts to NO₂ according to the reaction



This also motivated the addition of O₂ to the mixture. All the gases, including the mixtures, have been provided by Linde gas.

The samples used in the experiments are granular activated carbon Filtrasorb 400 from Calgon Carbon Corporation. The grain size is between 1 and 1.5 mm.

The sorption experiments have been conducted using a manometric set up previously described in Chapter 2. A Quadrupole Pfeiffer Vacuum mass spectrometer (QMS 422) was used to monitor the gas composition during desorption. After equilibrium, at the end of each desorption step, the valve between the sample cell and the reference cell is closed and the gas concentration has been measured using the MS (Mass Spectrometer). The reference cell is connected to the MS via a reducing valve and a capillary tube. Measurements have been taken until the pressure in the MS was showing a constant profile. Two vacuum pump working in series keep the required pressure of the MS below 10^{-6} bar. The MS was controlled by a PC via the software Quadstar 32-bit.

5.2 Experimental method and materials

The identification of the desorbed gases was done by using the major mass of the molecules, see Table 1. Measurements have been conducted using the

Table 5.1: *molecular weight of the molecules measured with the MS.*

He	C	O	H ₂ O	N ₂	O ₂	CO ₂	NO ₂
4	12	16	18	28	32	44	46

qualitative Multiple Ion Detection (MID) method and the detector used is the SEM (Secondary Emission Multiplier). The software acquires the ion current (A) of each different element produced by the ionization on the MS filament on 8 separate channels. The ion current gives a qualitative indication of the specific element concentration. A separate channel was used for pressure measurements. Presence of N₂ and H₂O traces can reveal a possible air leakage in the system.

5.2.1 Data analysis

Mass Spectrometer measurements

As described above, after every desorption step, the gas composition has been analyzed using a mass-spectrometer. The data interpretation has been conducted using helium as a reference gas. Due to its non adsorptive characteristics it has been assumed that its concentration is constant during the desorption process. The concentration of the gas in the cylinder has been measured prior to the beginning of the experiment with the MS and it has been used as an internal standard for the gas calibration. At every measurement, the ion current of each gas component measured with the MS has been normalized by multiplying it by the ratio between the helium ion current of the current step, $[He_{step}]$, and the ion current of the measurement taken from the reference bottle, $[He_{ref}]$.

$$\frac{[He_{step}]}{[He_{ref}]} \quad (5.2)$$

Fig.5.1 shows the normalized ion concentration of NO₂ plotted versus the pressure in each desorption step for the so-called helium mixture (see Section 5.2). As it can be observed, Fig. 5.1 shows a constant concentration of NO₂ within a fluctuation of 17% throughout the desorption experiment.

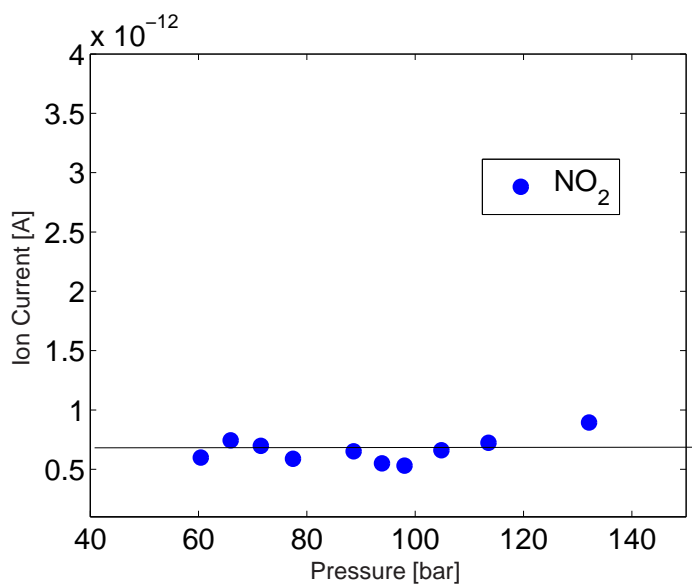


Figure 5.1: Ion current measurements conducted with the mass spectrometer of NO₂ plotted versus the desorption pressure steps.

5.2 Experimental method and materials

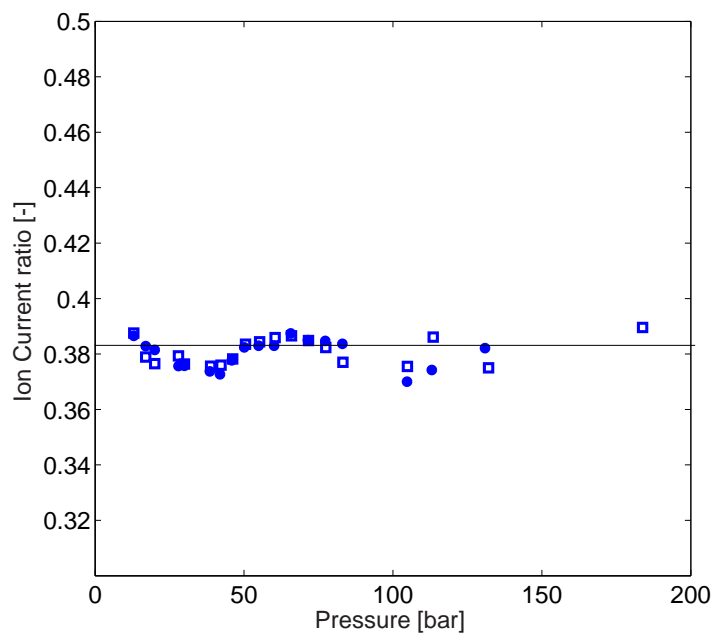


Figure 5.2: Ratio of the ion current measurements conducted with the mass spectrometer of NO_2 and CO_2 plotted versus the desorption pressure steps. These are the duplo results (full and empty dots).

Fig. 5.2 shows the data for the so-called CO₂ mixture. The values of the ion current relative to the two gases are strongly related to the pressure in the MS. The set up, as designed, cannot keep a constant flow of gas because of the nature of the experiments. As the pressure decreases in the MS, the concentration of the molecules increases. This is why the values in Fig. 5.2 have been plotted as the ratio between the NO₂ and the CO₂ concentration. The concentration of the different components is constant throughout the desorption steps within a range of 3.7 %.

It is important to notice that the data were not taken continuously but only when equilibrium was reached. At equilibrium, the gas was allowed to flow from the manometric set up to the MS. The results do not reveal anything about the rate of desorption of the different gases present in the mixture, but they indicate that there is no chemical reaction between the activated carbon and the gas mixture when equilibrium is attained and that the gas mixture can be assumed constant in concentration at each pressure step.

sorption measurements

All the excess sorption isotherms have been measured at 318.15 K. The excess sorption isotherm of the helium rich mixture can be calculated using the Mc Carty EoS (McCarty and Arp, 1990). This EoS is accurate for the density calculations of the helium rich mixture used in this study (Chapter 4). The results (Fig. 5.3) show that at this pressure range the excess sorption isotherm does not show a maximum. The amount of gas adsorbed can be fully ascribed to the NO₂ and O₂, which are present in the helium mixture in small concentration (2%). This is why the sorption curve shows such low values. The experiment has been repeated twice on two different activated carbon samples. Results show that at 165 bar (the highest pressure value) the amount of gas adsorbed is 0.25 mmol/g.

In the case of a CO₂ mixture the excess sorption isotherm cannot be calculated accurately with any of the existing EoS (Battistutta et al., 2011).

In Chapter 4 a method was developed to derive the density values for each single pressure step by measuring the volume ratio between the empty sample cell and the reference cell, using pure helium. With this known volume ratio, the density can be calculated backwards either starting from the highest pressure point or vice versa from the lowest pressure point. In order to apply this procedure, the initial P, T, ρ point has to be accurately determined. Therefore, the density of the mixture has been measured at high pressures using the density meter DMA 512 Paar. In contrast, the density of the mixture at low

5.2 Experimental method and materials

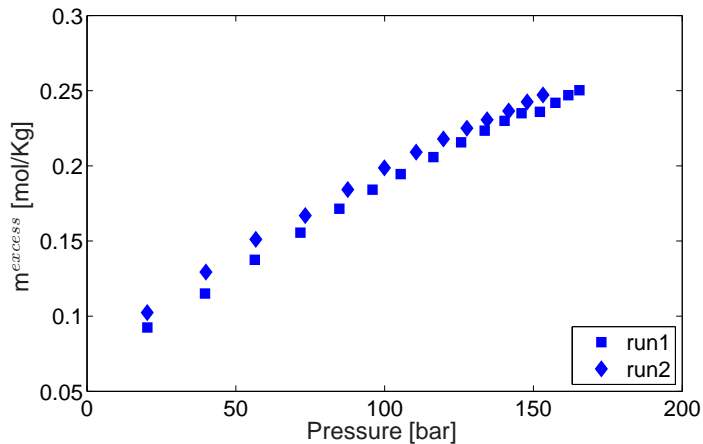


Figure 5.3: Excess sorption isotherm on activated carbon (Filtrisorb 400) of a mixture mainly composed of helium at 318.15 K. The experiments have been repeated twice (diamonds and squared symbols indicating the two separate experiments).

pressures has been determined averaging the density values obtained using different EoS. The different EoS used are: the Span and Wagner EoS (Span and Wagner, 1996), the SRK EoS (Soave, 1972) with standard Van der Waals mixing rules (Kwak and Mansoori, 1986) and volume correction (Peneloux and Freze, 1982), which we indicate as SRKI, the GERG EoS (Kunz et al., 2007) and the PSRK EoS (Holderbaum and Gmehling, 1991). The results are shown in Table 5.2.

Table 5.2: P, T of the lowest and highest data point of the void volume ratio measurements using the CO_2 mixture. Densities, ρ , at low pressures have been calculated using different EoS and for the case of high pressure, with the density meter.

P [bar]	T [K]	ρ [mol/dm ³]				
		SW	SRKI	PSRK	GERG	experiment
5.89	318.15	0.228	0.231	0.229	0.228	
152.0	318.15					16.131

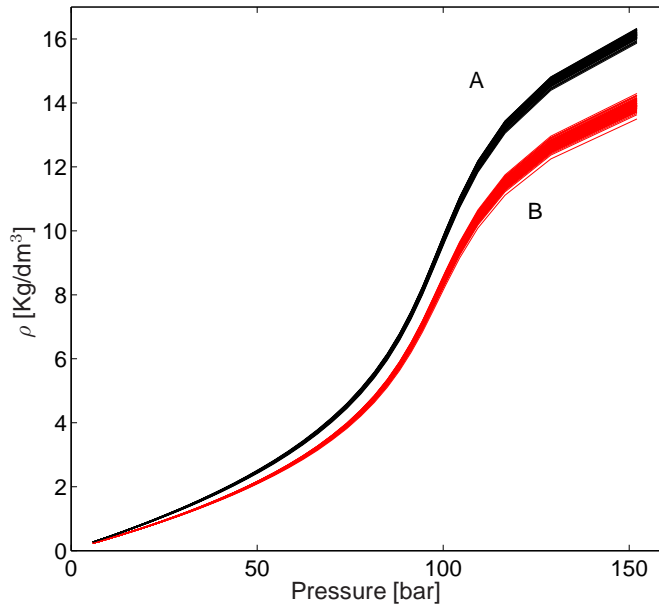


Figure 5.4: Montecarlo simulation of the density of the CO_2 mixture versus pressure. The results are obtained from the manometric set up, knowing the volume ratio between the empty sample cell and the reference cell. The results have been perturbed knowing the error on the first density value and on the measured volume ratio. For the A set, densities are calculated backward from the highest density value. For the B set, densities are calculated backward from the lowest density value.

5.2 Experimental method and materials

In order to determine any possible variation in these calculations, in both cases we made a sensitivity analysis perturbing the initial value of the density with its standard deviation and the volume ratio with the error given by the experiment conducted with pure helium in the empty cells (Battistutta et al., 2011). In the case of the high density value, the standard deviation is given by the density meter accuracy (10^{-4} kg/dm³). In the case of the low density value, the error on the density is given by the standard deviation over the average of the density values of the SW, SRKI, PSRK and the GERG EoS. Using the standard deviation, a set of 100 different initial density values and 100 volume ratios has been randomly generated, both for the high pressure case and the low pressure case. The densities of the other experimental points have been calculated backwards. Fig. 5.4 shows the two sets of curves resulting from this Montecarlo simulation. Each curve is the result of a different initial density and volume ratio value. The thickness of each set of curves gives an indication of the error that follows from the procedure. The set B leads to lower densities than the set A. This is attributed to the fact that all the EoS used in this study underestimate the density at low pressure. We prefer to use the method starting with the measured value at high pressure, because it is entirely based on experiments. The procedure described above gives the required P , T , ρ points.

For the fitting of the P , T , ρ points we choose the SRK EoS with standard mixing rule equation and the volume correction.

$$P = \frac{RT}{v - b_m} - \frac{a_m}{(v + c(P))(v + b + 2c(P))}. \quad (5.3)$$

The only parameter that can be changed without affecting the physics of the EoS is the Peneloux volume correction c (see the Appendix D for further details). Rewriting the SRK EoS in a different form with the Peneloux volume correction, the parameter c has been calculated knowing the experimental values of the gas mixture of P , T , ρ . The volume parameter b and the force parameter a have been calculated from the specific critical properties of each gas. As a result, we find a second order equation for c , which has two solutions. Fig. 5.5 shows both results plotted as a function of pressure and fitted using an exponential function of the type:

$$c(P) = -\beta \exp\left(\frac{-P}{P_0}\right)^\gamma + \delta, \quad (5.4)$$

The parameters used in the fitting are entirely empirical and their values have been summarized in table 5.3. It is noticed that the main deviation occurs

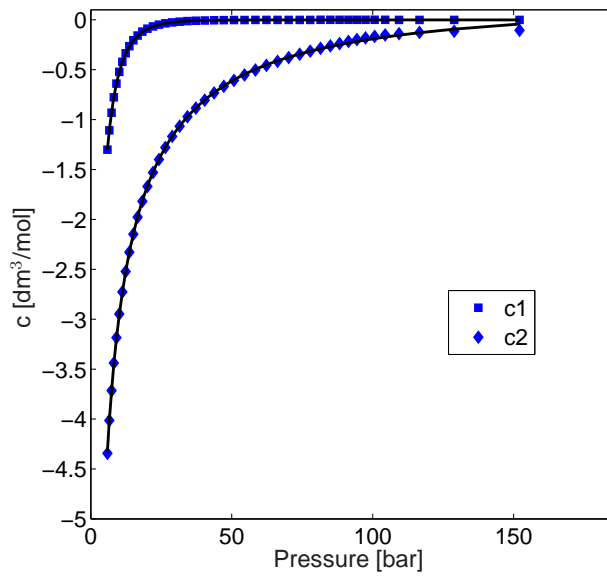


Figure 5.5: Volume correction parameter (Peneloux and Freze, 1982) obtained from the empty cell measurements of the CO₂ mixture plotted as a function of pressure.

5.2 Experimental method and materials

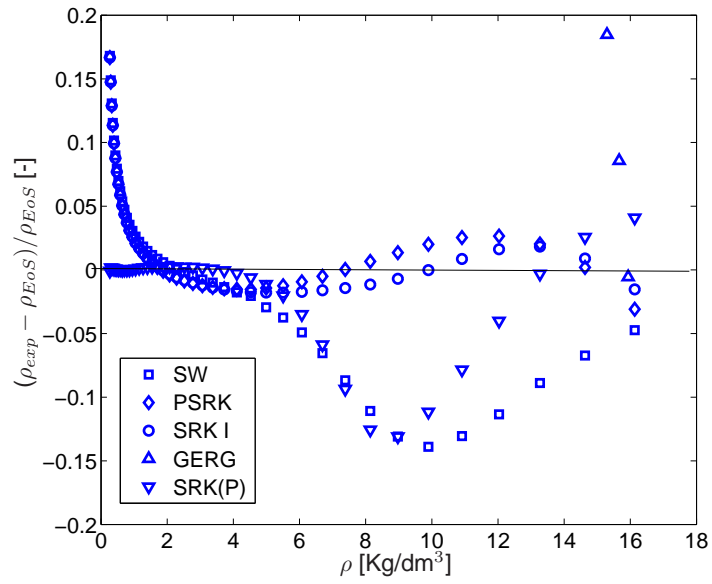


Figure 5.6: *The relative difference of the calculated density versus the experimentally determined density.*

Determination of Adsorption of Gas Mixtures in a Manometric Set Up

Table 5.3: *Fitting parameters of the volume correction calculated as a function of pressure.*

constants	β [dm ³ /mol]	P_0 [bar]	δ [dm ³ /mol]	γ
c1	66.783	0.0838	-0.1646	0.23364
c2	10.76	1.9222	0.0012	0.668

at low pressures. We used *c1* because it is giving a better fit. However, this new volume correction (SRK(P)) is very efficient at low pressures, correcting the effect that was common to all the other EoS (see Fig. 5.6). Though, its accuracy is limited at high pressures, where the SRKI is more accurate. All the EoS described in Fig. 5.6 have been tested in order to establish the validity of an accurate EoS (Battistutta et al., 2010). Four different samples of activated carbon (Filtrisorb 400) have been used for the study.

Fig. 5.7 describes the excess sorption isotherms curves of sample number 4. Every curve is obtained using a different EoS (S&W, SRKI, SRK(P), PSRK, GERG). It can be observed that the use of different EoS influences the final result. When using a manometric set up with gas mixtures, it is always necessary to test the actual density of the mixture because, as observed here, the final excess sorption isotherm can be affected by the choice of different EoS. Already at low pressures the different EoS are giving different results, changing also the maximum of the excess sorption. Between the SRKI and PSRK, that give respectively the highest maximum (7.07 mol/kg) and the lowest maximum (5.24), there is a 25.88% difference. The largest deviation occurs after 80-90 bar. The reason is that around the critical point all the EoS become extremely inaccurate and that the curve is calculated cumulatively. The negative values for the case of the S&W and the SRK(P) are due to the fact that these EoS are not accurate at high pressure and underestimates the density of the mixture (see Fig. 5.6).

Therefore, a combined EoS has been developed, using two different EoS at two different pressure ranges. It has been arbitrary chosen 75 bar as the transition point to obtain a combined EoS that is valid over the entire pressure range. The excess sorption isotherms have been measured combining the SRK(P) at low pressures (below 75 bar) and the SRKI at high pressures (above 75 bar). Fig. 5.8 shows the results for the four different excess sorption isotherms measured at 318.15 K on four different samples. At high pressures the behavior of the excess sorption isotherms is not satisfactory. The last 4

5.2 Experimental method and materials

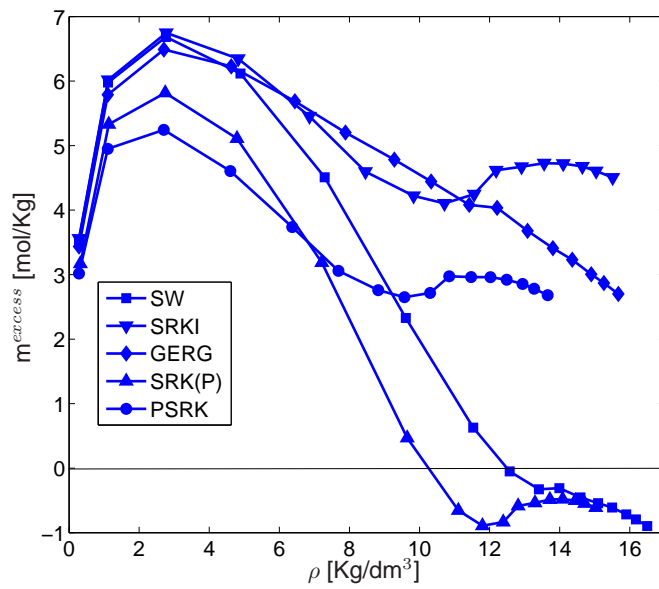


Figure 5.7: Excess sorption isotherm on activated carbon (Filtrisorb 400) of a mixture mainly composed by CO₂ at 318.15 K. Every curve describes the same experiment (sample #4) processed with different EoS.

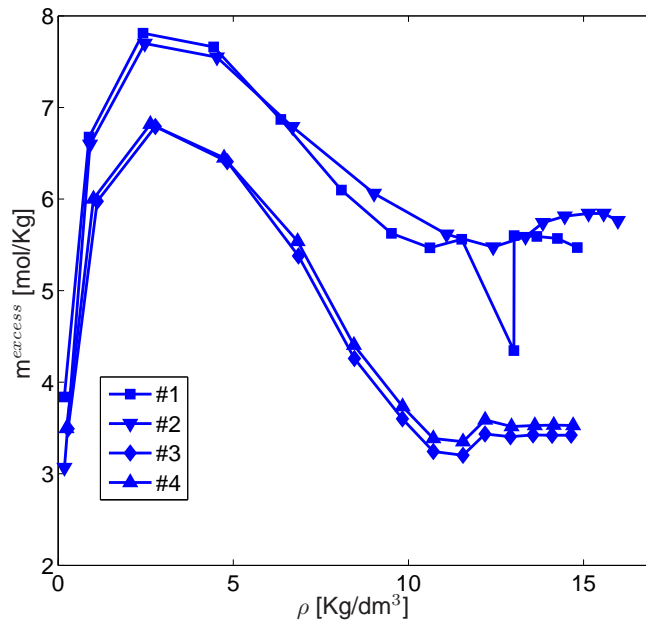


Figure 5.8: Excess sorption isotherm on 4 different activated carbon (Filtrisorb 400) samples of a mixture mainly composed by CO_2 at 318.15 K.

5.3 Conclusions

points of each excess sorption have an almost linear behavior. Assuming that these values are correct would imply an unrealistic high adsorbed density. The reason for this behavior is that at high pressures, the SRKI slightly overestimates the density (see Fig.5.6). The maximum sorption is 7.81 mol/Kg at 49.13 bar. This value is in the same range as for the pure CO₂ sorption measurements on activated carbon, Gensterblum et al. (2009) reported an average maximum value of 8 ± 0.16 mol/kg. Hence the presence of impurities does not significantly influence the maximum sorption capacity of activated carbon.

5.3 Conclusions

Pure gases have their own specific EoS, as in the case of the CO₂, built up with many fitting parameters. In the case of a mixture we cannot follow the same procedure because of the presence of more variables, such as the concentration of the different components. An optimal choice is to use an experimental procedure to obtain an acceptable EoS. A lack of accuracy always affects such measurements.

In this paper we determined that:

- at the range of P and T of this study, the gas mixtures are not reacting with the activated carbon;
- the mixture concentration is constant at each equilibrium step during a desorption process;
- the amount of helium mixture adsorbed by the activated carbon at 165 bar is 0.25 mol/kg;
- no theoretical EoS is accurately describing the CO₂ mixture;
- in our type of experiments the amount of CO₂ mixture adsorbed on activated carbon cannot be calculated accurately. The maximum of the excess sorption can vary of 25.88% depending on which EoS is used for the calculations;
- when a combination of two different EoS has been used, the maximum sorption is 7.81 mol/kg at 49.13 bar. This is in agreement with the literature concerning pure CO₂ sorption on activated carbon.

5.4 Acknowledgement

The experiments have been performed under the GRASP (Green-House Gas Removal Apprenticeship) Marie Curie programme. Experiments of gas sorption on coal have been performed at GeoLab of the Department of Applied Earth Sciences, TU Delft. We thank Henk Van Asten for his technical support and expertise. We also thank the LEK RWTH-Aachen group, in particular Yves Gensterblum for providing us the data concerning the GERG-2004 EoS.

Chapter 6

Conclusions

Worldwide the injection of CO₂ for CH₄ production (CO₂-ECBM) is considered to be a pure gas. As mentioned in the introduction, purification of CO₂ will cost a considerable amount of energy when compared with the use of less purified CO₂. In this thesis we looked at impurities in the CO₂, either flue gas components or water, and their effects on coal behavior. First of all the base values were determined by using pure gases. Secondly, combinations of gases were introduced to verify whether EoS for single gases and multicomponent gases, for dry and wet coal could be adopted.

This thesis presents experimental results, conducted with manometric set ups, of pure gases sorption on dry and wet coal and sorption of flue gas type of gas mixtures on activated carbon. The new aspect of the thesis is on the enumeration of different ways to obtain sufficiently accurate EoS to be used in the manometric set up. The EoS have been tested for gas mixtures and the presence of water by using a combination of manometric set ups, a density meter and a mass spectrometer. In addition, we have measured swelling of coal under gas sorption, equilibration times for different gases and the influence of temperature. The experimental results allowed to interpret and test different models concerning sorption and thermodynamic behavior of gases. The most important conclusions of each chapter are discussed below.

- Chapter 2 investigates the time required for attaining equilibrium for gas sorption on coal. This time is dependent on the gas type and the temperature used in the experiment. Sorption and desorption isotherms for N₂, CH₄, CO₂ have been measured on Selar Cornish coal at 318 K and

338 K up to 160 bar. An increase in temperature is reducing the sorption capacity. N_2 and CH_4 do not show hysteresis during the desorption, CO_2 do show hysteresis. Swelling measurements on unconfined cubic samples reveal that CO_2 sorption induces a swelling effect on coal that is fully reversible. The excess sorption isotherm have been converted to absolute sorption and fitted with a Langmuir type of curve. In order to convert excess to absolute sorption, the adsorbed phase density has been derived. The physical meaning of the extrapolated absolute density of CO_2 obtained from the excess sorption isotherm is not clear. This can indicate that either the line extrapolation is not a valid method or the model of adsorbate storage is oversimplified.

- Chapter 3 experimentally shows that the density of CO_2 and H_2O mixture in the gas phase can be calculated using the Span & Wagner EoS for pure CO_2 and that the dissolution of CO_2 in water can be calculated using a model derived from the Strijek-Vera EoS. The density of the CO_2 has been measured in its sorbed phase in water showing a good agreement with literature data. A Monte Carlo simulation has been run in order to establish the error on the excess sorption measurements. Errors are ranging from a minimum of 0.6% to a maximum of 4.2%. Comparison of sorption experiments conducted on wet coal and dry Tupton coal reveal that the presence of water is reducing the CO_2 sorption capacity of the coal. In a coal with 4.6% content of water, the maximum sorption is reduced by 16%.
- Chapter 4 studies the behavior of two different gas mixtures, both containing NO_x . The first one is a He mixture composed of 98% He, 1% O_2 and 1% NO_2 ; the second is a CO_2 mixture composed of 97% CO_2 , 1% He, 1% O_2 and 1% NO_2 . The first mixture has been introduced to test the procedure with a gas of which the EoS can be easily obtained. The second mixture is representative for the flue gas after removing N_2 . In order to test the adequacy of the EoS we measured in the manometric set up the volume ratio between the empty sample cell and the reference cell at different pressures. Results show that the Mc Carty EoS of pure Helium can also be used to accurately describe the He rich mixture. In this case, the maximum relative difference from the experimentally determined density is of $6 \cdot 10^{-3}$. None of the considered EoS and mixing rule can be used for the CO_2 rich mixture. Measurements concerning CO_2 mixtures are more sensitive to an accurate EoS because the experimental conditions are close to the CO_2 critical point. It is also well known

that the other gases in the mixture change the location of the critical point and thus have a large influence on the densities, reducing the adequacy of the EoS. The manometric set up can be used to measure the density values of a gas mixture provided that at least a single density value has been measured at the same conditions with another available technique, e.g., with a density meter. These experimental values can be used in order to determine an accurate EoS to process sorption experiments on coal.

- Chapter 5 uses the density data for the CO₂ rich mixture in order to obtain a model that could predict efficiently enough density data from P, T, V values. A combination of two different EoS has been used for this purpose. Sorption experiments have been conducted using a manometric set up and activated carbon as sorbent at a constant temperature of 318.15 K and up to a pressure of 160 bar. The composition of the gas mixture has been measured after every desorption step. For this we used a mass spectrometer. It turns out that when equilibrium is reached, the concentration of the different components of the mixture is constant throughout the desorption experiment. Consequently, no reaction, in this range of pressures and temperatures, occurs between the gas mixture and activated carbon. It turns out that the amount of the Helium mixture adsorbed by activated carbon at 165 bar is 0.25 mol/kg, meanwhile the amount of CO₂ mixture adsorbed on activated carbon cannot be calculated accurately. The maximum of the excess sorption can vary of 25.88% depending on which EoS is used for the calculations. The maximum of the excess sorption using the combination of two different EoS is giving a value of 7.81 mol/kg, which is in agreement with the literature concerning pure CO₂ sorption on activated carbon.

This study provides input data for EoS and sorption behavior for flue gas and it is a starting point for flue gas-coal interaction. Additional research can be built on the results of this thesis. The models used in this study should be validated also for other NO_x and SO_x concentrations in the flue gas. The competitive adsorption of the different gas components can be determined using a combination of core flooding experiments and mass spectrometer detection. The presence of impurities and their effects on the wettability can be measured and compared with the existing data on pure CO₂. The results here presented can be used as input parameters in reservoir simulations dealing with CO₂ or flue gas driven ECBM.

Appendix A

Absolute sorption

The absolute sorption is the total amount of fluid residing per unit mass. In the sorption experiments it can be described as

$$m_{abs} = n_T - \rho_g V_g, \quad (\text{A.1})$$

where V_g is the volume of the gas in the sample cell in the free phase, ρ_g is the density of the CO_2 in its free phase, n_T is the total amount of CO_2 present in the sample cell, m_{abs} is the absolute amount of CO_2 adsorbed per mass of coal and m_{exc} is the excess amount of CO_2 adsorbed per mass of coal. The volume of the sample cell (V_{sc}) is assumed to be constant and can be expressed as

$$V_{sc} = V_g + V_{coal} + V_a, \quad (\text{A.2})$$

where V_a is the volume occupied by the CO_2 in the adsorbed state and V_{coal} is the volume occupied by the coal sample. The volume occupied by the CO_2 in the adsorbed state can be defined as

$$V_a = \frac{m_{abs}}{\rho_a}, \quad (\text{A.3})$$

where ρ_a is the density of the gas in the adsorbed phase and it is assumed to be constant. The coal is swelling due to the CO_2 sorption. The volume of coal can be expressed as

$$V_{coal} = V_0(\epsilon_v + 1), \quad (\text{A.4})$$

where V_0 is the initial volume of coal, ϵ_v is the volumetric swelling that can be obtained using the Langmuir isotherm:

$$\epsilon_v = \frac{\epsilon_{\max} \rho_g}{b_V + \rho_g}, \quad (\text{A.5})$$

where ϵ_{\max} is the maximum swelling and b_v is the Langmuir constant. The absolute sorption can be calculated including also the swelling effect in it. Substituting Eq.A.2, Eq.A.3 and Eq.A.4 in Eq.A.1, we obtain:

$$m_{abs} = n_T - \rho_g [V_{sc} - (\rho_a m_a) - (V_0(\epsilon_v + 1))]. \quad (\text{A.6})$$

The unknown of the system are: m_{abs} , V_a , V_g and V_{coal} . The value of the density of the gas in its adsorbed phase has been extrapolated from the excess sorption curve and compared with the model results on the excess sorption fitting (see 2.3.4), the b_V and ϵ_{max} parameter of the Langmuir fitting have been taken from the experimental results.

Appendix B

Error determination

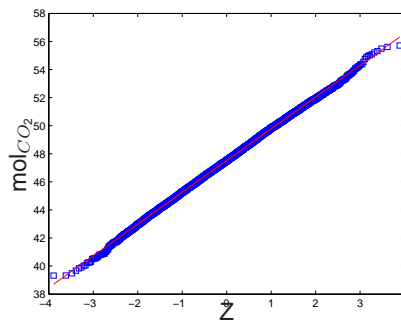


Figure B.1: Probability plot of an excess sorption value. The obtained value is plotted versus the variable Z in its standard normal form. The average is obtained for $z=0$ and the slope is equal to the standard deviation.

Table B.1: Accuracy of data measurements

Pressure [bar]	Temperature [K]	Ref cell volume [dm ³]	volume ratio [-]
0.1	0.02	10 ⁻⁵	0.007

The purpose of this appendix is to determine the error in the excess sorption measurements. The excess sorption n_{excess} is calculated cumulatively, i.e., using the equation

$$n_{excess,N} = \sum_{i=1}^N (\rho_{fill,i} - \rho_{eq,i}) V_{ref} - \rho_{eq,N} \chi V_{ref}, \quad (B.1)$$

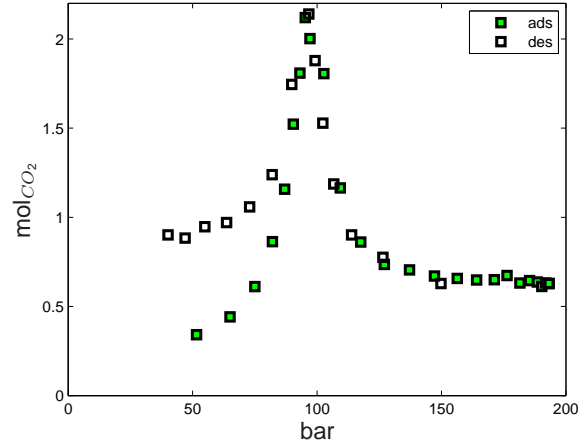


Figure B.2: Standard deviation of each pressure step plotted versus pressure (full dots are the adsorption steps, empty dots are representative of the desorption steps). Data are obtained from a CO_2 excess sorption isotherm on coal measured at 318.15 K.

where in this case $N = 42$, including all the sorption and desorption steps of the examined excess sorption experiment. The last point of the sorption curve is the first point of the desorption. It is expected by the way that B.1 is defined, that the error propagates and becomes bigger after each step in the calculations. In order to predict the influence of the error in our excess sorption isotherms, a Monte Carlo simulation has been performed using a Matlab program. This simulation takes into account the random errors in the experimental measurements. The precision of the pressure and temperature is given by the manufacturer who calibrated the instrument. The error (standard deviation) in the volume ratio and the volume of the reference cell can be equated to the

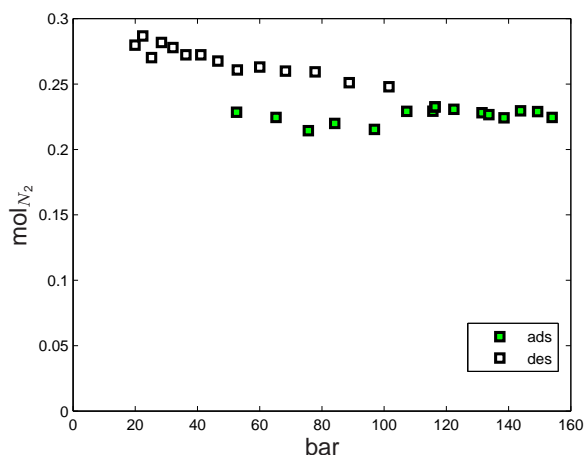


Figure B.3: Standard deviation of each pressure step plotted versus pressure (full dots are the adsorption steps, empty dots are representative of the desorption steps). Data are obtained from a N_2 excess sorption isotherm on coal measured at 318.15 K.

precision determined from the experimental data. B.1 reports all the standard deviations. All the errors are assumed to be random as the systematic error has been put to zero after calibration. It is assumed that errors are normally distributed. In the simulation the volume of the reference cell and the volume ratio are assumed to be constant and not affected by an error. Eq. B.1 is applied using a pressure and a temperature to which a normally distributed random error is added before it is substituted into the Span and Wagner EoS to obtain the density values. As a result N excess adsorption values, $n_{excess,i}$, are obtained. Subsequently this procedure is repeated one thousand times. As a result, for each pressure step, there are $M = 1000$ values. For each pressure step $i = 1, \dots, N$, the M values are ordered in ascending order and the estimated cumulative distribution function $(j - 1/2)/M$ has been assigned to them. Fig. B.1 shows the probability plot (i.e. the obtained values are plotted versus the variable Z in its standard normal form) for one pressure step by way of example. These plots are used to find the average and the standard deviation of each excess sorption value. Fig. B.2 shows the standard deviation of each single pressure step plotted versus pressure. The random error, given by

the pressure and temperature accuracy, is cumulative as can be observed by the increasing trend of the error. However, around the critical region another phenomenon takes place. We assert that this behavior can be attributed to the non-linear behavior of the EoS, in particular near the critical point of CO₂. By way of example, Fig. B.3 describes the standard deviation calculated following the same procedure applied to a nitrogen excess sorption experiment on coal. The experimental conditions are the same as for the CO₂ measurements. In this case there is not a non-linear behavior. The reason for it is that, in this case, the nitrogen density is approximately linear with the pressure. This is due to the fact that, for the conditions of interest, nitrogen is far away from its critical point.

Appendix C

UNIFAC model

Here the theory that can be found in Fredenslund et al. (1977) has been followed. This part has been included for easy reference. The UNIFAC model can be used in order to obtain the Gibbs free energy for the calculation of the density of a gas mixture using Eq.4.18. The mixture is considered to be composed of its different affinity groups, each of them composed of different molecules. The Gibbs free energy is

$$g_0^E = \sum_{i=1}^N \ln \gamma_i, \quad (\text{C.1})$$

where γ_i is the activity coefficient of component (i). Using the UNIFAC theory it can be expressed as the sum of a combinatorial (C) part, essentially due to differences in size and shape of the molecules in the mixture, and a residual (R) part, essentially due to energy interactions. Therefore it can be written for the activity coefficient

$$\ln \gamma_i = \ln \gamma_i^C + \ln \gamma_i^R. \quad (\text{C.2})$$

The combinatorial activity coefficient for component (i) is

$$\ln \gamma_i^C = \ln \frac{\Phi_i}{x_i} + \frac{z}{2} q_i \ln \frac{\Theta_i}{\Phi_i} + l_i - \frac{\Phi_i}{x_i} \sum_{j=1}^{N_c} x_j l_j, \quad (\text{C.3})$$

where N_c is the number of components, z is a parameter equal to 10 and

$$l_i = \frac{z}{2}(r_i - q_i) - (r_i - 1). \quad (\text{C.4})$$

The molecular surface area fraction Θ_i is defined as

$$\Theta_i = \frac{q_i x_i}{\sum_{j=1}^{N_c} q_j x_j}, \quad (\text{C.5})$$

here q_i denotes the van der Waals surface area that is given by

$$q_i = \sum_{k=1}^{N_g} v_k^{(i)} Q_k, \quad (\text{C.6})$$

where $k=1\dots N_g$ is the number of groups in molecule (i), $v_k^{(i)}$ is the number of groups of kind k in molecule (i). The molecular volume fraction Φ_i can be expressed as

$$\Phi_i = \frac{r_i x_i}{\sum_{j=1}^{N_c} r_j x_j}, \quad (\text{C.7})$$

where r_i is the van der Waals volume expressed as

$$r_i = \sum_{k=1}^{N_g} v_k^{(i)} R_k. \quad (\text{C.8})$$

The parameters R_k and Q_k can be found in the literature (Fischer and Gmehling, 1995; Gmehling et al., 1997; Horstmann et al., 2005) and are reported in Table 4.1.

The residual part is assumed to be the sum of the individual contributions of each solute group in the solution minus the sum of the individual contributions in the pure-component environment, i.e.,

$$\ln \gamma^R = \sum_{k=1}^{N_g} v_k^{(i)} \left[\ln \Gamma_k - \ln \Gamma_k^{(i)} \right], \quad (\text{C.9})$$

where Γ_k is the residual activity coefficient of group k in a solution and Γ_k^i is the residual activity coefficient of group k in a reference solution containing only molecules of type (i). The residual activity coefficient $\ln \Gamma_k^{(i)}$ and $\ln \Gamma_k$ are

$$\ln \Gamma_k = Q_k \left[1 - \ln \left(\sum_{m=1}^{N_g} \Theta_m \Psi_{mk} \right) - \sum_{M=1}^{N_g} \left(\frac{\Theta_m \Psi_{km}}{\sum_{n=1}^{N_g} \Theta_n \Psi_{nm}} \right) \right], \quad (\text{C.10})$$

with $m=1\dots N_g$ and $n=1\dots N_g$ that are all the different groups present in the mixture. In our case, where the family of the molecules coincide with the groups, we have $\ln \Gamma_k^i = 0$.

The group surface area Θ_m is equal to

$$\Theta_m = \frac{Q_m X_m}{\sum_{n=1}^{Ng} Q_n X_n}, \quad (\text{C.11})$$

where the group fraction is

$$X_m = \frac{\sum_{j=1}^{Ng} v_m^{(j)} x_j}{\sum_{j=1}^{Ng} \sum_{n=1}^{Ng} v_n^{(j)} x_j}, \quad (\text{C.12})$$

and the parameter Ψ_{nm} is given by:

$$\Psi_{nm} = \exp\left(-\frac{a_{nm}}{T}\right). \quad (\text{C.13})$$

The group interaction parameters a_{nm} can be found in the literature (Fischer and Gmehling, 1995; Gmehling et al., 1997; Horstmann et al., 2005) and are reported in Table 4.3. There are no data concerning the group interaction parameters for NO_2 , then in these case we assume it to be zero.

The UNIFAC method has been implemented in Matlab.

Appendix D

Peneloux volume correction

In a system containing n_c components, the fugacity coefficients ϕ_i are given by

$$\ln \phi_i = \int_0^P \left(\frac{v_i}{RT} - \frac{1}{P} \right) dP, \quad (\text{D.1})$$

where $i=1 \dots n_c$ and v_i is the partial molar volume of component i . The equilibrium conditions for two phases ' and '' are given by

$$x'_i \phi'_i(T, P, x'_1, \dots, x'_{n_c}) = x''_i \phi''_i(T, P, x''_1, \dots, x''_{n_c}), \quad (\text{D.2})$$

In the case of a volume correction, a pseudo partial molar volume is defined as

$$\bar{v} = v + \sum_{i=1}^{N_c} c_i x_i, \quad (\text{D.3})$$

with

$$\bar{v}_i = v_i + c_i, \quad (\text{D.4})$$

where the volume correction c_i is dependent on the total pressure. Based on the experimental data we propose that c_i can be written as (see Eq. 5.4 for the definition of the terms)

$$c_i = -\beta_i e \left(\frac{-P}{P_0} \right)^{\gamma_i} + \delta_i. \quad (\text{D.5})$$

The pseudofugacity $\bar{\phi}_i$, i.e., the fugacity that includes the volume corrections, is

$$\ln \bar{\phi}_i = \int_0^P \left(\frac{\bar{v}_i}{RT} - \frac{1}{P} \right) dP = \ln \phi_i + \left(\frac{\beta_i e^{\alpha_i} + \delta_i P}{RT} \right), \quad (\text{D.6})$$

where

$$\alpha_i = - \left(\frac{P}{P_0} \right)^{\gamma_i}. \quad (\text{D.7})$$

Therefore, the pseudo EoS leads to the following equilibrium conditions given by

$$x'_i \phi'_i(T, P, x'_1, \dots, x'_{nc}) + \left(\frac{\beta_i e^{\alpha_i} + \delta_i P}{RT} \right) = x''_i \phi''_i(T, P, x''_1, \dots, x''_{nc}) + \left(\frac{\beta_i e^{\alpha_i} + \delta_i P}{RT} \right), \quad (\text{D.8})$$

where the apostrophes are indicating the two different phases of the system. Therefore, the equilibrium condition is not affected by a pressure dependent volume correction.

References

- Agarwal, R., Li, Y., Santollani, O., Satyro, M., Vieler, A., 2001a. Uncovering the realities of simulation. *Chemical Engineering Progress* 97, 42–51.
- Agarwal, R., Li, Y., Santollani, O., Satyro, M., Vieler, A., 2001b. Uncovering the realities of simulation. part 2. *Chemical Engineering Progress* 97, 64–72.
- Arri, L., Yee, D., Morgan, W., Jeansonne, M., 1992. Modeling coalbed methane production with binary gas sorption. *SPE Rocky Mountain Regional Meeting* .
- Bachu, S., 2008. CO₂ storage in geological media: Role, means, status and barriers to deployment. *Progress in Energy and Combustion Science* 34, 254 – 273.
- Battistutta, E., van Hemert, P., Lutynski, M., Bruining, H., Wolf, K., 2010. Swelling and sorption experiments on methane, nitrogen and carbon dioxide on dry Selar Cornish coal. *International Journal of Coal Geology* 84, 39 – 48.
- Battistutta, E., Lutynski, M., Rudolph, S., Bruining, H., Wolf, K., 2011. Adequacy of equation of state models for determination of adsorption of gas mixtures in a manometric set up. *International Journal of Coal Geology*, accepted .
- van Bergen, F., 2009. Effect of coal swelling on enhanced coalbed methane production: a field laboratory study. *Utrecht University, PhD Thesis* .
- van Bergen, F., Pagnier, H., Krzystolik, P., 2006. Field experiment of enhanced coalbed methane-CO₂ in the upper Silesian basin of Poland. *Environmental Geosciences* 13, 201–224.

- van Bergen, F., Spiers, C., Floor, F., Bots, P., 2009. Strain development in unconfined coals exposed to CO₂, CH₄ and Ar: Effect of moisture. *International Journal of Coal Geology* 77, 43 – 53.
- Bhatia, S., 1987. Modeling the pore structure of coal. *AIChE Journal* 33, 1707–1718.
- Brunetti, A., Scura, F., Barbieri, G., Drioli, E., 2010. Membrane technologies for CO₂ separation. *Journal of Membrane Science* 359, 115–125.
- Busch, A., Gensterblum, Y., 2011. CBM and CO₂-ECBM related sorption processes in coal: A review. *International Journal of Coal Geology* 87, 49 – 71.
- Busch, A., Gensterblum, Y., K., B.M., Littke, K., 2004. Methane and carbon dioxide adsorption-diffusion experiments on coal: upscaling and modeling. *International Journal of Coal Geology* 60, 151 – 168.
- Busch, A., Gensterblum, Y., Krooss, B., 2003. Methane and CO₂ sorption and desorption measurements on dry Argonne premium coals: pure components and mixtures. *International Journal of Coal Geology* 55, 205 – 224.
- Busch, A., Gensterblum, Y., Krooss, B.M., 2007. High-pressure sorption of nitrogen, carbon dioxide, and their mixtures on Argonne Premium coals. *Energy and Fuels* 21, 1640–1645.
- Busch, A., Gensterblum, Y., Krooss, B.M., Siemons, N., 2006. Investigation behaviour of high-pressure selective adsorption/desorption CO₂ and CH₄ on coals: An experimental study. *International Journal of Coal Geology* 66, 53 – 68.
- Bustin, R., Clarkson, C., 1998. Geological controls on coalbed methane reservoir capacity and gas content. *International Journal of Coal Geology* 38, 3–26.
- CDIAC, . Carbon dioxide information analysis center.
- Chaback, J., Morgan, W., Yee, D., 1996. Sorption of nitrogen, methane, carbon dioxide and their mixtures on bituminous coals at in-situ conditions. *Fluid Phase Equilibria* 117, 289–296.
- Chapel, D., Mariz, C., 1999. Recovery of CO₂ from flue gases: commercial trends. *Canadian Society of Chemical Engineers annual meeting* .

- Chapoy, A., Mohammadi, A.H., Chareton, A., Tohidi, B., Richon, D., 2004. Measurement and modeling of gas solubility and literature review of the properties for the carbon dioxide water system. *Industrial and Engineering Chemistry Research* 43, 1794–1802.
- Chen, J., Fischer, K., Gmehling, J., 2002. Modification of PSRK mixing rules and results for vapor-liquid equilibria, enthalpy of mixing and activity coefficients at infinite dilution. *Fluid Phase Equilibria* 200, 411 – 429.
- Chikatamarla, L., Cui, X., Bustin, R., 2004. Implications of volumetric swelling/shrinkage of coal in sequestration of acid gases. *International Coalbed Methane Symposium Proceedings Alabama*.
- Chueh, P.L., Prausnitz, J.M., 1967. Vapor-liquid equilibria at high pressures: Calculation of critical temperatures, volumes, and pressures of nonpolar mixtures. *AIChE Journal* 13, 1107–1113.
- Ciembroniewicz, A., Marecka, A., 1993. Kinetics of CO₂ sorption for two polish hard coals. *Fuel* 72, 405–408.
- Clarkson, C.R., Bustin, R.M., 1999a. The effect of pore structure and gas pressure upon the transport properties of coal: a laboratory and modeling study. 1. Isotherms and pore volume distributions. *Fuel* 78, 1333 – 1344.
- Clarkson, C.R., Bustin, R.M., 1999b. The effect of pore structure and gas pressure upon the transport properties of coal: a laboratory and modeling study. 2. Adsorption rate modeling. *Fuel* 78, 1345–1362.
- Clarkson, C.R., Bustin, R.M., 2000. Binary gas adsorption/desorption isotherms: effect of moisture and coal composition upon carbon dioxide selectivity over methane. *International Journal of Coal Geology* 42, 241 – 271.
- Connell, L.D., Lu, M., Pan, Z., 2010. An analytical coal permeability model for tri-axial strain and stress conditions. *International Journal of Coal Geology* 84, 103 – 114.
- Cook, P., 2009. Demonstration and deployment of carbon dioxide capture and storage in Australia. *Energy Procedia* 1, 3859 – 3866. *Greenhouse Gas Control Technologies 9, Proceedings of the 9th International Conference on Greenhouse Gas Control Technologies (GHGT-9), 16-20 November 2008, Washington DC, USA.*

- Cosam, A., Eiber, R., 2007. Fracture control in carbon dioxide pipeline. *Journal of pipeline Engineering* 6, 147–158.
- Cui, X., Bustin, R., Dipple, G., 2004. Selective transport of CO₂, CH₄, and N₂ in coals: Insights from modeling of experimental gas adsorption data. *Fuel* 83, 293–303.
- Cui, X., Bustin, R.M., Chikatamarla, L., 2007. Adsorption-induced coal swelling and stress: implications for methane production and acid gas sequestration into coal seams. *Journal of geophysical research solid earth* 112.
- Dahl, S., Michelsen, M.L., 1990. High-pressure vapor-liquid equilibrium with a UNIFAC-based equation of state. *AIChE Journal* 36, 1829–1836.
- Damen, K., 2007. The merits, costs and risks of carbon dioxide capture and storage. TU Delft PhD Thesis .
- Damen, K., Faaij, A., van Bergen, F., Gale, J., Lysen, L., 2003. Identification of early opportunities for CO₂ sequestration–worldwide screening for CO₂-EOR and CO₂-ECBM projects. *Energy* 30, 1931 – 1952.
- Day, S., Duffy, G., Sakurovs, R., Weir, S., 2008a. Effect of coal properties on CO₂ sorption capacity under supercritical conditions. *International Journal of Greenhouse Gas Control* 2, 342 – 352.
- Day, S., Fry, R., Sakurovs, R., 2007. Swelling of australian coal in supercritical CO₂. *International Journal of Coal Geology* 74, 41–52.
- Day, S., Sakurovs, R., Weir, S., 2008b. Supercritical gas sorption on moist coals. *International Journal of Coal Geology* 4, 203 – 214.
- DeGance, A., Morgan, W., Yee, D., 1993. High pressure adsorption of methane, nitrogen and carbon dioxide on coal substrates. *Fluid Phase Equilibria* 82, 215 – 224.
- Diamond, L.W., Akinfiev, N.N., 2003. Solubility of CO₂ in water from -1.5 to 100 C and from 0.1 to 100 MPa: evaluation of literature data and thermodynamic modelling. *Fluid Phase Equilibria* 208, 265 – 290.
- Dreisbach, F., Staudt, R., Keller, J.U., 1999. High pressure adsorption data of methane, nitrogen, carbon dioxide and their binary and ternary mixtures on activated carbon. *Adsorption-Journal of the International Adsorption Society* 5, 215–227.

- Duan, Z., Sun, R., 2003. An improved model calculating CO₂ solubility in pure water and aqueous NaCl solutions from 273 to 533 K and from 0 to 2000 bar. *Chemical Geology* 193, 257 – 271.
- Durucan, S., Ahsanb, M., Shia, J., 2009. Matrix shrinkage and swelling characteristics of european coals. *Energy Procedia* 1, 3055 – 3062.
- Eftekhari, A., Bruining, H., 2011. Energy analysis of underground coal gasification with simultaneous storage of carbon dioxide. *Chemical Geology under submission*.
- Fathi, E., Akkutlu, I., 2009. Matrix heterogeneity effects on gas transport and adsorption in coalbed and shale gas reservoirs. *Transport in Porous Media* 80, 281–304.
- Feron, P., Hendriks, C., 2005. CO₂ capture process principles and costs. *Oil and gas technology* 60, 451–459.
- Fischer, K., Gmehling, J., 1995. Further development, status and results of the PSRK method for the prediction of vapor-liquid equilibria and gas solubilities. *Fluid Phase Equilibria* 112, 1 – 22.
- Fitzgerald, J., Pan, Z., Sudibandriyo, M., Robinson, R., Gasem, K., Reeves, S., 2005. Adsorption of methane, nitrogen, carbon dioxide and their mixtures on wet Tiffany coal. *Fuel* 84, 2351 – 2363.
- Forster, A., Norden, B., Zink-Jorgensen, K., Frykma, K., Kulenkampff, J., Spangenberg, E., 2006. Baseline characterization of the CO₂ SINK geological site at ketzin, germany. *Environmental Sciences* 13, 145–161.
- Fredenslund, A., Gmehling, J., Rasmussen, P., 1977. Vapor-liquid equilibria using UNIFAC, a group-contribution method. Elsevier .
- Fujii, T., Sato, Y., Lin, H., Inomata, H., Hashida, T., 2009. Evaluation of co₂ sorption capacity of rocks using a gravimetric method for co₂ geological sequestration. *Energy Procedia* 1, 3723 – 3730.
- Gensterblum, Y., van Hemert, P., Billemont, P., Battistutta, E., Busch, A., Krooss, B., De Weireld, G., Wolf, K.H., 2010. European inter-laboratory comparison of high pressure CO₂ sorption isotherms II: Natural coals. *International Journal of Coal Geology* 84, 115–124.

- Gensterblum, Y., van Hemert, P., Billefont, P., Busch, A., Charriere, D., Li, D.f., Krooss, B., de Weireld, G., Prinz, D., Wolf, K.H., 2009. European inter-laboratory comparison of high pressure CO₂ sorption isotherms. I: Activated carbon. *Carbon* 47, 2958–2969.
- Gmehling, J., Li, J., Fischer, K., 1997. Further development of the PSRK model for the prediction of gas solubilities and vapor-liquid -equilibria at low and high pressures II. *Fluid Phase Equilibria* 141, 113 – 127.
- Gmelin, J., 1978. *Gmelin handbook of inorganic and organometallic chemistry*
- Goodman, A., Busch, A., Bustin, R., Chikatamarla, L., Day, S., Duffy, G., Fitzgerald, J., Gasem, K., Gensterblum, Y., Hartman, C., Jing, C., Krooss, B., Mohammed, S., Pratt, T., Robinson, R., Romanov, V., Sakurovs, R., Schroeder, K., White, C., 2007. Inter-laboratory comparison II: CO₂ isotherms measured on moisture-equilibrated Argonne premium coals at 55 C and up to 15 MPa. *International Journal of Coal Geology* 72, 153 – 164.
- Goodman, A.L., Busch, A., Duffy, G.J., Fitzgerald, J.E., Gasern, K.A.M., Gensterblum, Y., Krooss, B.M., Levy, J., Ozdemir, E., Pan, Z., Robinson, L., Schroeder, K., Sudibandriyo, M., White, C., 2004. An inter-laboratory comparison of CO₂ isotherms measured on Argonne premium coal samples. *Energy and Fuels* 18, 1175–1182.
- Goodman, A.L., Favors, R.N., Larsen, J.W., 2006. Argonne coals rearrangement caused by sorption of CO₂. *Energy and Fuels* 20, 2537–2543.
- Gray, P.G., Do, D., 1993. Modelling of the interaction of nitrogen dioxide with activated carbon. II kinetics of reaction with pore evolution. *Chemical Engineering communications* 125, 109–120.
- Gruskiewicz, M., Naney, M., Blencoe, J., Cole, D., Pashin, J., Carroll, R., 2009. Adsorption kinetics of CO₂, CH₄, and their equimolar mixture on coal from the Black Warrior Basin, West-Central Alabama. *International Journal of Coal Geology* 77, 23 – 33.
- Gunter, W., Mavor, M., Robinson, J., 2005. CO₂ storage and enhanced coal-bed methane production: field testing at Fenn-Big Valley, Alberta, Canada. *Proceeding of the 7th international conference on greenhouse gas control technologies* 1, 413–422.

- Hall, F., Zhou, C., Gasem, K., Jr., R.R., 1994. Adsorption of pure methane, nitrogen, and carbon dioxide and their binary mixtures on Wet Fruitland coal. SPE Eastern Regional Meeting, 8-10 November 1994, Charleston, West Virginia .
- Harpalani, S., Chen, G., 1997. Influence of gas production induced volumetric strain on permeability of coal. *Geotechnical and Geological Engineering* 15, 303–325.
- Hemert, P.v., Bruining, J., Rudolph, E.S.J., Wolf, K., Maas, J., 2009. Improved manometric set-up for the accurate determination of supercritical carbon dioxide sorption. *Adsorption-Journal of the International Adsorption Society* 8, 111–123.
- Herzog, H., 2001. What future for carbon capture and sequestration? *Environmental science and technology* 35, 148–153.
- Hol, S., Peach, C., Spiers, C., 2011. A new experimental method to determine the CO₂ sorption capacity of coal. *Energy Procedia* 4, 3125 – 3130. 10th International Conference on Greenhouse Gas Control Technologies.
- Holderbaum, T., Gmehling, J., 1991. PSRK: A group contribution equation of state based on UNIFAC. *Fluid Phase Equilibria* 70, 251 – 265.
- Horkova, S., Benson, S., Doughty, C., Freifield, B., Sakurai, A., Daley, T., 2006. Measuring permanence of CO₂ storage in saline formations: the frio experiment. *Environmental Geosciences* 13, 105–121.
- Horstmann, S., Jabloniec, A., Krafczyk, J., Fischer, K., Gmehling, J., 2005. PSRK group contribution equation of state: comprehensive revision and extension IV, including critical constants and [alpha]-function parameters for 1000 components. *Fluid Phase Equilibria* 227, 157 – 164.
- Huang, X., Margulis, C., Li, H., Berne, B.J., 2005. Why is the partial pressure of CO₂ so small when dissolved in a room temperature ionic liquid? Structure and dynamics of CO₂ dissolved in [Bmin+][PF6-]. *Journal of American Chemical Society* 127, 17842–17851.
- Huijgen, W., Ruijg, G., Comans, R., Witkamp, G., 2006. Energy consumption and net CO₂ sequestration of aqueous mineral carbonation. *Industrial & engineering chemistry research* 45, 9184–9194.

Huron, M., Vidal, J., 1979a. New mixing rules in simple equations of state for representing vapour-liquid equilibria of strongly non-ideal mixtures. *Fluid Phase Equilibria* 3, 255 – 271.

Huron, M., Vidal, J., 1979b. New mixing rules in simple equations of state for representing vapour-liquid equilibria of strongly non-ideal mixtures. *Fluid Phase Equilibria* 3, 255 – 271.

IEA, 2007. International energy outlook 2007. US DOE www.eia.doe.gov/oiaf/ieo/index.html.

IEA, G., 2004. Impact of impurities on CO₂ capture transport and storage , Report Number PH4/32.

Jacquemet, N., Le Gallo, Y., Estublier, A., Lachet, V., von Dalwigk, I., Yan, J., Azaroual, M., Audigane, P., 2009. CO₂ streams containing associated components—A review of the thermodynamic and geochemical properties and assessment of some reactive transport codes. *Energy Procedia* 1, 3739 – 3746.

Joubert, J.I., Grein, C.T., Bienstock, D., 1974. Effect of moisture on the methane capacity of american coals. *Fuel* 53, 186 – 191.

King, A.D., Coan, C.R., 1971. Solubility of water in compressed carbon dioxide, nitrous oxide, and ethane. evidence for hydration of carbon dioxide and nitrous oxide in the gas phase. *Journal of the American Chemical Society* 93, 1857–1862.

King, G., Ertekin, T., 1995. State-of-the-art modeling for unconventional gas recovery, part II: recent developments. *Low Permeability Reservoirs Symposium*, 19-22 March 1995, Denver, Colorado .

King, M., Mubarak, A., Kim, J.D., Bott, T.R., 1992. The mutual solubilities of water with supercritical and liquid carbon dioxides. *The Journal of Supercritical Fluids* 5, 296 – 302.

Krooss, B.M., van Bergen, F., Gensterblum, Y., Siemons, N., Pagnier, H.J.M., David, P., 2002. High-pressure methane and carbon dioxide adsorption on dry and moisture-equilibrated pennsylvanian coals. *International Journal of Coal Geology* 51, 69 – 92.

- Kunz, O., Klimeck, R., Wagner, W., Jaeschke, M., 2007. The GERG-2004 wide-range equation of state for natural gases and other mixtures. GERG TM15, Fortschritt-Berichte VDI 6.
- Kwak, T., Mansoori, G., 1986. Van der Waals mixing rules for cubic equations of state. Applications for supercritical fluid extraction modelling. *Chemical Engineering Science* 41, 1303 – 1309.
- Levine, J., 1996. Model study of influence of matrix shrinkage on absolute permeability of coal bed reservoirs. Geological Society, London, special publications 109, 197–212.
- Li, H., Yan, J., 2009a. Evaluating cubic equations of state for calculation of vapor-liquid equilibrium of CO₂ and CO₂-mixtures for CO₂ capture and storage processes. *Applied Energy* 86, 826 – 836.
- Li, H., Yan, J., 2009b. Impacts of equations of state (EOS) and impurities on the volume calculation of CO₂ mixtures in the applications of CO₂ capture and storage (CCS) processes. *Applied Energy* 86, 2760 – 2770.
- Li, H., Yan, J., Anheden, M., 2009. Impurity impacts on the purification process in oxy-fuel combustion based CO₂ capture and storage system. *Applied Energy* 86, 202 – 213.
- Liu, H., Shao, Y., 2010. Predictions of the impurities in the CO₂ stream of an oxy-coal combustion plant. *Applied Energy* 87, 3162 – 3170.
- Majewska, Z., Ceglarska-Stefanska, G., Majewski, S., Zietek, J., 2009. Binary gas sorption/desorption experiments on a bituminous coal: Simultaneous measurements on sorption kinetics, volumetric strain and acoustic emission. *International Journal of Coal Geology* 77, 90 – 102.
- Marecka, A., Mianowski, A., 1998. Kinetics of CO₂ and CH₄ sorption on high rank coal at ambient temperatures. *Fuel* 77, 1691–1696.
- Mastalerz, M., Gluskoter, H., Rupp, J., 2004. Carbon dioxide and methane sorption in high volatile bituminous coals from Indiana, USA. *International Journal of Coal Geology* 60, 43 – 55.
- Mather, A.E., Franck, E.U., 1992. Phase equilibria in the system carbon dioxide-water at elevated pressures. *The Journal of Physical Chemistry* 96, 6–8.

- Mathias, P.M., Copeman, T.W., 1983. Extension of the Peng-Robinson equation of state to complex mixtures: Evaluation of the various forms of the local composition concept. *Fluid Phase Equilibria* 13, 91 – 108.
- Mavor, M., Hartman, C., Pratt, T., 2004. Unvertainty in sorption isotherm measurements. *Proceeding International Coalbed Methane Symposium Tuscaloosa*.
- Mazumder, S., 2007. Dynamics of CO₂ in coal as a reservoir. TU Delft PhD Thesis .
- Mazumder, S., Bruining, H., Wolf, K.H., 2006a. Swelling and anomalous diffusion mechanism of CO₂ in coal. *International coalbed methane symposium* .
- Mazumder, S., Bruining, J., 2007. Anomalous diffusion behavior of CO₂ in the macromolecular network structure of coal and its significance for CO₂ sequestration, pp. 627–633.
- Mazumder, S., van Hemert, P., Busch, A., Wolf, K.H., Tejera-Cuesta, P., 2006b. Flue gas and pure CO₂ sorption properties of coal: A comparative study. *International Journal of Coal Geology* 67, 267 – 279.
- Mazumder, S., Wolf, K.H., 2007. Differential swelling and permeability change of coal in response to CO₂ injection for ECBM. *International Journal of Coal Geology* 74, 123 – 138.
- Mazumder, S., Wolf, K.H., Elewaut, K., Ephraim, R., 2006c. Application of x-ray computed tomography for analyzing cleat spacing and cleat aperture in coal samples. *International Journal of Coal Geology* 68, 205 – 222.
- Mazzotti, M., Pini, R., Storti, G., 2009. Enhanced coalbed methane recovery. *The Journal of Supercritical Fluids* 47, 619 – 627.
- McCarty, R., Arp, V., 1990. A new wide range equation of state for helium. *Advances in cryogenic engineering* 35.
- van der Meer, L., Hartman, J., Geel, C., Kreft, E., 2005. Re-injecting CO₂ into an offshore gas reservoir at a depth of nearly 4000 metres sub-sea, in: Rubin, E., Keith, D., Gilboy, C., Wilson, M., Morris, T., Gale, J., Thambimuthu, K. (Eds.), *Greenhouse Gas Control Technologies* 7. Elsevier Science Ltd, pp. 521 – 529.

- Metz, B., Davidson, O., de Coninck, H., Loos, M., Mayer, L., IPCC 2005. Special report on carbon dioxide capture and storage. Cambridge, UK and New York, NY, USA Cambridge University press.
- Mikelic, A., Bruining, H., 2008. Analysis of model equations for stress-enhanced diffusion in coal layers. part I: Existence of a weak solution. *SIAM Journal on Mathematical Analysis* 40, 1671–1691.
- Mimura, T., Simayoshi, H., Suda, T., Iijima, M., Mituoka, S., 1997. Development of energy saving technology for flue gas carbon dioxide recovery in power plant by chemical absorption method and steam system. *Energy Conversion and Management* 38, S57 – S62. Proceedings of the Third International Conference on Carbon Dioxide Removal.
- Mohammad, S., Fitzgerald, J., Robinson, R.L., Gasem, K.A.M., 2009a. Experimental uncertainties in volumetric methods for measuring equilibrium adsorption. *Energy and Fuels* 23, 2810–2820.
- Mohammad, S.A., Chen, J.S., Fitzgerald, J.E., Robinson, R.L., Gasem, K.A.M., 2009b. Adsorption of pure carbon dioxide on Wet Argonne coals at 328.2 K and pressures up to 13.8 MPa. *Energy and Fuels* 23, 1107–1117.
- Moritis, G., 2006. CO₂ injection gains momentum. *Oil and gas journal* 104, 37–57.
- Muller, G., Bender, E., Maurer, G., 1988. Das dampf-flüssigkeitsgleichgewicht des ternären systems ammoniak-kohlendioxid-wasser bei hohen wassergehalten im bereich zwischen 373 und 473 Kelvin. *Energy and Fuels* 23, 2810–2820.
- Murata, K., El-Merraoui, M., Kaneko, K., 2001. A new determination method of absolute adsorption isotherm of supercritical gases under high pressure with a special relevance to density-functional theory study. *The Journal of Chemical Physics* 114, 4196–4205.
- Neathery, J.K., Rubel, A.M., Stencel, J.M., 1997. Uptake of NOX by activated carbons: bench-scale and pilot-plant testing. *Carbon* 35, 1321 – 1327.
- Ottiger, S., Pini, R., Storti, G., Mazzotti, M., 2008. Measuring and modeling the competitive adsorption for CO₂, CH₄, and N₂ on a dry coal. *Langmuir* 24, 9531–9540.

- Ottiger, S., Pini, R., Storti, G., Mazzotti, M., Bencini, R., Quattrocchi, F., Sardu, G., Derui, G., 2006. Adsorption of pure carbon dioxide and methane on dry coal from the Sulcis coal province (SW Sardinia, Italy). *Environmental Progress* 25, 355–364.
- Oyenekan, B.A., Rochelle, G.T., 2006. Energy performance of stripper configurations for CO₂ capture by aqueous amines. *Industrial and Engineering Chemistry Research* 45, 2457–2464.
- Ozdemir, E., Schroeder, K., 2009. Effect of moisture on adsorption isotherms and adsorption capacities of CO₂ on coals. *Energy and Fuels* 23, 2821–2831.
- Palmer, I., Mansoori, J., 1998. How permeability depends on stress and pore pressure in coalbeds: A new model. *SPE Reservoir Evaluation and Engineering* 1, 539–544.
- Pan, Z., Connell, L., 2007. A theoretical model for gas adsorption-induced coal swelling. *International Journal of Coal Geology* 69, 243–252.
- Panagiotopoulos, A.Z., Reid, R.C., 1986. New Mixing Rule for Cubic Equations of State for Highly Polar, Asymmetric Systems. chapter 29. pp. 571–582.
- Pekot, L., Reeves, S., 2003. Modeling the effects of matrix shrinkage and differential swelling on coal methane recovery and carbon sequestration. *International Coalbed Methane Symposium* .
- Peneloux, A. and Rauzy, E., Freze, R., 1982. A consistent correction for Redlich-Kwong-Soave volumes. *Fluid Phase Equilibria* 8, 7 – 23.
- Peng, D., Robinson, D., 1976. A new two-constant equation of state. *Industrial and Engineering Chemistry Fundamentals* 15, 59–64.
- Pini, R., Ottiger, L., Storti, G., Mazzotti, M., 2009. Role of adsorption and swelling on the dynamics of gas injection in coal. *Journal of Geophysical Research, Solid Earth* 114.
- Prinz, D., Littke, R., 2005. Development of the micro- and ultramicroporous structure of coals with rank as deduced from the accessibility to water. *Fuel* 84, 1645 – 1652.

- Prusty, B., 2008. Sorption of methane and CO₂ for enhanced coalbed methane recovery and carbon dioxide sequestration. *Journal of Natural Gas Chemistry* 17, 29 – 38.
- Reeves, S., 2001. Geological Sequestration of CO₂ in Deep, Unmineable Coalbeds: An Integrated Research and Commercial-Scale Field Demonstration Project. SPE Annual Technical Conference and Exhibition .
- Reeves, S., 2003. Coal-seq project update: field studies of ecbm recovery/CO₂ sequestration in coal seams. *Proceeding of the 6th international conference on greenhouse gas control technologies* 1, 557–562.
- Reeves, S., 2006. An overview of CO₂-ecbm/sequestration in coal seams. AAPG Special publication on Geological sequestration of CO₂ 59, 17–32.
- Reucroft, P., Patel, H., 1986. Gas-induced swelling in coal. *Fuel* 65, 816–820.
- Riahi, K., Rubin, E., Schratzenholzer, L., 2004. Prospects for carbon capture and sequestration technologies assuming their technological learning. *Energy* 29, 1309 – 1318. 6th International Conference on Greenhouse Gas Control Technologies.
- Riddiford, F., Tourqui, A., Bishop, C., Taylor, B., Smith, M., 2004. A cleaner development: the In Salah gas project, Algeria. Gale, J.J. and Kaya, Y. editors 1, 601–606. 6th International Conference on Greenhouse Gas Control Technologies.
- Ritger, P., 1987. Transport of penetrants in the macromolecular structure of coals. *Fuel* , 66.
- Robertson, E., 2005. Measurements and modelings of sorption-induced strain and permeability changes in coal. prepared for the U.S. department of energy through the INL LDRD program under DOE Idaho operations office. [contract de-ac07-051d14517] .
- Romanov, V., 2007. Coal chemistry for mechanical engineers: From macromolecular thermodynamics to reservoir simulation. *Energy and Fuels* 21, 1646–1654.
- Romanov, V.N., Goodman, A.L., Larsen, J.W., 2006. Errors in CO₂ adsorption measurements caused by coal swelling. *Energy and Fuels* 20, 415–416.

- Rubel, A.M., Stencel, J.M., 1996. Effect of pressure on NO_x adsorption by activated carbons. *Energy and Fuels* 10, 704–708.
- Rubel, A.M., Stencel, J.M., 1997. The effect of low-concentration SO₂ on the adsorption of NO from gas over activated carbon. *Fuel* 76, 521 – 526.
- Rubin, E., Chen, C., Rao, A., 2007. Cost and performance of fossil fuel power plants with CO₂ capture and storage. *Energy Policy* 35, 4444 – 4454.
- Ruckenstein, E., Vaidyanathan, A., Youngquist, G., 1971. Sorption by solids with bidisperse pore structures. *Chemical Engineering Science* 26, 1305–1318.
- Saghafi, A., Faiz, M., Roberts, D., 2007. CO₂ storage and gas diffusivity properties of coals from Sydney Basin, Australia. *International Journal of Coal Geology* 70, 240–254.
- Sakurovs, R., Day, S., Duffy, G., , Weir, S., 2007. Application of a modified Dubinin-Radushkevich equation to adsorption of gases by coals under supercritical conditions. *Energy and fuels* 21, 992–997.
- Sakurovs, R., Day, S., Weir, S., 2009. Causes and consequences of errors in determining sorption capacity of coals for carbon dioxide at high pressure. *International Journal of Coal Geology* 77, 16–22.
- Salem, M.M.K., Braeuer, P., von Szombathely, M., Heuchel, M., Harting, P., Quitzsch, K., Jaroniec, M., 1998. Thermodynamics of high-pressure adsorption of argon, nitrogen, and methane on microporous adsorbents. *Langmuir* 14, 3376–3389.
- Sass, B., Monzyk, B., Ricci, S., Gupta, A., B., H., Gupta, N., 2005. Impact of SO_x and NO_x in flue gas on CO₂ separation, compression, and pipeline transmission. *Carbon dioxide capture for storage in deep geologic formations , results from CO₂ capture project 2*, 955–981.
- Sebastian, J., Jasra, R.V., 2005. Sorption of nitrogen, oxygen, and argon in silver-exchanged zeolites. *Industrial & Engineering Chemistry Research* 44, 8014–8024.
- Shi, J., Durucan, S., 2005. A model for changes in coalbed permeability during primary and enhanced coalbed methane recovery. *SPE reservoir evaluation and engineering* 8, 291–299.

- Shi, J.Q., Durucan, S., 2003. A bidisperse pore diffusion model for methane displacement desorption in coal by CO₂ injection. *Fuel* 82, 1219 – 1229.
- Siemons, N., Busch, A., 2007. Measurement and interpretation of supercritical CO₂ sorption on various coals. *International Journal of Coal Geology* 69, 229 – 242.
- Siemons, N., Busch, A., Bruining, H., Krooss, B., Gensterblum, Y., 2003. Assessing the kinetics capacity of gas adsorption in coals by combined adsorption/diffusion method. SPE annual technical conference and exhibition, 5-8 October, Denver, Colorado .
- Siemons, N., Wolf, K.H., Bruining, J., 2007. Interpretation of carbon dioxide diffusion behavior in coals. *International Journal of Coal Geology* 72, 315–324.
- Soave, G., 1972. Equilibrium constants from a modified Redlich-Kwong equation of state. *Chemical Engineering Science* 27, 1197 – 1203.
- Solano-Acosta, W., Mastalerz, M., Schmmelman, A., 2004. Experimental CO₂ adsorption in coal versus particle size: implications for CO₂ sequestration. Annual AAPG Eastern Section meeting, October 3-6, Program with Abstracts, Columbus, Ohio , 126.
- Span, R., Wagner, W., 1996. A New Equation of State for Carbon Dioxide Covering the Fluid Region from the Triple-Point Temperature to 1100 K at Pressures up to 800 MPa. *Journal of Physical and Chemical Reference Data* 25, 1509.
- Spycher, N., Pruess, K., Ennis-King, J., 2003. CO₂ – H₂O mixtures in the geological sequestration of CO₂. I. assessment and calculation of mutual solubilities from 12 to 100 C and up to 600 bar. *Geochimica et Cosmochimica Acta* 67, 3015 – 3031.
- Stanmore, B., Tschamber, V., Brillhac, J.F., 2008. Oxidation of carbon by NO_x, with particular reference to NO₂ and N₂O. *Fuel* 87, 131 – 146.
- Stevenson, M., Pinczewski, W., Somers, M., Bagio, S., 1991. Adsorption/Desorption of Multicomponent Gas Mixtures at In-Seam Conditions . SPE Asia-Pacific Conference, 4-7 November 1991, Perth. Australia .

- Stryjek, R., Vera, J.H., 1986. PRSV: An improved Peng-Robinson equation of state for pure compounds and mixtures. *The Canadian Journal of Chemical Engineering* 64, 323–333.
- Sudibandriyo, M., Pan, Z., Fitzgerald, J.E., Robinson, R.L., Gasem, K.A.M., 2003. Adsorption of methane, nitrogen, carbon dioxide, and their binary mixtures on dry activated carbon at 318.2 K and pressures up to 13.6 MPa. *Langmuir* 19, 5323–5331.
- Syed, S., 2011. Permeability and injectivity enhancement of near wellbore region for CO₂ enhanced coalbed methane recovery and CO₂ storage. PhD Thesis, Imperial College London .
- Thomas, N., Windle, A., 1982. A theory of case II diffusion. *Polymer* 23, 529 – 542.
- Todheide, K., Franck, E.U., 1963. Das zweiphasen gebiet die kritische kurve im system kohlendioxid wasser bis zu drucken von 3550 bar. *Z. Phys. Chem.* 37, 387.
- Torp, A.T., Gale, J., 2004. Demonstrating storage of CO₂ in geological reservoirs: The Sleipner and SACS projects. *Energy* 29, 1361 – 1369. 6th International Conference on Greenhouse Gas Control Technologies.
- Valderrama, J., Silva, A., 2003. Modified Soave-Redlich-Kwong equations of state applied to mixtures containing supercritical carbon dioxide. *Korean Journal of Chemical Engineering* 20, 709–715.
- Wagner, W., Span, R., 1993. Special equations of state for methane, argon, and nitrogen for the temperature-range from 270-K to 350-K at pressures up to 30 MPa. *International Journal of Thermophysics* 14, 699 – 725.
- Wahanik, H., Eftekhari, A., Bruining, J., Marchesin, D., 2010. Analytical solution for mixed CO₂-water injection in geothermal reservoirs. Canadian unconventional resources and international petroleum conference, SPE 19.
- Walker, P., Verma, S., Rivera-Utrilla, J., Davis, A., 1988. Densities, porosities and surface areas of coal macerals as measured by their interaction with gases, vapours and liquids. *Fuel* 67, 1615 – 1623.
- Wang, G., Massarotto, P., Rudolph, V., 2009a. An improved permeability model of coal for coalbed methane recovery and CO₂ geosequestration. *International Journal of Coal Geology* 77, 127 – 136.

- Wang, G., Wei, X., Rudolph, V., Wei, C., Qin, Y., 2009b. A multi-scale model for CO₂ sequestration enhanced coalbed methane recovery. *Frontiers of Chemical Engineering in China* 3, 20–25.
- White, C., Smith, D., Jones, K., Goodman, A., Jikich, S., LaCount, R., DuBose, S., Ozdemir, E., Morsi, B., Schroeder, K., 2005. Sequestration of carbon dioxide in coal with enhanced coalbed methane recovery—a review. *Energy and Fuels* 19, 659–724.
- Wiebe, R., Gaddy, V.L., 1939. The solubility in water of carbon dioxide at 50, 75 and 100 C, at pressures to 700 atmospheres. *Journal of the American Chemical Society* 61, 315–318.
- Wiebe, R., Gaddy, V.L., 1940. The solubility of carbon dioxide in water at various temperatures from 12 to 40 C and at pressures to 500 atmospheres. critical phenomena. *Journal of the American Chemical Society* 62, 815–817.
- Wiebe, R., Gaddy, V.L., 1941. Vapor phase composition of carbon dioxide-water mixtures at various temperatures and at pressures to 700 atmospheres. *Journal of the American Chemical Society* 63, 475–477.
- Wong, S., Gunter, W., Law, D., Mavor, M., 2000. Economics of Flue Gas Injection and CO₂ Sequestration in Coalbed Methane Reservoirs. 5th International Conference on Greenhouse Gas Control Technologies, Aug .
- Wong, S., Law, D., Deng, X., Robinson, J., Kadatz, B., Gunter, W., Jianping, Y., Sanli, F., Zhiqiang, F., 2007. Enhanced coalbed methane and CO₂ storage in anthracitic coals—micro-pilot test at South Qinshui, Shanxi, China. *International Journal of Greenhouse Gas Control* 1, 215 – 222. 8th International Conference on Greenhouse Gas Control Technologies - GHGT-8.
- Yamaguchi, S., Ohga, K., Fujioka, M., Nato, M., Muto, S., 2006. Field experiment of Japan CO₂ geosequestration in coal seams project (JCOP). *Proceeding of the 7th international conference on greenhouse gas control technologies CD-ROM*.
- Yang, H., Xu, Z., Fan, M., Gupta, R., Slimane, R., Bland, A., Wright, I., 2008. Progress in carbon dioxide separation and capture: A review. *Journal of Environmental Sciences* 20, 14 – 27.
- Yi, J., Akkutlu, I., Deutsch, C., 2008. Gas transport in bidisperse coal particles: Investigation for an effective diffusion coefficient in coalbeds. *Journal of Canadian Petroleum Technology* 47, 20–26.

- Yi, J., Akkutlu, I., Karacan, C., Clarkson, C., 2009. Gas sorption and transport in coals: A poroelastic medium approach. *International Journal of Coal Geology* 77, 137–144.
- Zhou, C., Hall, F., Gasem, K.A.M., Robinson, R.L.J., 1994. Predicting gas adsorption using two-dimensional equations of state. *Industrial and Engineering Chemistry Research* 33, 1280–1289.
- Zhu, J., Wang, Y., Zhang, J., Ma, R., 2005. Experimental investigation of adsorption of NO and SO₂ on modified activated carbon sorbent from flue gases. *Energy Conversion and Management* 46, 2173 – 2184.

Acknowledgments

These four years would not have been successful for me without the academic, technical, social support of so many people! I hope to be able to mention here all of them.

First of all, I am really grateful to Hans Bruining and Karl-Heinz Wolf, what a combination of elements! Hans for his constant support and unlimited spontaneous willing of helping his students; for his pindaric flights around the world of transport phenomena and mathematics that were filling my mind for entire weeks. Apart for the academic aspect I really enjoyed his humor and he really helped me and pushed me when I was feeling that my work was just simply going nowhere. Karl-Heinz, especially in my last months of writing, was always present, clarifying my mind about the general overview of my work. He also made all my PhD possible, offering me the possibility to join the GRASP European Project and the dutch CATO2 project.

I feel very lucky to have had such these two supervisors. I have learnt a lot from them and I could not expect a better treatment.

The technical expertise and help of Henk van Asten, who was my rough and efficient guide to the laboratory world, was fundamental. A big thanks goes also to all the other technicians in the lab that were helping me a lot: Jan Etienne, Karel Heller, Mark Friebe, Henny, Gerard, Yolanda, Ellen, Dick, ... Thanks also for all my strange external requests in which the technicians were involved, such as cutting the stones to make out a musical instrument, or using the lab to shoot a musical video.

I want to thank my friend and colleague Marcin Lutynski. Part of the thesis wouldn't be possible without his help in the period he was in Delft. Our endless struggles with the mass spectrometer were a bit less sour thanks to his company and help. I want to thank also Susanne Rudolph, I am happy that she accepted to be a member of the committee, she is as a person that I really

esteem. Another mention has to go to Patrick that patiently taught me how to deal with the manometric set up. Amer in Imperial College helped me a lot with the swelling measurements, without him I do not know if I could run all the experiments in London in just three months. A thanks goes also to Eshan (aka Ali Akbar) that was helping me a lot with all the thermodynamic aspects of my thesis. Thanks to all the secretaries and administrative side of our department: Ralph, Lydia, Margot, Marlijn, Guus, Lianne, Annie,...especially for all the campus card they made for me in these four years. A thanks goes also to Maarten for his help in my thesis cover and Maarten de Groot for letting me be part of the LOT 12 project.

Marcin, Andrea, Mattia, Negar, Roozbe, Saskia, Sanaz, Elham, Mariam, Amin, Michel, Chris, Anna, Christiaan thanks a lot for resisting to my hyper active mood and for sharing all the funny lunches we had together and especially the good italian coffee.

A big thanks goes to all my friends in here that spent with me these 4 years. They represented for me my second family, my home: Eugenia, Valeria, Rachele and Giacomo, my four sisters. My amazing flatmates Miguel Hiroshi and Jean-Christophe and all the friends that temporary lived in my beautiful flat and shared the small and always crowded kitchen. Jordi, the best saxophone teacher ever, Alberto Novel, Erin, Thanos, Carlitos, Raluca, Annika, Julius and Jenny, Gonzo, Agnese, all the sonology crew in den Haag ...I am always having so much fun with you guys, also if you are now all spread around the world.

When you leave your own country, you really realize, especially after four years, who are the people that will stay forever in your life. This is what happened to me and with my life long friends: Michela, Chiaretti, Titta, Caty, Paolo, Laura and Gullo.

And now I want to give a special thanks to my family, because they are really the best. Patiently they were constantly supporting me, when I was a bit sad because it was always raining and I could not see any progress in my thesis, they were always there, always for me. Mamma, papa' e Marco, grazie, vi voglio tanto bene!

About the Author

Elisa Battistutta was born on August 13, 1981 in Palmanova, Italy. After having obtained her diploma at Liceo Scientifico 'G. Marinelli' (Udine) with 100/100 in 2000, she started studying Environmental Engineering at the Università degli Studi di Trieste, Italy. She graduated with Laude in 2006 with a thesis conducted at the OGS (Oceanographic and Geophysical National Institute) on Lidar Remote Sensing. The thesis was based on the implementation of data image resolution, using Digital Signal Processing analysis tools. After a brief experience as exhibition designer, she moved to the Netherlands and started in 2007 her PhD at TUDelft under the supervision of Prof. Dr. Hans Bruining and Dr. Karl-Heinz Wolf, which resulted in this dissertation.

Publications

1. E. Battistutta, P. van Hemert, M. Lutynski, H. Bruining and K.H. Wolf, Swelling and sorption experiments on methane, nitrogen and carbon dioxide on dry Selar Cornish coal, *International Journal of Coal Geology*, Vol.84 (1),pp. 39 - 48, 2010.
2. E. Battistutta, M. Lutynski, S. Rudolph, H. Bruining and K.H. Wolf, Adequacy of Equation of State models for determination of adsorption of gas mixtures in a manometric set up, *International Journal of Coal Geology*, accepted, 2011.
3. E. Battistutta, A.A. Eftekhari , H. Bruining and K.H. Wolf, Sorption measurements of CO₂ on wet bituminous coal, *Fuel and Energy*, accepted, 2011.
4. E. Battistutta, M. Lutynski, S. Rudolph, H. Bruining and K.H. Wolf, Determination of adsorption of gas mixtures in a manometric set up, *International Journal of Coal Geology*, accepted, 2011.
5. Y. Gensterblum, P. van Hemert, P. Billefont, E. Battistutta, A. Busch, B.M. Krooss, G. De Weireld and K.-H.A.A. Wolf, European inter-laboratory comparison of high pressure CO₂ sorption isotherms II: Natural coals, *International Journal of Coal Geology*, Vol.84 (2),pp. 115-124, 2010.
6. M. Lutynski, E. Battistutta, H. Bruining and K.H. Wolf, Discrepancies in the assessment of CO₂ storage capacity and methane recovery from coal with selected equations of state. Part I. Experimental isotherm calculation, *Physicochemical Problems of Mineral Processing journal*, Vol.47 , 2011.

7. M. Lutynski, E. Battistutta, H. Bruining and K.H. Wolf, Discrepancies in the assessment of CO₂ storage capacity and methane recovery from coal with selected equations of state. Part II. Reservoir simulation, *Physico-chemical Problems of Mineral Processing journal*, Vol.47 , 2011.